

**Guided vasculogenic sprouting induced by the immobilized  
fusion construct CaM-VEGF120**

by

Malcolm Robb

A thesis

presented to the University of Waterloo

in fulfillment of the

thesis requirement for the degree of

Master of Science

in

Chemistry

Waterloo, Ontario, Canada, 2012

© Malcolm Robb 2012

## **Author's declaration**

I hereby declare that I am the sole author of this thesis. This is a true copy of this thesis, including any required final revisions, as accepted by my examiners.

I understand that my thesis may be made electronically available to the public.

Malcolm Robb

## Abstract

This project is intended to utilize an immobilized bio-active first generation fusion constructed cytokine inducing in receptive cell lines guided vasculogenic development. This research through the assembly, expression and purification of a bio-active molecule the CaM-VEGF120 fusion construct permitted the creation of a first generation smart-gel platform. Cell culture bringing together HUVECs or cBOECs with soluble or immobilized CaM-VEGF120 coupled with a type-I collagen platform are the main components intended to induce guided vascular sprouting. Purification of the CaM-VEGF120 was achieved utilizing HIC coupled with size exclusion chromatography. Mass Spectrometry and cellular augmentation noted by survivability and proliferation suggests the correct CaM-VEGF120 properties were achieved. Cell culture interactive changes were recorded utilizing fluorescent and phase microscopy. The 66 KDa dimeric CaM-VEGF120 was able to phosphorylate the cytoplasmic Tyr<sup>1175</sup> localized to the C-terminal portion of the transmembrane VEGFR2. GNP immobilized CaM-VEGF120 induced VEGFR2 expressing cell lines as were imaged over a week's period recording vascular pseudo-tube formation. These events resulting from contact with the immobilized CaM-VEGF120 and VEGFR2 induced activity thus presenting *in vitro* guided vascular pseudo-tube development. This research is being pursued utilizing HUVEC and cBOECs as guided vascular pseudo-tube structural formation is possible. This successful model implies a first generation model for physiological vascular development having therapeutic applications.

## **Acknowledgements**

Many people to thank, but my supervisor's Dr. Guy Guillemette did provide the expertise to complete this thesis and to compile the experiments pointing the project in the right direction, and of course Dr. Eric Jervis for much expertise and vision if only there was more time for this project, that has so much vast potential.

Of course all the people I had the pleasure to interact with that provided support, such as Val Taiakina and even Odi Israel for the help to lift the project off the ground, and the rest of the Jervis lab for there help especially with Microscope number 5.

Much Thanks from Malcolm J Alexander Robb.

## **Dedication**

This can be dedicated to perhaps; to a further strengthening for the foundation to which medical research has been established.

# Table of Contents

<b>Author's declaration.....</b>	<b>ii</b>
<b>Abstract.....</b>	<b>iii</b>
<b>Acknowledgements.....</b>	<b>iv</b>
<b>Dedication.....</b>	<b>v</b>
<b>Table of Contents.....</b>	<b>vi</b>
<b>List of Figures.....</b>	<b>xii</b>
<b>List of Tables.....</b>	<b>xiii</b>
<b>List of Abbreviations.....</b>	<b>xiv</b>
<b>Chapter I The properties of vasculogenesis, the extra-cellular matrix complemented with the ligand-receptor requirements.....</b>	<b>1</b>
1.1 Modified Vascular Development.....	1
1.1.1 Properties of vasculogenesis.....	3
1.1.2 Properties of Angiogenesis.....	4
1.1.3 Sprouting angiogenesis.....	5
1.2 The family of angiogenic growth factors.....	7
1.2.1 Bio-Active VEGF cytokine family and properties.....	7
1.2.2 VEGF-A an endothelial specific bio-active cytokine.....	9
1.2.3 VEGF-A biology and regulation.....	10
1.3 ECM.....	10
1.3.1 Biology of the ECM.....	12
1.4 VEGFR2.....	12
1.4.1 Properties of the VEGF receptors, receptor tyrosine kinase family.....	13
1.4.2 VEGFR2 receptor tyrosine kinase.....	14
1.4.3 Biology of VEGFR2 phosphorylation and signaling pathways.....	15

1.4.4 Modification of VEGFR2 signaling.....	16
1.4.5 The biological effects of VEGFR2 .....	17
1.5 Research Objectives.....	18
<b>Chapter II The production, purification and biochemical characterization of the putative CaM-VEGF120 fusion construct.....</b>	<b>19</b>
2.1 Summary.....	19
2.2 Introduction.....	20
2.2.1 Characteristic description of the VEGF120.....	21
2.2.2 Calmodulin and its properties involving the CaM-VEGF120 fusion construct.....	22
2.2.3 Properties of the CaM-VEGF120 Fusion Construct feed-back system.....	23
2.2.4 Potential properties of the CaM-VEGF fusion construct.....	24
2.2.5 Chapter II objective.....	24
2.3 Methodology.....	25
2.3.1 Preparation and characterization of the pET-15b CVFC expression vector.....	25
2.3.1.1 Excision of the fusion construct fragment CaM-VEGF120 from pET-9b, 315 residues or 945 bases.....	25
2.3.1.2 pET-15b CaM-VEGF120 subcloning, amplification and purification .....	26
2.3.1.3 PCR Parameters for amplification and subcloning the VEGF120.....	27
2.3.2 CaM-VEGF120 protein translation utilizing pET-15b.....	27
2.3.2.1 CaM-VEGF120 production and purification.....	27
2.3.2.2 Protein production and purification; CaM-VEGF120 translation and amplification.....	28
2.3.2.3 Bacterial cell lysis and construct separation.....	28
2.3.2.4 Phenyl sepharose CaM-VEGF120 separation from cell lysate.....	29
2.3.3 SDS-page reducing gel protein analysis.....	29
2.3.4 CaM-VEGF120 preparation for bio-activity.....	30
2.3.4.1 Sample preparation for utilization of gel column purification .....	30
2.3.4.2 Superdex 75 gel column purification.....	31

2.3.5 Characterization.....	31
2.3.5.1 Mass spectrometry.....	31
2.3.5.2 Membrane separation of CaM-VEGF120 utilizing 50KDa size exclusion spun column....	32
2.3.5.3 CaM-VEGF120 MMP-9 Digest.....	32
2.3.6 Modification of CaM-VEGF120.....	32
2.3.6.1 FITC labeling of CaM-VEGF120 required for isotherm and tissue culture.....	33
2.4 Results.....	34
2.4.1 Characterization of the DNA clone for CaM-VEGF120.....	34
2.4.2 CaM-VEGF120 translation, purification and analysis.....	37
2.4.3 Final conformational experiments confirming CaM-VEGF120 properties.....	39
2.5 Discussion .....	40
2.5.1 Cloning of the CaM-VEGF120 DNA fragment.....	40
2.5.2 Supporting evidence for the CaM-VEGF120 properties .....	41
2.5.2.1 Construct Description and conformation.....	42
2.5.2.2 CaM-VEGF120 modification.....	42
<b>Chapter III Properties of the gold nanoparticles, CaM binding peptide and the numerical</b>	
<b>quantification of the CaM-VEGF120 per gold nanoparticle.....</b>	<b>43</b>
3.1 Summary.....	43
3.2 Introduction.....	44
3.2.1 The GNP complex and immobilization.....	45
3.2.2 Chapter III objective.....	46
3.3 Methods.....	47
3.3.1 Preparation of GNPs using the tri-sodium citrate reduction method.....	47
3.3.2 Properties of the iNOS CBP and CAP.....	48
3.3.3 CBP Nanopartz GNP capping procedure.....	49
3.3.4 CaM-VEGF120 interaction and binding to the CBP capped GNPs.....	49

3.3.5 GNP immobilization.....	50
3.3.6 Collagen adhesion utilizing the CAP.....	50
3.3.7 Isotherm construction, CaM-VEGF120 binding affinity and quantity per single CBP capped GNP.....	50
3.3.7.1 Standard curve construction to determine fluorescent values to established CaM-VEGF120 concentration.....	50
3.3.7.2 Isotherm plot construction.....	52
3.4 Results.....	53
3.4.1 In house production of the GNPs.....	53
3.4.2 Nanopartz GNP peptide capping.....	53
3.4.3 Characterization and properties of the CBP capped GNPs.....	54
3.4.4 Determination of CaM-VEGF120 per GNP.....	56
3.4.5 Isotherm.....	56
3.5 Discussion.....	58
3.5.1 In house GNP production and applicability.....	58
3.5.2 CBP capped GNPs.....	59
3.5.3 Characterization and properties of the CBP capped GNPs.....	59
3.5.4 Optimization of CaM-VEGF120 per GNP.....	60
3.5.5 Isotherm.....	60
3.5.6 CaM-VEGF120 complex immobilization.....	62
<b>Chapter IV CaM-VEGF120 bio-active response of VEGFR2 expressing cell lines.....</b>	<b>63</b>
4.1 Summary.....	63
4.2 Introduction.....	64
4.2.1 HUVEC properties.....	64
4.2.2 MSCs properties.....	65

4.2.3 SMCs and pericytes.....	66
4.2.4 Lineage committed stem cells.....	66
4.2.4.1 EPC characterization.....	67
4.2.4.2 Early out-growth EPCs.....	67
4.2.4.3 Late out-growth EPCs.....	68
4.2.5 Objective.....	68
4.3 Methodology.....	69
4.3.1 Tissue culture.....	69
4.3.2 Scratch assay preparation.....	70
4.3.3 Random pseudo-tube formation.....	70
4.3.4 Advanced tissue culture.....	71
4.3.5 IP and western analysis of VEGFR2.....	71
4.3.5.1 Immunoprecipitation of the VEGFR2.....	72
4.3.5.2 Western blotting.....	73
4.4 Results.....	74
4.4.1 Scratch Assay.....	74
4.4.2 CaM-VEGF120 bio-active properties.....	77
4.4.3 GNP internalization.....	78
4.4.4 3D Collagen gel structures.....	82
4.4.5 VEGFR2 Tyrosine 1175 auto-phosphorylation.....	86
4.5 Discussion.....	87
4.5.1 Cell culture demonstration of CVFC bio-activity.....	87
4.5.2 CaM-VEGF120 Vasculogenesis.....	88
4.5.3 CaM-VEGF120 complex interaction with putative VEGFR2.....	89
4.5.4 Enhancing GNP immobilization to survive rigorous conditions.....	90
<b>Chapter V Conclusion.....</b>	<b>91</b>
5.1 Alternatives to the CaM-VEGF120.....	92

5.2 Modifications to tissue culture.....	93
References.....	94

## List of Figures

<b>Figure 1.1</b> - Image depicting vasculogenic sprouting induced by VEGF120.....	6
<b>Figure 1.2</b> – Basic outline depicting the CaM-VEGF120 fusion construct.....	7
<b>Figure 2.1</b> - Nucleic acid and amino acid sequence describing the CaM-VEGF120.....	22
<b>Figure 2.2</b> - SDS-PAGE demonstrating presence of putative CaM-VEGF120 in crude bacterial lysate..	35
<b>Figure 2.3</b> - SDS-PAGE of CaM-VEGF120 fractions collected from Phenyl Sepharose chromatography .....	36
<b>Figure 2.4</b> - Superdex 75 purification profile analyzed by SDS-PAGE, image depicting the putative CaM- VEGF120 on SDS-page gel.....	37
<b>Figure 2.6</b> - MMP-9 digest of CaM-VEGF120.....	39
<b>Figure 3.1</b> - Simplistic image of the CaM-VEGF120 complex.....	46
<b>Figure 3.2</b> - CaM-VEGF120 Isotherm and complementary standard curve. ....	55
<b>Figure 3.3</b> - The original isotherm with 6 to 7 FITC labels per CaM-VEGF120.....	57
<b>Figure 4.1</b> - cBOEC scratch assay .....	75
<b>Figure 4.2</b> - HUVEC scratch assay demonstrating CaM-VEGF120 induced cell confluency. ....	76
<b>Figure 4.3</b> - Day 1 to Day 4 HUVEC CaM-VEGF120 complex stimulation and response.....	78
<b>Figure 4.4</b> - Image at time zero of HUVEC and CaM-VEGF120 stimulation and exposure.....	79
<b>Figure 4.5</b> – 14 hour HUVEC exposure to CaM-VEGF120 complex, with emphasis on tube formation. 80	
<b>Figure 4.6</b> - Day 2 imagery following CaM-VEGF120 complex exposure. ....	81
<b>Figure 4.7</b> – Final images at day three, emphasizing the robust pseudo-tube formation and fluorescent CaM-VEGF120.....	83
<b>Figure 4.8</b> - Collagen spot interaction with HUVECs, time zero. ....	84
<b>Figure 4.9</b> - Day 3.5 cellular invasion into the collagen CaM-VEGF120 diffusible spot.....	85
<b>Figure 4.10</b> - Western images of VEGFR2 IP demonstrating Tyr <sup>1175</sup> phosphorylation.....	86

## List of Tables

<b>Table 2.1</b> – FITC protein labeling.....	33
<b>Table 2.2</b> - Mass Spectrometry Data depicting the native CVFC and FITC labeled version in monomer form.....	38
<b>Table 3.1</b> – (FITC) CaM-VEGF120 concentrations for standard curve. ....	51

## List of Abbreviations

Ang-1	Angiopoietin-1
AP1	Activated Protein 1
aPC	activated Protein C
APS	Ammonium per Sulfate
BM	Bone Marrow
cBOEC	canine Blood Outgrowth Endothelial Cell
BSA	Bovine Serum Albumin
CaM	Calmodulin
sCaM-VEGF120	soluble CaM-VEGF120
CAP	Collagen Adhesion Peptide
CBP	CaM Binding Peptide
CD	Cluster of Differentiation
CVFC	CaM-VEGF120 Fusion Construct
DLS	Dynamic light scattering
DTT	Dithiothreitol
EC	Endothelial Cell
ECM	Extra Cellular Matrix
<i>E. coli</i>	<i>Escherichia coli</i>
EDTA	Ethylenediaminetetraacetic Acid
EET	Epoxyeicosatrienoic acid
EPC	Endothelial Progenitor Cell
bFGF	basic Fibroblast Growth Factor
FITC	Fluorescein isothiocyanate
GNP	Gold Nanoparticle
G-CSF	Granulocyte-colony stimulating factor

HEPES	Hydroxyethyl Piperazineethanesulfonic Acid
HIF-1 $\alpha$	Hypoxic Response Factor 1 $\alpha$
HRE	Hypoxic Response Element
HSPG	Heparin Sulfate Proteoglycan
HUVECs	Human Umbilical Vascular Endothelial Cells
IL 1	Interleukin 1
IP	Immuno-Precipitation
IPTG	Isopropyl beta-D-Thiogalactopyranoside
KDa	Kilo Daltons
LB	Lysogeny broth
LMW	Low Molecular Weight
LPS	Lipo-Polysaccharide
MAPK	Mitogen-Activated Protein Kinase
MEK	MAPK Extracellular-Regulated Signaling Kinase
MMP	Matrix-Metallo Protease
MSC	Mesencimal Stem Cells
NAD	Nicotinamide Adenine Dinucleotide
NF- $\kappa\beta$	Nuclear Factor kappa beta
p38	protein 38
PBS	Phosphate Buffered Saline
PDGF	Platelet Derived Growth Factor
PDDA	Poly(Diallyl Dimethyl Ammonium Chloride)
PiGF	Placental Growth Factor
PKC	Protein Kinase C
PLC $\gamma$	Phospholipase gamma
PMSF	Phenylmethylsulphonylfluoride
PS	Phenyl Sepharose

RGD	Arginine Glycine
RT	Restriction Digest Enzymes
RTK	Receptor Tyrosine Kinase
SANH	Succinimidyl 4-Hydrazinonicotinate Acetone Hydrazone
SDS-PAGE	Sodium Dodecyl Sulphate Polyacrylamide Gel Electrophoresis
SFB	Succinimidyl 4-formylbenzoate
SMC	Smooth Muscle Cell
SOD	Super-Oxide Dismutase
SP1	Specific Protein 1
TACE	TNF- $\alpha$ -converting enzyme
TBS	Tris-Buffered Saline
TEM	Transmission Electron Microscopy
TEMED	Tetramethylethylenediamine
TGF $\beta$	Transformation Growth Factor beta
Tie-2	Tyrosine-2
TM	Thrombomodulin
TNF $\alpha$	Tumor necrosis factor-alpha
TP	ThromboxaneA2 Receptor
TRITC	Tetramethyl Rhodamine Isothiocyanate
VEGF	Vascular Endothelial Growth Factor
VEGFR2	VEGF Receptor 2
VHD	VEGF Homology Domain
VPF	Vascular Permeability Factor
UV	Ultra Violet

## Chapter I

### **The properties of vasculogenesis, the extra-cellular matrix complemented with the ligand-receptor requirements**

#### **1.1 Modified Vascular Development**

Compromised tissue due to damage or disease once considered irreversible now has a chance at repair, utilizing a promising new approach described as *in vitro* tissue engineering or scaffolding modification (Nerem RM, 2006). Our approach is a blend of bio-active cytokines coupled with an insoluble matrix suitable for an optimal choice of a putative cell line, a cocktail with intent to create a system suitable to tackle these challenging medical issues. As tissue engineering undergoes developmental modifications supported by the latest materials, it should begin to hold substantial medical promise (Nerem RM, 2006). To date there are still major obstacles to overcome, identified as limitations of diffusion or sufficient blood supply for delivery of oxygen and metabolic waste removal. Previously it has been shown that seeding of endothelial cells into experimental tissues grafts or constructs has enhanced tissue survival, perhaps due to augmented circulation supplying cytokines favouring the quiescent vascular state, but the ideal long-term graft remains elusive (Batten *et al.*, 2007). In relation to this project, vasculogenesis, an event that describes *in vitro* vascular formation from individual cell sources, is the intended objective.

### 1.1.1 Properties of Vasculogenesis

Vasculogenesis describes vascular development independent of any pre-existing vascular network; early stage embryogenesis presents an excellent example (Francis *et al.*, 2008). Cytokine response can initiate tip cell developmental profiles or angiogenic sprouting laying the foundation for pseudo-tube formation (Carmona *et al.*, 2008). These events take place in receptive cell lines expressing the VEGFR2, activated upon interaction with its ligand VEGF-A. During embryogenesis vascular development derives from angioblast cell lines (Loffredo and Lee, 2008). Alternatively vasculogenesis can be utilized as an *in vitro* model on a collagen surface, 3D collagen slab or Matrigel. Mesodermal precursor cells (hemangioblast) or angioblasts (EPCs) differentiate into endothelial cells during the formation of vessels (Jakobsson *et al.*, 2006; Loffredo and Lee, 2008); this can take place *in vitro* for direct transfer to animal models or to sites of induced ischemia, noting this event is neo-vascularization or vasculogenesis (Lokmic and Michell, 2008). So far not much is known about EPC recruitment to active sites of vasculogenesis; however growth factors in the peripheral blood such as stromal-derived factor-1, erythropoietin, angiopoietin-1, estrogen and even exercise all have the affects of EPC recruitment and increased numbers of EPCs within the peripheral blood (Lokmic and Michell, 2008).

A functional *in vivo* micro-vascular network is one of the major challenges facing bio-engineering if the intent is to aid the recovery of damaged tissues. Pericytes derived from MSCs are deemed essential to help stabilize developing vessels otherwise they fall short of full development with minimal vascular connection to the host, regression becomes inevitable. Pericytes themselves migrate towards and attach to developing vessels in direct contact with ECs creating a system of paracrine signaling enhancing stability, differentiation and growth arrest (Lokmic and Michell, 2008).

### 1.1.2 Properties of angiogenesis

Briefly this is an event describing vasculature development dependent on preexisting vessels where resident endothelial cells from the pre-existing vessels are recruited forming tube and luminal structures suitable for blood flow. This is essential during embryonic development and notably pathological demands do produce functional although unstable vascular structures (Nacak *et al.*, 2007; Labrecque *et al.*, 2003; Francis *et al.*, 2008). This process requires a break from the quiescent state, an active re-modeling of the existing vasculature. These events can be induced by pericytes or lymphocytes that supply a cocktail of cytokines that act directly on receptive cells that express receptors such as bFGF or TP, or indirectly through TGF $\beta$  and TNF $\alpha$  (Gao *et al.*, 2011; Terpos *et al.*, 2012). Currently the most important of the angiogenic cytokines is VEGF-A, and from observations VEGF-A is ubiquitously present at sites of active angiogenesis targeting endothelial cells (Robinson and Stringer, 2001; Compagni *et al.*, 2000; Bhattacharya *et al.*, 2009).

The arterial vascular wall contains progenitor cells; however their exact role remains elusive although they do express the VEGFR2. Advancing micro-vascularization within atherosclerotic plaques is problematic as this leads to the advancement of atherosclerotic progression and plaque instability. Healthy vessels do have a microvascular network but it is restricted to the vasa vasorum (Zampetaki *et al.*, 2008). Finally upon completion of development, angiogenesis is blocked as homeostatic ligands and their receptors come into play, such as TM, aPC, SOD, Tie-2, Ang-1 and TGF- $\beta$  (Song *et al.*, 2009; Thomas and Augustin, 2009).

### 1.1.3 Sprouting angiogenesis

Angiogenic sprouting describes the earliest known stage of vascular development. This can occur either *in vivo* in preexisting vessels marking the initial point of angiogenesis, or *in vitro* as individual cells begin the cascade of vasculogenesis following receptor stimulation induced by specific ligand interactions (Moss *et al.*, 2009). Changes in physical characteristics displayed include cellular elongation. This is best observed on type-1 collagen as this insoluble matrix predisposes committed cells towards pseudo-tube formation. VEGF-A stimulated events observed on fibronectin or gelatin coated surfaces are conditions predisposed for cell proliferation, perhaps a pathological developmental predisposition. Interestingly, early stage sprouting on collagen could in fact be simulating the earliest stages of physiological angiogenesis, as on fibronectin conditions seem to favor that found in wound healing and the properties of tumor hypoxia, a known source of massive VEGF-A production (Holderfield and Hughes, 2008).

On the other hand, sustained and excessive amounts of VEGF-A on mature vessels can lead to vascular leakage and remodeling, where angiogenic sprouting is absent. Therefore the amount of VEGF-A exposure may be an important consideration. To date the only cytokine reported to induce angiogenic sprouting appears to be VEGF-A, other cytokines may act to only cause receptive cells to augment VEGF-A (Mellberg *et al.*, 2009).

Cells reported to have excessive amounts of VEGFR2 are favored to form the tip cells, these undergo elongation and migration towards VEGF-A gradients. Tip cells rarely divide and are not the lumen forming cells but align in the direction towards the VEGF-A gradient. Lumen

forming cells are those that follow tip cell signaling and do proliferate; these cells are referred to as trunk cells and reportedly form the vascular lumen (Holderfield and Hughes, 2008).

## **1.2 The family of angiogenic growth factors**

### **1.2.1 Bio-Active VEGF cytokine family and properties**

Classified as cytokines with bio-active properties the VEGF family possesses mitogenic and chemotactic properties with extended effects on vasodilation, survival and permeability (Hu *et al.*, 2009). Vascular permeability fluctuations were the events leading to the discovery of VEGF-A or VPF (Prahst *et al.*, 2008). The VEGF family of cytokines specifically target endothelial cells and at present the current classification consists of six genes VEGF-A, VEGF-B, VEGF-C, VEGF-D, VEGF-E (encoded by virus), VEGF-F (snake venom) and PiGF (Prahst *et al.*, 2008; Roy *et al.*, 2006; Gabhann and Popel, 2008; Bahram and Claesson-Welsh, 2010).

Inclusion into this family requires recognition and activation of the RTK receptors VEGFR1, VEGFR2 and VEGFR3 (Roy *et al.*, 2006; Mellberg *et al.*, 2009; Bahram and Claesson-Welsh, 2010). This family of cytokines contains the VEGF Homology domain (VHD), a unique feature whose amino acid identity is in the range of 29-64%. There are eight conserved Cysteine residues in the VHD in a structural form described as the Cysteine Knot Motif (Muller *et al.*, 1997).

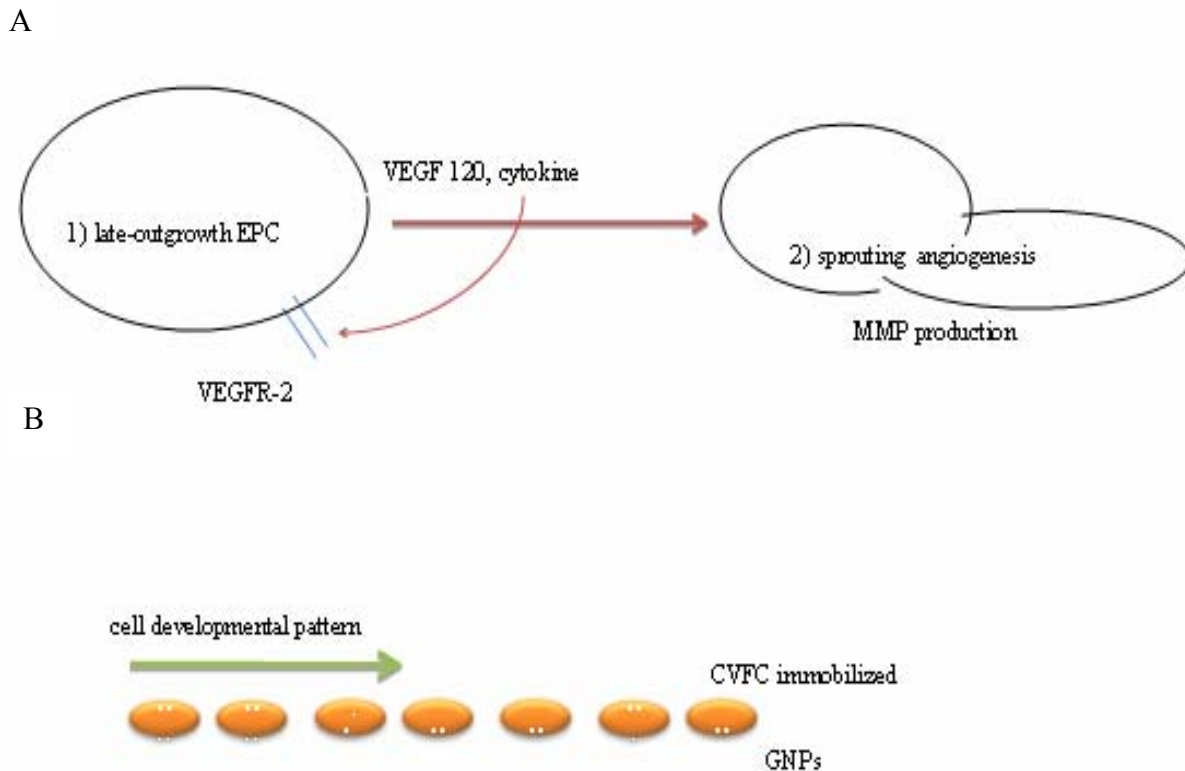


**Figure 1.1 - Image depicting vasculogenic sprouting induced by VEGF120.** A) A visual presentation to highlight the basic events leading to angiogenic sprouting as the tip cell is acted on by a soluble cytokine, including an illustration for protease production that is augmented, for example MMP production and activity. B) An illustration to present in simple terms GNP's with immobilized CaM-VEGF120 intended to be visible to the VEGFR2 expressing cells, the result is guided angiogenesis. Noting the GNP pattern is flexible as trunk cells follow the tip cell intended for pseudo-tube formation intended for a functional lumen.

These Cysteines are naturally involved with inter- and intramolecular disulfide bridge formation residing in a conserved central four-stranded  $\beta$ -sheet per monomer, and all display the characteristic anti-parallel dimer (Robinson and Stringer, 2001; Gabhann and Popel, 2008; Muller *et al.*, 1997).

Excessive amounts of VEGF-A and other similar ligands can result in a dilated vasculature with an inflated size and excessive permeability to fluids. Briefly, hVEGF-A consists of the

following isoforms each representative of the number of amino acids, such as VEGF121, VEGF145, VEGF165, VEGF183, VEGF189 and VEGF206 (rare); VEGF121, VEGF145 and VEGF165 are secreted while the rest remain matrix bound (Zygalaki *et al.*, 2008). The VEGF165 is believed to be the most active and the VEGF145 is absent within the vasculature (Roy H *et al.*, 2006). Since only three isoforms are relevant and the most characterized reference will be made only to VEGF121, VEGF165 and the VEGF189, or the VEGF120, 164 and 188 being designations mouse and rat.



**Figure 1.2 – Basic outline depicting the CaM-VEGF120 fusion construct.** The full size 576 amino acids, 66 kDa, displayed as an anti-parallel homo-dimer connected by 3 disulfide bridges, the bio-active form. Solid blocks represent the CaM portion; open blocks the VEGF120 connected by a solid horizontal line the protease linker.

### 1.2.2 VEGF-A an endothelial specific bio-active cytokine

VEGF-A induces proliferation and migration of endothelial cells in conjunction with nitric oxide, and may contribute to vascular remodeling following hypoxic conditions, which augments VEGF-A expression. Interestingly what is currently known about VEGFR2 transcriptional expression and signaling remain relatively elusive (Gabhann and Popel, 2008; Kim BS *et al.*, 2002; Tam *et al.*, 2009; Linares and Gisbert, 2011). VEGF-A is encoded from 8 exons (exon 8a) that gives rise to a number of splice variants. The human VEGF-A isoforms are slightly different

having an extra residue (Tozer *et al.*, 2008; Houck *et al.*, 1992; Kim *et al.*, 2007). The active form comprises of single peptides bound by two disulfide bridges Cys-51 and Cys-60 in an anti-parallel fashion. The VEGF120 is slightly acidic and readily diffusible, and represents secreted soluble isoform of VEGF-A (Roy *et al.*, 2006).

VEGF165 forms an active homodimeric heparin binding glycoprotein about 45 KD in size and is diffusible having a weak capacity to interact with the glycoproteins of the ECM (Roy H, 2006; Kim *et al.*, 2002). The C-terminal of the VEGF165, which includes the family of VEGF-A isoforms, has a six residue alternative form that upon conversion becomes antagonistic preventing VEGFR2 signaling, VEGF165b (Gabhann and Popel, 2008). The other two isoforms of interest, VEGF121 and the VEGF189, have different signaling properties evident if present in only their individual forms. Interestingly, the vasculature is seemingly more fragile if only the VEGF 121 is available to induce angiogenic development. Observations of tumor models stimulated with the VEGF189 isoform reveal enhanced vascular stability with extensive development (Tozer *et al.*, 2008). VEGF189, being one of the largest and most basic form is only found immobilized to the cell surface ECM bound to the heparin proteoglycans. Characterization of the VEGF189 suggests this isoform is highly angiogenic, inducing the formation of large vessels with extensive branching. Investigations with each isoform demonstrates a unique characteristic morphological difference in the resulting vasculature however full characterization has yet to be completed (Tozer *et al.*, 2008; Houck *et al.*, 1992; Kim *et al.*, 2002). VEGF121 cannot bind heparin or the ECM as it is lacking the heparin binding domain. This is not the case for VEGF165 since this cytokine has an extra 44 residues and a single HSPG binding site making possible interaction with heparin and the ECM. VEGF189 is increasingly basic, having

an additional 29 residues and an additional HSPG binding site binding heparin and the ECM essentially irreversibly (Houck *et al.*, 1992).

Finally VEGF-A has a very high affinity for VEGFR-1, a  $K_d$  of 15–100 pM and VEGFR-2 a  $K_d$  of 400–800 pM, still robust but 10 times less than that of VEGFR1. However VEGFR1 has yet to demonstrate anything but minimal bio-activity in endothelial cells, but might incur some form of negative regulation such as the removal of excess VEGF-A. Therefore the transcriptional regulation of VEGFR1 would be of interest (Roy *et al.*, 2006; Gabhann and Popel, 2008). The mature endothelium should not respond to VEGF-A as only minimal levels of the receptors are present under homeostatic states, noting the activated endothelium may have a robust level of VEGFR2 predisposing the vasculature to re-modeling.

### **1.2.3 VEGF-A biology and regulation**

An important feature identifying the regulatory region of VEGF-A is the presence of a hypoxic response element that can augment transcription in response to hypoxia or glycemia. HIF-1 $\alpha$  is up-regulated and protected against proteolytic degradation during O<sub>2</sub> depletion and is the transcription factor acting on the VEGF-A HRE. The expression cascade takes place in the vascular wall localized to the smooth muscle cells hence acting in a paracrine manner on the endothelial monolayer. Other transcription factors regulating VEGF-A include Sp-1, Ap-1 and NF- $\kappa$ B (Zahlten *et al.*, 2010). VEGF-A is found actively expressed in areas such as the parenchyma tissue and stromal cells, and can also include an autocrine expression pattern from endothelial cells themselves however it is unclear if this occurs during development. The reason may be to sustain cell survival if the vessels are lacking a muscular wall characteristic of capillaries. Other known factors affecting VEGF-A expression are growth factors; these include

bFGF, TGF- $\beta$  and IL-1. As mentioned above, hypoxia is directly linked to the regulation of VEGF-A, and is also up-regulated by inflammatory signals. It seems pathological angiogenesis relating to carcinomas, diabetic retinopathy or arthritis demonstrate augmented expression favoring the shift towards the expression of VEGF165, as VEGF165b is attenuated, implying a potent angiogenic environments (Gabhann and Popel, 2008; Kim *et al.*, 2002).

## **1.3 ECM**

### **1.3.1 Biology of the ECM**

Collagens, including elastin, are some of the major structural features of the vascular wall forming the ECM providing tensile strength and elasticity. Collagen, an insoluble component of the ECM, predisposes endothelial cells towards sustained angiogenic differentiation (Heydarkhan-Hagvall *et al.*, 2006; Francis *et al.*, 2008). Thus, for engineering vascular development this represents a suitable platform for cytokine immobilization, providing an ideal simplistic first generation matrix (Rusnati *et al.*, 2006). Matrigel is another possible matrix, however due to the amount of various bio-active cytokines present, Matrigel has been ruled out as this will mask the effects of the experimental immobilized VEGF120 (Hughes *et al.*, 2010). At present, there are 20 known different types of collagen in the human body and the most abundant are types I and III. The major sources of collagen are derived from fibroblast and connective cell lines. Upon secretion, they form three poly-peptide strands bundled into what is described as a triple helix, thus forming the collagen fibrils and fibers. Collagen does undergo extra-cellular modification, including the process of cross-linking mediated by lysyl oxidase generating bond formation between lysine and hydrolysine which enhances strength and insolubility to the

collagen ECM (Henriksen *et al.*, 2011). Type-I collagen and to a lesser extent type-III collagen are generally found in abundance in the skin, ligaments, fascias and fibrous tissues. Type-III collagen levels however are augmented during the wound healing process due to serum activation of the regional fibroblast cells. Both type I and type III do coexist in the same fibrils but special organization places type-III collagen towards or on the surface. With an increasing ratio of type-III collagen relative to type-I, the fibril diameter decreases (Henriksen *et al.*, 2011; Haas *et al.*, 1998). Collagen is the first generation material for generating scaffolding complexes that will be used this project. However the optimal scaffolding complex for cell growth and development as suggested would be a blend of type-1 collagen and fibronectin (Francis *et al.*, 2008). Integrins like  $\alpha_v\beta_3$  are examples of some receptors that respond through signaling when interacting with the ECM and their structural features. A good example is RGD thus influencing cellular properties that can involve differentiation and survivability (Mihardja *et al.*, 2010; Smadja *et al.*, 2008). Collagen is itself also subject to modification such as cross-linking, and thus can act as an adhesive surface for the collection and binding of bio-active cytokines. Cross-linking creates a resistant barrier to proteolytic degradation (MMPs), however collagen gels *in vitro* are not cross-linked and are easily degraded by MMPs due to cellular activity induced by immobilized cytokines such as bFGF and VEGF188/189 (Fernandes *et al.*, 2009; Heydarkhan-Hagvall *et al.*, 2006). *In vitro* collagen can be augmented by cyclic strain, growth factors (probably VEGF-A) and ascorbic acid through SMCs. Tendons are a good example of an *in vivo* collagen based ECM linking muscle to bone, as when compromised tendons result in an augmentation of VEGF-A to attract VEGFR2 expressing cells. Since VEGF-A is abundantly expressed in the compromised tendon, ECM implicates angiogenesis as a source for recovery. However invading cells responding to VEGF-A, augmentation of proteolytic activity has to be

taken into account, noting endothelial cells do not excrete much ECM (Petersen *et al.*, 2003). VEGF-A signaling has been linked with MMP activity. This is important as it suggests not only angiogenic activity but tendon ECM remodeling, and presents an excellent model system for comparing to *in vitro* models utilizing VEGF-A and collagen scaffolding. (Petersen *et al.*, 2003; Chachques *et al.*, 2008).

## **1.4 VEGFR2**

### **1.4.1 Properties of the VEGF receptors, the receptor tyrosine kinase family**

These receptors are trans-membrane and therefore possess a ligand binding domain extending into the luminal region. This also includes an intra-cellular cytoplasmic domain shown to have kinase activity. The VEGF receptors appear to be found in clusters or within lipid rafts on the cell surface as opposed to even distribution throughout the cell surface (Gabhann and Popel, 2008). Co-factors or HSPGs are the main cell surface structures binding and immobilizing cytokines, having complimentary binding sites capable of contact with the extra-cellular domains of relevant RTKs to induce signaling. Briefly, there are four main regions or domains that describe the physical structure of the VEGF receptors, of which there are three isoforms belonging to this RTK receptor family, the VEGFR1, VEGFR2 and the VEGFR3 (Bahram and Claesson-Welsh, 2010). Each receptor possesses multiple tyrosine residues located within the cytoplasmic-cellular domain and are predisposed to auto and trans-phosphorylation. It becomes much more complex considering the variations in the types of ligands that can bind these receptors, affecting different sub-sets of tyrosine residues, and differing cellular responses (Gabhann and Popel, 2008).

The basic map of the VEGF receptor and individual domains includes an N-terminus extra-cellular ligand binding domain as the site of interaction with specific ligands. Following this is the trans-membrane, including the juxta-membrane domain and the complex region recognized for intracellular signaling segmented into RTK domains, then terminates with the C-terminal tail. The RTK and C-terminal tail are predisposed to undergo phosphorylation at their residing tyrosine residues. Phosphorylation can be either auto or a *trans* induced event. Auto-phosphorylation is a result of ligand interaction that induces dimerization between two VEGFR monomers within the extra-cellular domains, this results in the phosphorylation of the tyrosine residues in the cytoplasmic domains (Bahram and Claesson-Welsh, 2010).

#### **1.4.2 VEGFR2 receptor tyrosine kinase**

VEGFR2 in the mature state is a glycosylated 230 KDa protein, a semi-glycosylated intermediate of 200 KDa, and the immature non-glycosylated form at 150 KDa having 1356 amino acids and a pI 5.6 (Genbank, Accession number NP 002244). The VEGFR2 extracellular domain possesses seven immunoglobulin (Ig) like sub-domains, similar to VEGFR1 and VEGFR3. The ligand binding domain interacts with available cytokines, the most relevant for angiogenesis is the VEGF-A. Binding takes place at the 2<sup>nd</sup> and 3<sup>rd</sup> Ig-like sub-domains, as is found for VEGFR1, however specific at the 2<sup>nd</sup> Ig-like domain. The fourth to the seventh Ig-like domains are the contact points of dimerization that follows upon the binding of VEGF-A (Wiesmann *et al.*, 1997). Dimerization at the 4<sup>th</sup> Ig domain is required for auto-phosphorylation within the VEGFR2 cytoplasmic domain (Koch *et al.*, 2011). The trans-membrane domain acts

as an anchor for support in the membrane and provides a scaffold for proper receptor orientation in the extra-cellular domain for binding to the target ligand (Shibuya M, 2006).

The region responsible for signaling within the cytoplasm, the Cytoplasmic Domain, or the Tyrosine Kinase Domain, is divided into two sub-domains consisting of roughly a 70 residue stretch referred to as Kinase Insert Sequence. The C-terminal domain is referred to as the Carboxyl Terminal Tail, whose role has to be specific in the intracellular region. Perhaps structural, although recent evidence has shown this domain to be involved in tyrosine phosphorylation and subsequent signaling inducing migration, proliferation and tube formation (Shibuya M, 2006).

#### **1.4.3 Biology of VEGFR2 phosphorylation and signaling pathways**

VEGFR2 ligand stimulation results in Tyrosine auto-phosphorylation affecting the residues identified as Tyr<sup>951</sup>, Tyr<sup>1054</sup>, Tyr<sup>1059</sup>, Tyr<sup>1175</sup> and Tyr<sup>1214</sup>. The phosphorylation of Tyr<sup>1175</sup> seems to have the most dramatic biological outcome. When Tyr<sup>1175</sup> is activated,  $\gamma$ -phospholipase (PLC $\gamma$ ) in turn is activated and this induces cellular migration, proliferation and angiogenesis. Phosphorylation of Tyr<sup>951</sup> seems to have only a single role, that of migration. The downstream activated sequence of events involves protein kinase C (PKC $\beta$ ) and in turn affecting c-Raf-MEK and MAPK pathways, thus augmenting survivability. Not much is known about VEGFR2 regulation but its expression is augmented by inflammatory signals, shear stress and this includes enhanced transcriptional expression by its own ligand VEGF-A. Other areas deemed to demonstrate augmented VEGFR2 expression occur during branching angiogenesis and angiogenic sprouting (Mellberg *et al.*, 2009). Physical factors affecting VEGFR2 levels were

shown are linked to exercise, but attenuation of VEGFR2 can occur through VEGF-A when linked to DII4-Notch signaling, a link to vascular regulation (Gabhann and Popel, 2008).

Transcriptional factor regulation of the VEGFR2 has yet to be published, so information in this area is limited (Gabhann and Popel, 2008). Finally, Tyrosine phosphorylation is cleared by the internalization of the VEGFR2, and from what is known, the clathrin-pathways are involved (Hoeben *et al.*, 2004; Holderfield and Hughes, 2008).

#### **1.4.4 Modification of VEGFR2 signaling**

VEGFR2 is important for physiological vascular development, but is also a requirement for pathological angiogenesis. Since VEGFR2 is essential for pathological angiogenesis, it is a target for therapeutic attempts at disrupting dependent pathways (Kim *et al.*, 2007). Section 1.4.3 presented some of the known pathways, thus small molecule inhibitors have been developed targeting the VEGFR2 signaling pathways, as examples are BAY43-9006, PTK 787/ZK222584, AZD6474, SU11248 and KRN951 (Shibuya M, 2006). BAY43-9006 has been given FDA approval targeting renal cancer by blocking VEGFR2 signaling (Shibuya M, 2006).

Pharmacological inhibitors have other uses, one being a means to unravel and map the VEGFR2 signaling pathways. For example M475271 blocks p38 through the kinase insert domain of VEGFR2. Small molecule inhibitors such as PD98059 have shown not to block migration however it specifically interferes with proliferation. M475271 disrupts both VEGF-A induced migration and proliferation (Ali *et al.*, 2005). *In vivo* M475271 specifically disrupts the Src kinase activity and tumor development, hence disrupting pathological angiogenesis. In HUVECs pathways affected are Src-ERK1/2 and p38, however Akt is unaffected and hence the affects seem to be specific for pathological angiogenesis (Ali *et al.*, 2005; Gabhann and Popel, 2008).

### **1.4.5 The biological effects of VEGFR2**

Late-outgrowth EPCs stimulated with VEGF-A can be affected differently depending on the level of expression of the VEGFR2 (Smadja *et al.*, 2007; Smadja *et al.*, 2008; Smadja *et al.*, 2009). Colony expansion at three weeks from point of seeding responds to VEGF-A with extensive proliferation. Interestingly, levels of expression of the VEGFR2 on the cell surface is quite low compared to the levels observed after 5 weeks of expansion, and demonstrate reduced proliferative activity (Smadja *et al.*, 2007). Integrins have been found to be essential such as the  $\alpha_6$  integrin. VEGFR2 is influenced by the  $\alpha_6$  integrin, pseudo-tube formation without  $\alpha_6$  integrin is prevented and proliferation becomes predominant. Therefore integrins play a role in angiogenesis, worthy of further investigation (Smadja *et al.*, 2007). Obesity and related issues show that VEGFR2 undergoes an increase in expression as adipose cells accumulate lipid. Obesity augmentation is dependent on and correlates with angiogenesis perhaps hypoxia is playing a role similar to expanding tumor tissue (Tam *et al.*, 2009; Rophael *et al.*, 2007; Lee *et al.*, 2009).

### **1.5 Research objectives**

This project is designed to develop technologies that might support development of sustainable vascular grafts to provide a therapeutic platform, and supplement potential bio-artificial organs or compromised tissue with needed cytokines and signalling context. Comparative models could come from analysis of transplant organs and the ensuing vascular developments. To date, there has been limited success with regards to long-term stability of *in*

*vivo* induced vascular networks including *in vitro* sources for transplants (Mertsching *et al.*, 2009). This project will address a component of these shortcomings on the assumption that guided angiogenesis, utilizing a platform presenting immobilized cytokine patterns, can set the stage for long-term engraftment or at least lead to a better understanding. Example applications might include de-cellularized matrix as outlined by Ott *et al.*, 2008, which utilized an entire rat heart, generating a potential natural platform for cellular re-seeding; however long-term viability still remains controversial (Ott *et al.*, 2008; Mertsching *et al.*, 2009).

Briefly, a first generation bio-active cytokine demonstrating angiogenic properties coupled with a means of immobilization will be constructed and isolated. Since VEGF120 has been modified in the past in the form of fusion constructs it is logical to proceed with a fusion construct of our own only utilizing CaM as the fusion partner. This protein is ideal for purification noting its hydrophobic properties and an irreversible binding capacity to certain short peptide segments. Upon obtaining the putative CaM-VEGF120 and knowing it can bind peptides in an irreversible fashion, it is logical then to proceed with the binding of the selected peptides to a solid substrate surface. For this function GNPs come to mind as they bind sulfur moieties in a covalent fashion. Therefore the decision to generate CBP capped GNPs predisposed for binding scaffolding complexes and the CaM-VEGF120 has been undertaken.

**It is hypothesized that;** an experimental immobilized bio-active cytokine can be produced, and with a suitable scaffold these immobilized cytokines can be organized into set patterns, and through guided cellular development produce pseudo-tube complex structures. To date, stem cell therapy has not met with the intended success. For example, treating myocardial infarcts with attempts at long-term exogenous vascular maintenance remain elusive, although suppression of inflammatory symptoms has been observed (Smadja *et al.*, 2009). BOECs, and HUVECs

assuming they are the optimal choice for vasculature development, (still controversial) are going to be the cell lines utilized for this project. It is in the design of this model that allows for flexibility influenced from literature or experimental protocol to make changes as required, as our approach is to strategically incorporate with design angiogenic growth factors coupled with optimal cell types into a therapeutic cocktail. Upon optimization a therapeutic platform can begin to be considered for the large scale manufacture of solid-tissue grafts. Presentation of bio-active molecules via immobilization to type-1 collagen utilizing GNPs as an intermediary should demonstrate physiological developmental properties.

## Chapter II

### **The production, purification and biochemical characterization of the putative CaM-VEGF120 fusion construct**

#### **2.1 Summary**

The CaM-VEGF120 was chosen as the first generation collagen-binding bio-active cytokine fusion protein for this project. VEGF-A and its splice variants are the predominant cytokines inducing vasculogenic sprouting. CaM for the purposes of this project has a limited but essential role. CaM will fulfill two roles in this project, first as an anchor utilized for the immobilization of the construct discussed in the next section. The other features unique to CaM are its hydrophobic properties where HIC can be utilized for CaM-fusion purification. Phenyl sepharose is a form of hydrophobic chromatography. Separation is achieved exploiting the hydrophobic properties of CaM which is regulated by  $\text{Ca}^{2+}$  concentrations, making purification from bacterial lysate straight forward. The CaM-VEGF120 fusion construct is linked together via a protease recognition site consisting of 20 amino acids found in the inactive precursor of  $\text{TNF}\alpha$ , an inflammatory cytokine that is activated upon proteolytic cleavage. MMP-9 is one of the proteases capable of cleavage within the linker peptide. In this section the correct CaM-VEGF120 sequence of the clone was verified and protease cleavage was confirmed. Conformational characterization of the CaM-VEGF120 was performed utilizing SDS-PAGE, Mass Spectrometry and size exclusion chromatography.

## 2.2 Introduction

### 2.2.1 Characteristic description of the VEGF120

VEGF-A knockout is embryonic lethal in murine models even with the removal of one allele (Claesson-Welch L, 2008). However mice do grow to term if only one of the splice variants is expressed. As noted in the first chapter, different VEGF isoforms reportedly exhibit different biochemical properties. Compared to the other isoforms VEGF120 is smaller, slightly acidic and has no heparin binding properties therefore is freely diffusible (Yaun *et al.*, 2011). The inability of VEGF120 to bind HSPGs impacts its properties with respect to the auto-phosphorylation of the VEGFR2, especially with comparison to the VEGF165 (Zachary and Glick, 2001; Rusnati *et al.*, 2006). Therefore mice exclusively expressing only the VEGF (120/120) do survive to term however display a lagging vascularization problematic for developing tissues (Zelzer *et al.*, 2002; Holderfield and Hughes, 2008). Given the type of applications motivating this project, it is still unclear as to the type of vascular development that can result from an immobilized VEGF120, and whether this form will have the properties of the VEGF164. However several studies show that the expression of the VEGF188 at least relating to tumor activity is implicated with a high tumor micro-vascular density and metastasis, and implies poor prognoses. VEGF164 and the VEGF120 also induce vascular development, responding to tumor activity but are characteristically a micro-vascular network predisposed to eruption and hemorrhage and lack stability (Yaun *et al.*, 2011). As mentioned earlier except for VEGF120, bio-active VEGF-A isoforms have two disulfide bridges. VEGF-C possesses an additional cysteine in close proximity of the VHD and has an additional third disulfide bridge, so that three sulfur bonds are involved in stabilizing this homo-dimer (Keck *et al.* 1997). VEGF120 is the main soluble isoform setting the foundation for proof of principle imparting bio-active structural features that

can be referred to as the first generation fusion construct. The other isoforms to consider would be the VEGF164 and the VEGF188. As mentioned, the angiogenic profile generated from the individual VEGF120 produces long thin vessels that have a propensity to vascular wall leakiness, that lack branching (Zygalaki *et al.*, 2008). However immobilization of VEGF120 may alter the biological effects, as noted there can be an effect on affinity up or down with regards to the modified properties towards the interaction with the VEGFR2 (Nillesen *et al.*, 2007; Zachary and Glikli, 2001).

### **2.2.2 Calmodulin and its properties involving the CaM-VEGF120 fusion construct**

Calmodulin the portion of the fusion construct used for one of the purification steps utilizing HIC to isolate the fusion construct from the bacterial cell lysate. CaM binding to its target peptide is specific with very high affinity due to interaction utilizing hydrophobicity and electrostatic interactions (Gifford *et al.*, 2007). The hydrophobic properties of the CaM fusion construct can be used to interact with a phenyl sepharose column (O'Neil and DeGrado, 1990).

CaM is involved with intra-cellular signaling that in many cases is calcium dependent. CaM has 148 residues and can bind specifically 4 calcium ions. Upon binding calcium CaM undergoes conformational changes and has strong interactive properties with a very wide range of proteins, some examples are kinases, NAD kinases, phosphor-diesterase, calcium pumps and motility proteins (O'Neil and DeGrado, 1990; Andruss *et al.*, 2004). CaM binds with very high affinity to its target substrate usually a 20 amino acid peptide or parts of the protein as is true for the peptide in this project; MRPRRREIRF RVLVRVFFFA SMLMRNNLAC derived from the iNOS protein. Other examples of peptide binding are calcium dependent events having a basic

amphiphilic  $\alpha$ -helical feature independent of a precise amino acid sequence. The dissociation constant for this interaction is in the range of high picomolar to low nanomolar values (O'Neil and DeGrado, 1990).

A) *TTTTGTTTAACTTTAAGAAGGAGANATACN* **ATG** GCT GAC CNA CTG ACT GAA GAG CAG ATC GCA GAA TTC AAA GAA GCT TTC TCC CTA TTT GAC AAG GAC GGG GAT GGG ACA ATA ACA ACC AAG GAG CTG GGG ACG GTG ATG CGG TCT CTG GGG CAG AAC CCC ACA GAA GCA GAG CTG CAG GAC ATG ATC AAT GAA GTA GAT GCC GAC GGT AAT GGC ACA ATC GAC TTC CCT GAA TTC CTG ACA ATG ATG GCA AGA AAA ATG AAA GAC ACA GAC AGT GAA GAA GAA ATT AGA GAA GCG TTC CGT GTG TTT GAT AAG GAT GGC AAT GGC TAC ATC AGT GCA GCA GAG CTT CGC CAC GTG ATG ACA AAC CTT GGA GAG AAG TTA ACA GAT GAA GAG GTT GAT GAA ATG ATC AGG GAA GCA GAC ATC GAT GGG GAT GGT CAG GTA AAC TAC GAA GAG TTT GTA CAA ATG ATG ACA GCG AAG **GAC GTC AGG CCT AGC CCG CTA GCG CAG GCG GTG CGT AGC AGC AGC CGT AGG CCT CAA TTG** GCA CCC ACG ACA GAA GGA GAG CAG AAG TCC CAT GAA GTG ATC AAG TTC ATG GAT GTC TAC CAG CGA AGC TAC TGC CGT CCG ATT GAG ACC CTG GTG GAC ATC TTC CAG GAG TAC CCC GAC GAG ATA GAG TAC ATC TTC AAG CCG TCC TGT GTG CCG CTG ATG CGC TGT GCA GGC TGC TGT AAC GAT GAA GCC CTG GAG TGC GTG CCC ACG TCA GAG AGC AAC ATC ACC ATG CAG ATC ATG CGG ATC AAA CCT CAC CAA AGC CAG CAC ATA GGA GAG ATG AGC TTC CTA CAG CAC AGC AGA TGT GAA TGC AGA CCA AAG AAA GAG AGA ACA AAG CCA GAA AAA TGT GAC AAG CCA AGG CGG ***TGA GGA TCC GGC TGC TAA CAA AGC CCG AAA GGA AGC***

B) MADQLTEEQ IAEFKEAFS LFDKDGDT ITTKELGTV MRSLGQNPT EAELQDMIN EVDADGNGT IDPPEFLTM MARKMKD TD S EEEIREAF RVFDKDGNG YISAAELRH VMTNLGEKL TDEEVD EMI READIDGDG QVNYEEFVQ MMTAK-**DVRP SPLA..QAVRS SSRRPQL**-APTTEGEQK SHEVIKFMD VYQRSYCRP IETLV DIFQ EYPDEIEYI FKPSCVPLM RCAGCNDE ALECVPTSE SNITMQIMR IKPHQSQHI GEMSFLQHS RCECRPKKD RTKPEKCDK PRR

**Figure 2.1 - Nucleic acid and amino acid sequence describing the CaM-VEGF120.** A) The cDNA sequence for the putative CaM-VEGF120 in relation to this project, outlining the various regions, in bold is the ATG the methionine N-terminus. The C-terminus in italicized bold is the stop codon TGA and in-between is the putative CaM-VEGF120 cDNA sequence matching published data with regards to the CaM and mVEGF120. B) The N-terminus is the CaM peptide, protease linker is in bold and downstream of the linker is the VEGF120. An IP of 4.68 implies a highly soluble acidic protein, with an estimated extinction coefficient of 9440 for the monomer, calculated by the software ExPASy a ProtParam tool. Noting no Tryptophans are present in the sequence thus implies a 10% error at best associated with the calculated deduction of  $\epsilon$ . The Cystiene residues in underlined bold form the disulfide bridges. Within the linker region the italicized *A..Q* is the potential putative MMP-9 cleavage site.

### **2.2.3 Properties of the CaM-VEGF120 fusion construct feed-back system**

Upon translation of CaM the N-terminal methionine is cleaved as expected, this is what is assumed to happen to the CaM-VEGF120 producing a putative total of 288 amino acids or double this amount for the formation of the active anti-parallel dimer shown in figure 1.2.

A unique feature included into the design of the CaM-VEGF120 is a linker region joining the fusion construct being a peptide sequence copied from the TACE cleavage recognition site belonging to the 26 kDa precursor TNF $\alpha$ . Upon cleavage a 17 kDa active soluble form is produced. The TACE cleavage site is also recognized by the MMPs however with reduced efficiency (Mohan *et al.*, 2002). It is well known that cellular stimulation of the VEGFR2 results in an augmented production of the MMPs. This separates the bound CaM from the bio-active cytokine separating the VEGF120-VEGFR2 ligand-complex during internalization. A form of feedback intended to minimize up-take of any of the solid surface components used to immobilize the fusion construct (Gabhann and Popel, 2008).

### **2.2.4 Potential properties of the CaM-VEGF fusion construct**

CaM binds many peptides sequences and this implies alterations in how this fusion construct may behave. For example, in its soluble form CaM could bind unknown cell surface structures if placed *in vitro*, perhaps determined by utilizing a fluorescent label. Unknowns to be considered by the reader, the immobilized fusion construct may affect receptor activation differently than the soluble VEGF120 (Helm *et al.*, 2005). This may lead to an enhanced and prolonged level of activation of the VEGFR2 as internalization may face resistance. This is the first generation construct that upon expression and purification possesses putative bio-active properties intended

to induce auto-phosphorylation of the VEGFR2 Tyr<sup>1175</sup>; keeping in mind this is a new molecule that will require characterization. Since VEGFR2 interaction with the VEGF120 ligands takes place within the central region of the VEGF120 molecule, steric interference from the CaM portion should not be an issue. The N-terminus of the VEGF120 is a rigid  $\alpha$ -helix that points away from the molecule therefore one would assume the CaM portion should also be pointed away from the receptor binding region (Muller *et al.*, 1997).

### **2.2.5 Chapter II objective**

The objective for this phase of the project is an introduction to the CaM-VEGF120 and the individual components. Included is an outline describing the subcloning into a suitable vector and modification of the CaM-VEGF120 DNA fragment for optimal bio-activity. This is followed by purification of a fully functional bio-active CaM-VEGF120 fusion construct. The main techniques to be presented are SDS-PAGE, Mass Spectrometry, HIC and size exclusion chromatography intended for characterization and purification. Verification at the genetic and biochemical level will be used prior to initiation of cell culture studies.

## **2.3 Methodology**

### **2.3.1 Preparation and characterization of the pET-15b CaM-VEGF120 expression vector**

#### **2.3.1.1 Excision of the fusion construct fragment CaM-VEGF120 from pET-9b, 315 residues or 945 bases**

The expression vector pET-15b (EMD chemicals, Gibbstown NJ) has been obtained to incorporate the complete bio-active cassette CaM-VEGF120 of 867bp. The full length inactive CaM-VEGF120 clone was extracted by RT digest from pET-9d utilizing the RT enzymes BamHI and NcoI. The insert DNA fragment from pET-9d (kan<sup>r</sup>) originally constructed by Val Taiakina from Dr. G Guillemettes lab required transfer to pET-15b as bacterial strain Origami 2 (DE3) is a kan<sup>r</sup> strain, but amp<sup>s</sup>, as pET-15b offers the amp<sup>r</sup> properties.

#### **2.3.1.2 pET-15b CaM-VEGF120 subcloning, amplification and purification**

Upon double digest and gel extraction of the vector pET-15b and the CaM-VEGF120 DNA fragment, ligation was carried out with a mix of 1:3 vector template to insert (50 ng of pET-15b and CaM-VEGF120), ligase buffer (10 X stock) with 0.5 µl T4 DNA ligase (M0202T, NEB Ipswich, MA) for a final reaction volume of 20 µl with incubation at room temperature for 1 hour, followed by bacterial transfection. On the following day, 10 colonies were selected and screened by RT digest analysis (EcoR I, Bam HI and Mun I) selecting suitable clones by identifying the putative fragment CaM-VEGF120. Further modification was required to prepare bio-active sequence, by removing a DNA fragment representing the 26 residue leader sequence of VEGF120; MNFLLSWVHW TLALLLYLHH AKWSQA. The VEGF120 with leader sequence using MunI and BamHI was separated from the rest of the pET-15b CaM-VEGF120.

VEGF120 minus the leader sequence was cloned back into the linearized pET-15b CaM, thus completing the pET-15b CaM-VEGF120 bio-active subclone outlined in 2.3.1.2. PCR primer design; Forward, VEGF120F; TGTACCAA**CAA TTGGCACCC** ACGACAGAA GGAGAGCAG, and Reverse, VEGF120R; ACAAAA GTT**GGATCC** TCACCGCCT TGGCTTGTC, obtained from Sigma Genosystems, the six bases in bold are restriction sites, MunI and BamHI intended for proper subcloning orientation. Bacterial transfections, and growth selective conditions were performed as previously mentioned with confirmation by RT analysis and DNA sequencing (McMaster, Hamilton ON). Vector isolation and purification were carried out with the Qiagen DNA miniprep kit following the manufacturer's protocol. Vector concentration was derived at OD<sub>260</sub>, pET-15b (CaM-VEGF120).

### **2.3.1.3 PCR parameters for amplification and subcloning the VEGF120**

To ensure sequence accuracy of the amplified product, a good starting point is amount of template per 25 µl PCR reaction and initial PCR contents. Vent<sub>R</sub> polymerase (M0254S) from NEB is a suitable choice because it includes proof reading capacity. Starting template of 0.5 ng was used to obtain desired quantities with a minimum number of cycles. PCR conditions were as follows; 2 minutes at 94°C denaturing step, followed by 16 cycles to obtain suitable product with cyclic condition set at 30 sec 95°C, 30 sec 65°C primer annealing step and a 20 sec 72°C extension. Completion of the PCR required incubation at 72°C for two minutes for DNA end polishing, with cooling to 4°C until sample recovery. VEGF120 fragment minus the leader sequence was removed from a 1.5% agarose gel followed with a second round of PCR using the

same conditions to obtain sufficient DNA. A purified fragment 372 bp subject to restriction end digest was cloned back into pET-15b complete with the CaM and protease linker portion.

### **2.3.2 CaM-VEGF120 protein translation utilizing pET-15b**

#### **2.3.2.1 CaM-VEGF120 production and purification**

The next procedure was to manufacture and purify a soluble bio-active CaM-VEGF120, a 66 kDa protein. The initial bacterial cell line used was the BL21 (DE3) *E. coli*, but was not suitable as the product demonstrated no evidence of dimer formation.

From the literature, an option appeared to be a bacterial *E. coli* Origami 2 strain AD494 (DE3) (Novagen Madison WI), which possesses a deficiency in the Thioredoxin system, creating an environment favoring disulfide bond formation. The AD494 *E. coli* bacterial cell line was chosen and following manufacturers recommendations utilizing 50 µg/ml ampicillin selective conditions, concluding with the preparation of cryopreservation stocks. SDS-PAGE was used to confirm appropriately sized product is abundantly expressed.

#### **2.3.2.2 Protein production and purification; CaM-VEGF120 translation and amplification**

A seed culture was prepared for overnight growth from a previously prepared frozen stock of the transfected CaM-VEGF120 *E. coli* AD494 strain inoculating 50 ml LB medium supplemented with ampicillin. 10 ml of the seed culture was used to inoculate a batch culture of 1 liter of LB medium per 4 liter Erlenmeyer flask; four flasks were grown. The four flasks were incubated at 37°C with a rotational motion at 200 rpm, until turbidity reached 0.9 at OD<sub>600nm</sub>.

The culture temperature was reduced to 23°C thus slowing bacterial proliferation to enhance accumulation of CaM-VEGF120 per bacterial cell induced with the addition of 0.1 mM IPTG. Rotational incubation was continued for an additional six hours following collection of bacterial paste and storage at -80°C until required for processing.

### **2.3.2.3 Bacterial cell lysis and construct separation**

The bacterial paste was resuspended on ice in lysis buffer (50 mM HEPES pH 7.5, 100 mM KCl and 1 mM EDTA) and brought to a final volume of 50 ml supplemented with protease inhibitors; one complex tablet per 50ml (04693132001, Roche Diagnostics, Indianapolis IN). Cell lysis was carried out by sonication utilizing 5 pulses for 10 seconds each aided by the addition of lysozyme to release the cellular contents. Insoluble cell lysate was removed by centrifugation at 20,000 rpm at 4°C, retaining the insoluble fraction for SDS-page analysis.

### **2.3.2.4 Phenyl Sepharose CaM-VEGF120 separation from cell lysate**

PS is used to separate CaM-VEGF120 from soluble cellular contents by means of hydrophobic interactions mediated by the CaM portion of the fusion construct. The required solutions are prepared with 50 mM HEPES buffer pH 7.5 holding the temperature at 4°C throughout the entire procedure. The storage solution 20% EtOH has to be flushed from the column, draining the column to just above the meniscus, washed with 50 ml of ddH<sub>2</sub>O followed by the addition of 100 ml of equilibration buffer (50 mM HEPES, 1 mM CaCl<sub>2</sub> and 1 mM DTT). Noting all fractions including wash buffers were retained for analysis to determine the fraction of

the product. Following equilibration the 50 ml solution of bacterial lysate was added to the column collecting the supernatants followed by two washes each of 100 mls utilizing high salt buffers (50 mM HEPES pH 7.5, 1 mM CaCl<sub>2</sub> and 0.5 M NaCl<sub>2</sub>). The final phase of the procedure was the application of the elution buffer C low salt (10 mM HEPES pH 7.5, 10 mM EDTA) with collection of 2 ml fractions, all collected solutions were imaged using coomassie blue stained 12% SDS-PAGE gels. From gel analysis the size of the product anticipated would be expected in the elution fractions, ideally the most abundant of the bands visible. Fractions containing at least 3 mg/ml were collected; pooled and concentrated 10 fold in preparation for size exclusion chromatography.

### **2.3.3 SDS-PAGE reducing gel protein analysis**

Analytical runs of SDS-PAGE gels of 12% acrylamide, optimal for proteins in the size range of 20 to 60 KDa, were used. Sample preparation were carried out with 4 X sample loading buffer (0.3 g Tris pH 6.8, 0.4 g SDS, 1.0 mg bromophenol blue, 4.0 ml glycerol, 0.2 ml 2-β-mercaptoethanol to 10 ml with ddH<sub>2</sub>O). A low molecular weight protein marker was included for every run ranging in size of 14-97 KDa (GE Healthcare). Upon completion gels were stained with coomassie blue to visualize the protein bands. Silver staining was used if increased sensitivity was required to reveal trace amounts of protein (10-100 ng), far below the sensitivity of the coomassie blue. This procedure was carried out as recommended by the manufacturer (Bio-Rad, 161-0443, Hercules CA) following coomasie blue staining. Upon completion of staining the gels were rinsed with ddH<sub>2</sub>O and placed in saran wrap for imaging.

## **2.3.4 CaM-VEGF120 preparation for bio-activity**

### **2.3.4.1 Sample preparation for utilization of gel column purification**

Samples from PS purification followed by a concentration step to obtain 10 to 35 mg/ml were ideal for further purification with the Superdex 75 gel column (10 x 30 cm). The Äkta purification system (Pharmacia, Uppsala Sweden) was used to maintain a flow rate of 0.5 to 0.8 ml/min and pressure below 1.8 kPa to prevent column damage.

Bio-Rad protein assay (Bradford Assay) was used for determination of protein concentration carried out following manufacturer's protocol (Bio-Rad, Richmond CA). Alternatively the extinction coefficient might be used, however there are no tryptophan's in the CaM-VEGF120, therefore the computational values provide only an estimate, as the best approximation would be a minimum error of 10% (Gill and von Hippel, 1989). Bradford Assay is reproducible and is more accurate when utilizing BSA standards. Absorbance was determined by Spectra Max Plus<sup>384</sup> (Molecular Devices, Sunnyvale CA).

### **2.3.4.2 Superdex 75 gel column purification**

Gel column purification was designed to optimize the purity of the sample preparation to remove remaining bacterial toxins. Volume size upon injection was 0.25 ml of the concentrated sample preparation and injected into 1ml sample loop passing the sample through a pre-packed Superdex 75 column (GE healthcare, Baie d'Urfe Quebec) maintaining a flow rate of 0.7 ml/min in equilibrated degassed buffer (25 mM HEPES pH 7.4, 150 mM NaCl and 1 mM EDTA pH 8), and collected in a series of 0.5 ml fractions. Sample recovery determined by UV detection was

displayed with peaks correlating with size and fraction number confirmed by SDS-PAGE, before proceeding to other methodologies for characterization. System calibration was carried out by the LMW protein standard 6500-75000 Da from GE-Healthcare.

## **2.3.5 Characterization**

### **2.3.5.1 Mass spectrometry**

Mass spectrometry is one means to verify the mass of the proteins presented in kDa allowing comparisons to theoretical values. Sample preparation requires a 100 mM sample in ddH<sub>2</sub>O as a desalting preparatory step is required (buffer and salt replaced with ddH<sub>2</sub>O) using the YM-30 Microcon mini-columns from Millipore.

### **2.3.5.2 Membrane separation of CaM-VEGF120 utilizing 50 kDa size exclusion spun column**

Spun columns utilized for protein concentration and buffer exchange can also be utilized in this case for product characterization. A column with a size exclusion limit of 50 kDa can be employed to demonstrate if a product over 60 kDa is prevented from passage (Amicon Ultra-.05, Millipore). A multi-subunit protein complex when intact should not pass through if it is larger than 50 kDa, however upon separation of into individual components passage should be possible. Therefore cleavage of the sulfur bonds disrupting the putative dimeric form of the CaM-VEGF120 should allow passage where as dimeric form should not. DTT sample loading buffer

and boiling of sample diluted to 400  $\mu$ l in ddH<sub>2</sub>O disrupts dimers. Staining the effluent with the Bradford Assay is a practical means to determine location of sample.

### **2.3.5.3 CaM-VEGF120 MMP-9 Digest**

Using 0.1  $\mu$ g of activated MMP-9 (activated MMP-9 prepared with p-amino-phenylmercuric acetate 1 mM, incubation at 37°C for 24 hr) was added to 100  $\mu$ l of substrate the CaM-VEGF120 fusion construct at 5  $\mu$ g/ml in MMP-9 digest buffer (50 mM Tris-HCl pH 7.5, 10 mM CaCl<sub>2</sub>, 150 mM NaCl and 0.05% nonionic surfactant Brij 35) with incubation at 37°C for a maximum of two to four days sufficient for near completion of digest. MMP-9 digest of the CaM-VEGF120 fusion construct in theory should generate a double band separated within the linker region. Following the digest reaction SDS-page gel analysis was performed and confirmed by mass spectrometry.

### **2.3.6 Modification of CaM-VEGF120**

#### **2.3.6.1 FITC labeling of CaM-VEGF120 required for isotherm and tissue culture**

CaM-VEGF120 was covalently linked to fluorescent tags according to manufactures protocols noting a few modifications (Molecular Probes, Eugene OR). Purity of protein sample is important as determined by SDS-page analysis collected from Superdex 75 gel column purification. The preparation to be labeled can assumed to be quite pure if the experimental band of reasonable amounts is visible compared to only trace amounts of any unidentified bands

present. Protein concentration is required as to adjust the ratio of the labeling reagent, the FITC reactive dye, to the target protein.

Upon completion, the unreacted FITC is separated from protein bound FITC using spin columns with the protocol supplied by manufacturer. The final part of the protocol requires the determination of the ratio of FITC label per protein; this requires a final sample concentration determination. Briefly the CaM-VEGF120 has a very high percent of lysine residues therefore highly reactive, to prevent over-labeling the reaction was reduced from one hour as recommended to 45 minutes and perhaps can be reduced further as the ideal label target is 2 fluorescent tags per molecule, Mass Spectrometry data determined the degree of FITC tag incorporation.

**Table 2.1 – FITC protein labeling.**

$$\mu\text{l dye stock solution} = \frac{\text{mg/ml substrate} \times .2\text{ml} \times 389 \times 100 \times \text{MR}}{\text{MW}_{\text{protein}}}$$

$$M = (A_{260} - (A_{494} \times .30)) \times \text{dilution factor} / \epsilon$$

$$\text{FITC per molecule} = A_{494} \times \text{dilution factor} / 68,000 \times \text{protein concentration}(M)$$

Protein solution or substrate vol., 0.20ml,

Reactive dye MW 389,

conversion factor 100

MR is the molar ratio dependent on the substrate concentration, an MR of 30 implies a substrate range of 4-10mg/ml

M= equation two determination of FITC labeled protein

## **2.4 Results**

### **2.4.1 Characterization of the DNA clone for CaM-VEGF120**

The construction of the putative clone for protein expression requires a suitable vector. The high copy expression vector pET-15b appeared to be optimal as it offers ampicillin selective capabilities to the transfected host AD494 (DE3) *E. coli* Amp<sup>s</sup>. Noting AD494 is Kan<sup>r</sup> ruling out the use of pET-9d the original vector as it only offers kanamycin resistance. The choice of vector also has to take into account the MCS dictating the type of RT enzymes suitable for the specific DNA fragment intended for cloning, as fragment orientation is one area of concern. Suitable RT enzymes for the putative CaM-VEGF120 are BamHI and NcoI, ideal for the full length fusion construct. Briefly a double digest was carried out with BamHI and NcoI to prevent vector self-ligation so that only colonies of bacteria able to grow in selective conditions are cultured. DNA sequence determination is the recommended protocol for absolute confirmation of the clone. Cloning of the CaM-VEGF120 into the pET-15b was confirmed by RT digest, producing the anticipated correct results of size and fragmentation data (image not shown) and sequencing data is absolute presented in Figure 2.1a.

### **2.4.2 CaM-VEGF120 translation, purification and analysis**

Prior to large scale purification of the putative CaM-VEGF120, a small aliquot was lysed with sample buffer; the insoluble was separated from the soluble fraction, and analyzed with SDS-PAGE. The CaM-VEGF120 was confirmed to be over whelming in the soluble bacterial fraction, results are presented in figure 2.2a.

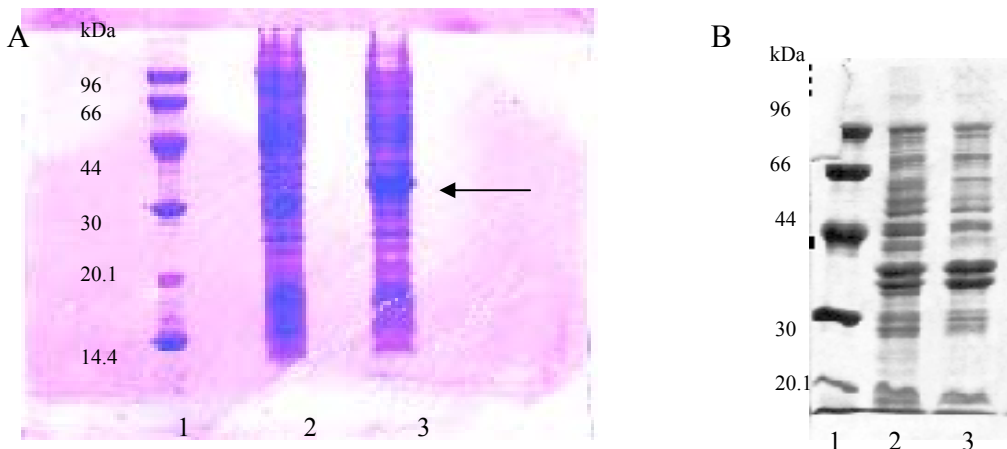


**Figure 2.2 - SDS-PAGE demonstrating presence of putative CaM-VEGF120 in crude bacterial lysate.** Image of 12% SDS-PAGE gels, initial phase of the project intended to highlight the putative CaM-VEGF120 translated in AD494 (*DE3*) *E. coli*. A) Lane 1, LMW; Lane 2, control sample vector only; lane 3 vector with fusion construct indicated by arrow corresponds to 33KDa product. B) Insoluble fraction of bacterial paste; lane 1, LMW marker; Lane 2 control vector only and Lane 3 putative CaM-VEGF120 clone, no detectable product.

4 grams of bacterial paste induced by IPTG produced approximately 100 mg of target protein. Using phenyl sepharose as seen in figure 2.3, large quantities of CaM-VEGF120 of right size was eluted and pooled for concentration (figure 2.4a). Following elution and isolation optimal samples were pooled and the resulting mass spectrometry data produced a monomer of exact size, with two concentrated sample fractions, A (35 mg/ml) and B (25 mg/ml) totaling 3-5 mls of CaM-VEGF120, presented in figure 2.4a.

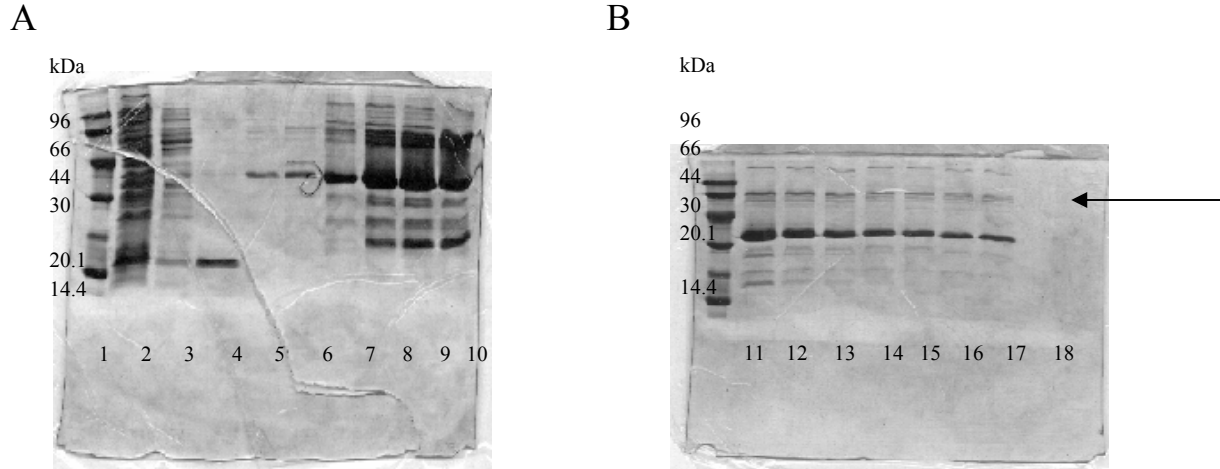


**Figure 2.3 - SDS-PAGE of CaM-VEGF120 fractions collected from Phenyl Sepharose chromatography.** CaM-VEGF120 indicated by arrow indicates putative monomer at 33 KDa. A) Lanes 1 LMW marker, 2 to 5 are controls; 2 elute from lysis buffer, lanes 3 and 4 wash steps and lane 5 is first fraction collected after addition of elution buffer; Fraction 1-5 (lanes 7-10) collected and pooled into group A. B) Lane 1 LMW, 6-12 fractions lanes 12-17, these fractions were pooled into group B. Sample fractions A and B are intended for purification utilizing size exclusion chromatography, see figure 2.5.

A final purification step was recommended with the results presented in figure 2.4b. SDS-PAGE shown in figure 2.4a demonstrates abundant impurities from the original bacterial lysate, for example LPS. Purification using the Äkta pump system and Superdex 75 gel column yielded sufficiently pure CaM-VEGF120 for various analytical and experimental purposes such as mass spectrometry, MMP-9 digest analysis, and (FITC) CaM-VEGF120 labeling. Sufficient amounts of labeled construct (70 mgs) for tissue culture experimentations and were collected from size exclusion chromatography, presented in figure 2.4b.

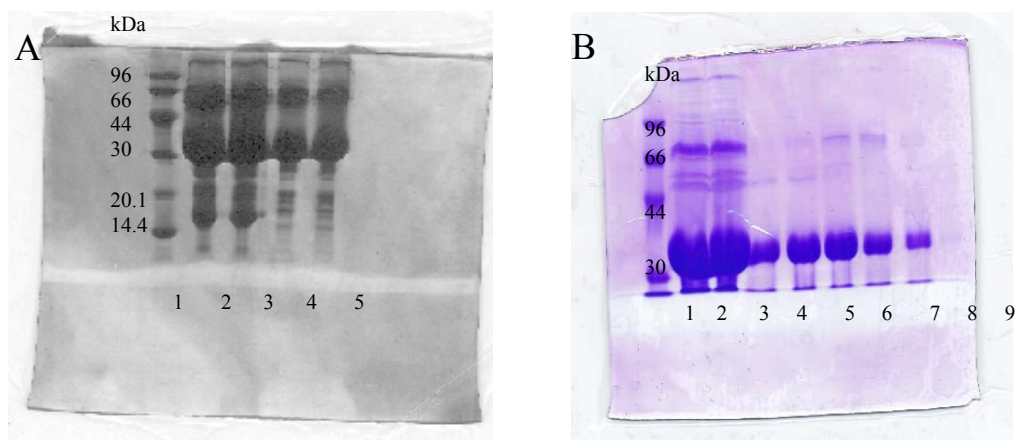


**Figure 2.4 - Superdex 75 purification profile analyzed by SDS-PAGE, image depicting the putative CaM-VEGF120 on SDS-PAGE.** A) CaM-VEGF120 concentrated following phenyl sepharose pooled fractions A and B, see figure 2.4a. Lanes 2 and 3 represent an approximate concentration, fraction A at 35 mg/ml and fraction B lanes 4 and 5 at 25 mg/ml. B) Superdex 75 gel column purification of samples from 2.4a. Lanes; 1, LMW marker; 2 and 3 samples prior to injection as in 2.4a; lanes 4 to 9 are collected fractions, lanes 5 and 6 were pooled obtaining a final concentration of 6.14 mg/ml.

The results for this section are straight forward. Evidence to confirm the proper protein sequence was acquired through mass spectrometry to confirm monomer size. The demands of bio-activity require this molecule to be in an anti-parallel homo-dimeric form. Sample collection from size exclusion chromatography separates based on size and places the CaM-VEGF120 within the expected dimer range of 60-70 kDa, the anticipated result (data not shown). Further confirmation was established using a spin column that prevents the passage of protein over 50 kDa. The intact construct should not pass through in native conditions, however when treated with DTT sample buffer, the dimeric CaM-VEGF120 upon boiling is 33KDa. Passage was confirmed by Bradford assay, therefore suggestive of disulfide bridge formation.

**Table 2.2 - Mass Spectrometry Data depicting the native CVFC and FITC labeled version in monomer form.** Utilizing Mass Spectrometry with comparison to theoretical ExPasy calculation. A) Full length monomer forms of CVFC, B) size determination of the monomer form of CaM-VEGF120 following MMP-9 digestion and C) FITC labeled CVFC size variations.

---

A) Full length CaM-VEGF120

32955 kDa (Mass Spectrometry)

32962 kDa (ExPasy software data)

B) CaM-VEGF120 following MMP-9 digest

17542 Da, deduced by Mass Spectrometry

17542 Da, calculated by the ExPasy software data

C) FITC (MW 389 per FITC) labeled CaM-VEGF120

35289 Da, deduced by Mass Spectrometry, a value with 6 added FITC tags

34122 Da, deduced by Mass Spectrometry, averaging 3 added tags

### **2.4.3 Final conformational experiments confirming CaM-VEGF120 properties**

The fractions collected following size exclusion chromatography suggest at the very least the monomer was recovered as noted by SDS-page and Mass Spectrometry, data presented in table 2.2 and figure 2.5. MMP-9 digestion using 1-2 µg of protein did in fact produce a cleaved fragment targeting the putative protease linker site separating the CaM from the VEGF120. Although there were some unexpected results, mass spectrometry demonstrates the CaM portion was recovered and produced an exact size of 17 kDa at the anticipated cleavage site, figure 2.1b. As it appears the VEGF portion must have been further degraded as no obvious identifiable fragment was obtained.

However, data suggests the protease site is functional as MMP-9 cleaves the putative CaM-VEGF120 presented in figure 2.5, and mass spectrometry confirms that the correct protein sequence has been obtained as the full length size is exactly as predicted (table 2.2), as is the putative remaining CaM fraction. Finally, FITC labeling of the CaM-VEGF120 confirmed by mass spectrometry shows the initial preparation having an average 6-7 labels, probably in excess as is very bright even to naked eye, other batches were prepared with much less intensity obtaining between 2-4 labels per molecule as anticipated, a shorter incubation time was run producing 1 ml of 6 mg/ml, sufficient for foreseeable experiments.

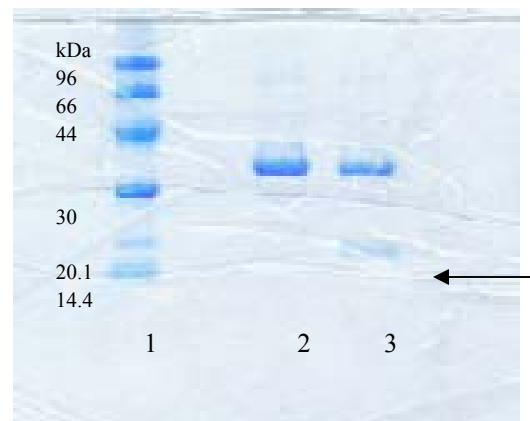


**Figure 2.5 - MMP-9 digest of CaM-VEGF120.** SDS-page image of the cleaved band seen at 17kDa indicated by the arrow compared to lane one control. Lane 3 shows two bands one at 33 kDa, remaining intact and a smaller at 17 kDa the MMP-9 cleaved product.

## 2.5 Discussion

### 2.5.1 Cloning of the CaM-VEGF120 DNA fragment

This chapter describes the creation of a suitable clone with the correct sequence to translate the product into a proper bio-active anti-parallel homodimeric molecule. The very first phase of this project was to construct an adequate sub-clone for protein expression within a suitable vector. The proper choice of bacteria host for protein expression and purification had to be determined. *E. coli* strain AD494 (DE3) was a suitable choice as this host favors disulfide bond formation due to lack of Thioredoxin. Double digestion for both the vector and fragment were recommended as self-ligation is prevented. Following transfection, bacterial colonies were screened for the putative CaM-VEGF120 insert. DNA sequencing confirmed the correct clone as presented in figure 2.1a, noting full-length translated intact CaM-VEGF120, the intended peptide at the very least in monomer form can be obtained. Thus, CaM-VEGF120 fusion construct clone was confirmed at the DNA level by sequencing supported by RT digest.

### **2.5.2 Supporting evidence for the CaM-VEGF120 properties**

Bacteria growth in batch culture with an optimized protocol for expression was determined for a small aliquot shown in figure 2.2a, and then scaled up to 4 L for CaM-VEGF120 purification. SDS-PAGE analysis suggested the product of interest was well expressed and yielded a protein product of 33 kDa as expected. The system has worked for the production and isolation of the monomer and possibly the dimer, fully intact as confirmed by Mass Spectrometry presented in Table 2.2. Large amounts of bacterial paste expressing the construct CaM-VEGF120 can easily be obtained and suitable quantities can be recovered in bio-active form. For example the percentage of dimeric CaM-VEGF120 produced per bacteria is not known; but it seems to be near 100% as determined by size exclusion chromatography. If only 25-50% was in

dimeric form perhaps the amount bacteria could easily be expanded, as sample collection is by size fractionation (Kim *et al.*, 2007). This implies optimized conditions for a functional bio-active protein that can first be purified using HIC and second utilizing the N-terminal CaM portion of CaM-VEGF120 to bind the intended target peptide. The main focus of this section is on preparation of conditions to generate the CaM-VEGF120 to be recovered as an anti-parallel intact homodimer in its full pure form. Quantity is also important, requiring enough for analysis, FITC modification and extended experimental purposes outlined in the next couple of chapters. SDS-PAGE suggest the fragment is correct as presented in Figure 2.4, and further supporting evidence suggesting the CaM-VEGF120 was in dimeric form noting an inability to pass through a 50 KDa cut off spin column confirmed using a Bradford assay. Most importantly, is the data from the purification profile collected from the Äkta gel column purification system, the collected fraction was in the size range of 60-70 KDa, further evidence disulfide bond formation took place and the CaM-VEGF120 must have bio-active properties. If one was to look closely at the gels in figure 2.4b there is slight contamination remaining at the 66 kDa size marker, keeping in mind this is a reducing gel and any contamination would be the same size as the product eluting from the Superdex 75 gel column. Purification is size dependent therefore if the size of the dimer is 66 kDa the contaminating product at 66 kDa cannot be separated by size exclusion.

### **2.5.2.1 Construct description with conformation**

The CaM-VEGF120 now complete, the N-terminus is the CaM portion and the C-terminus is comprised of the VEGF120 with the putative characteristic bio-active anti-parallel homo-dimer of 66 kDa or 566 amino acids. It is not likely the CaM portion folds back onto the VEGF120 as an  $\alpha$ -helix at the N-terminus of the VEGF are known for their rigidity, suggesting the CaM is pointed away from the VEGFR2 interactive domain of the VEGF-A, thus the CaM-VEGF120 is probably not any different in its activation of the VEGFR2 as the native VEGF120, of course excluding potential added properties of the CaM. Alternatively how would the VEGF120 influence the properties of CaM interactive behavior, noting purification and separation from the bacterial lysate was successful, protein separation is CaM dependent therefore the influence of the VEGF120 perhaps is minimal.

#### **2.5.2.2 CaM-VEGF120 modification**

The final protocols before continuing to the next sections require completion, fluorescent tag modification that is intended to covalently link FITC tags to the CaM-VEGF120 assuming two tags per fusion construct would be ideal and still result in a relatively intense signal leaving intact bio-activity minimizing interference. FITC was the label of choice as there seems to be cellular uptake issues with TRITC, an observation made by others, noting the TRITC-CaM label was internalized by the same cell, it is speculation but a potential source for error. Since isotherms and cellular imaging are required for various experimentation, an amount of 5mg/ml of (FITC) CaM-VEGF120 labeled product was produced and probably sufficient for all required procedures.

## Chapter III

### **Properties of the gold nanoparticles, CaM binding peptide and the numerical quantification of the CaM-VEGF120 per gold nanoparticle**

#### **3.1 Summary**

Gold nanoparticles (GNPs) are the intermediary to immobilize the CaM-VEGF120 to a solid or insoluble matrix allowing presentation of immobilized bio-active cytokines to cellular membrane receptors. The CaM-VEGF120 can specifically bind short peptide sequences comprised of a mixture of basic and hydrophobic residues. The CaM binding peptide chosen for this project is a 30 amino acid CBP that derives from a region in the iNOS protein recognized by CaM. GNPs can covalently bind sulfur moieties hence the importance of including a Cys residue within the peptides intended for GNP binding. To complete this section a collagen adhesive peptide has been obtained for the immobilization of the GNPs to the platform of choice, solidified type-1 collagen.

## 3.2 Introduction

### 3.2.1 The GNP complex and immobilization

GNPs due to their ease of preparation, stability and optical properties have been under intense investigation especially with regards to their biological compatibility (Krpetić *et al.*, 2009). The stability of GNPs is established through capping reagents that can bind gold (Lévy, 2006).

Peptides are one such capping agent, a sulfur possessing moiety is the only requirement, as this permits covalent binding to the GNP providing a protective coat to produce a capped GNP. Other examples of compounds that offer a capping protective coat are mercaptodextranes, thiolated PEG derivatives and thiol-based ligands (Krpetić *et al.*, 2009; Majzik *et al.*, 2009).

The most common means of producing GNPs are the protocols for citrate reactive GNPs, although not fully stable until the citrate coating is exchanged with cysteine capped peptides. Tri-sodium citrate GNPs generally can form in the 10-100 nm range and are highly reactive to sulfur groups, one being thiolated ligands or the Cys residue, as this implies biological applications (Gong and Ito, 2008; Lévy, 2006). The Cys side chain can bind citrate reactive GNPs due to the negative surface charge creating a very favorable chemistry to react with functional groups like thiols, amines, cyanide or diphenylphosphine (Krpetić *et al.*, 2009; Majzik *et al.*, 2009). Binding of thiols is optimal at neutral pH as in this project; however reactivity of GNPs for  $\alpha$ -amino groups is optimal at a lower pH (Majzik *et al.*, 2009). The binding reaction can be described as cleavage of the S-H bond that makes it possible for chemisorbed covalent bond formation on the gold surface, forming the S-Au covalent bond (Gong and Ito, 2008). Initially during the early developmental phase of GNPs, concentration and size were determined utilizing TEM and DLS. From these techniques comparative charts were constructed for UV and Visible spectra, having

specific absorbance properties to estimate particle size and concentration, as citrate coated GNPs have a unique size dependent extinction coefficient (Zhou *et al.*, 1994; Haiss *et al.*, 2007).

For cell culture the optimal size appears to be in the size range of 50-60 nm as it seems if they are too large, stability and solubility may become an issue. If they are too small difficulties might occur with regards to recovery when bound to soluble molecules. Noting reproducibility in GNP production is determined by the ratio of gold ions to sodium citrate, as the protocol for their manufacture is quite simple once established (Lévy, 2006). Tri-sodium citrate is the most common reducing agent however others are available such as ascorbic acid, 3-thiophene-malonic acid and PDDA, as PDDA is used to produce stable gold nanoparticles in the size range of 12 nm (Majzik *et al.*, 2009).

Metal nanoparticles, gold being the obvious, however silver is also an option as its optical properties invites interest from the biological sciences, this is due to their surface plasmon oscillations well within the visible spectrum. GNPs upon formation are colored which correlates with their size and reflects on the plasmon band (collective oscillation of electrons in the nanoparticle), as the surface area is sensitive to the refractive index (Lévy, 2006).

---

CaM-VEGF120; CaM outline n-terminus, protease site middle section  
and VEGF120 solid structure



**Figure 3.1 - Simplistic image of the CaM-VEGF120 complex.** This image is presented in the monomer form, consisting of 288 amino acids; it is much more complex as an anti-parallel dimer, its true form. Au indicates the GNP, showing a representative of the two peptide types the CBP and the CAP bound from the Cysteine capped terminus.

### 3.2.4 Chapter III objective

The properties of the GNPs allow binding to sulfur moieties; to enable the covalent binding of Cysteine capped peptides. Therefore CBP capped GNPs once established are recognized by the CaM-VEGF120 as a substrate. Having obtained the CaM-VEGF120, amounts of the CaM-VEGF120 per capped GNPs can be established, by means of an isotherm plot.

The final objective to be addressed in this chapter is how to immobilize this CaM-VEGF120 complex to a suitable structure intended for modified cytokines in any variable desired pattern presented to receptive cell types. The choice of scaffolding utilized is type-1 collagen that can bind collagen adhesion peptides complemented with a Cys amino acid.

### **3.3 Methods**

#### **3.3.1 Preparation of GNPs using the tri-sodium citrate reduction method**

GNPs were prepared by the Frens method modified for GNP production in preliminary experiments (Turkevich, 1985). A 125 ml Erlenmeyer flask with addition of 50 ml of 0.25 mM gold ions (precursor) is prepared. While stirring, the sample is boiled for 3 minutes and then 0.4 ml of 34 mM tri-sodium citrate (reducing and stabilizing agent) is added, continuing with boiling for 5 minutes, followed by removal of the heat source with continued stirring for ten minutes. This protocol is intended to produce 40-50 nm diameter GNPs, size confirmation was determined by UV/vis spectrophotometry (Majzik *et al.*, 2009). Each size variation has a characteristic peak in the visible spectrum. 50 nm particles have maximum absorbance at 534 nm. This procedure generates a product that should be stable for one month at 4°C, freezing is never recommended.

#### **3.3.2 Properties of the iNOS CBP and CAP**

The CBP peptide was chosen as it is recognized by CaM with a demonstrated high binding affinity independent of calcium having a  $K_d$  between 1-10 nM, forming a virtually irreversible reaction that can only be separated by strong detergents. This is a 30 residue peptide that includes a cysteine cap, in this case at the C-terminus. With a high percentage of hydrophobic residues this molecule is semi-soluble in water at or near neutral pH. To enhance solubility extra hydrophilic residues could be included at either terminus as these regions will not involve CaM binding. Concentration of CBP at 5 mg/ml was prepared re-suspending 8 mg's of the lyophilized peptide in 1.6 ml ddH<sub>2</sub>O having a MW of 3739 Da. At 5 mg/ml the CBP is only semi-soluble, but is the required condition to optimize binding to GNPs, acidic conditions would increase solubility noting a theoretical pI of 12.22; however acidic conditions are not favorable for sulfur

and gold binding as GNPs are optimally stable at pH 7.0 and sensitive to pH fluctuations. Obtaining optimized solubility the CBP solution was dispensed in 50  $\mu$ l aliquots for -80°C storage. The CBP concentration converting from grams using avocadro's constant represents 268 pmol per 1  $\mu$ g. The Sequence of the CBP is **MRPRRREIRF RVLVRVVF**FA SMLMRNNL**AC**, noting the 5' cysteine is in bold (GenScript Corporation, Piscataway NJ).

### **3.3.3 CBP Nanopartz GNP capping procedure**

Nanopartz GNPs (Nanopartz, Loveland CO) are 50 nm in diameter at a concentration of 4.48 E+10 particles per ml with a surface area of 7.85  $\mu$ m<sup>2</sup>. This implies a theoretical capacity to bind approximately 4.0 E+5 sulfur atoms which can translate for the same number of CBPs. The CBP peptide has a single cysteine cap at the C-terminus. The combination of 9.0 E+5 CBPs per GNP are sufficient to ensure successful and complete saturation of the gold nanoparticles surface, CBP capped GNPs are very stable. Long-term storage can be insured by lyophilization, naked GNPs are soluble in salt solutions including PBS. Prior to capping maximum stability is at 4°C in ddH<sub>2</sub>O, pH 7.0 for a period of one year.

Following the manufacturers methodology CBP capped GNPs are acquired by mixing 25  $\mu$ g (5  $\mu$ l ddH<sub>2</sub>O) or 4.03 E+15 CBP peptides per 4.48 E+9 50 nm GNPs in a volume of 100  $\mu$ l in ddH<sub>2</sub>O. This cocktail then requires over night gentle agitation at room temperature followed by washing twice (5000 rpm, 3 minutes) in 1 X PBS for the removal of possible excess CBPs, with re-suspension in 1 X PBS to a volume of 100  $\mu$ ls.

The protocol is easily modified if scaffolding immobilizations are required. For collagen binding the CBP is mixed with a 10:1 ration with CAP, choice of linker is dependent on type of substrate intended for immobilization.

### **3.3.4 CaM-VEGF120 interaction and binding to the CBP capped GNPs**

Adhesion or binding of the CaM-VEGF120 to the CBP capped GNPs has been worked out and can present a standard protocol (obtaining 8,000 CaM-VEGF120 molecules per CBP capped GNPs), noting this procedure has to take into account sterile protocol procedure. To 100  $\mu$ l of CBP capped GNPs ( $4.48E+9$ ) was added 5  $\mu$ l or 25  $\mu$ g's of CaM-VEGF120 (379 pmoles) and incubated at room temperature for 1 to 4 hours sufficient for completion of reaction (addition of 1  $\mu$ l of 1 M  $CaCl_2$  is optional). Following adhesion of the CaM-VEGF120 complex the unbound CaM-VEGF120 was removed with two washes in 1 X PBS at 8,000 rpm, with re-suspension to 100  $\mu$ l. This is optional, a brief sonication for 10 seconds to disrupt any aggregation however gold particles in their individual form are not visible with phase contrast microscopy.

### **3.3.5 GNP immobilization**

There are two methods available for the immobilization of GNPs to collagen based scaffolds, one being the SANH-SFB kit (Solulink, San Diego CA) that requires collagen modification coupled with a modified GNP bound peptide both having chemical structures that specifically recognize each other creating the link. Another and possible superior means is the utilization of a collagen adhesive peptide, CAP (GenScript, Piscataway, NJ). CAP was chosen because it can readily bind to collagen in the liquid state or during collagen solidification as these are the required conditions upon addition of the CaM-VEGF120 complex. This minimizes any destructive side affects especially for the CaM-VEGF120 complex. Noting the SANH-SFB conjugation process is overnight utilizing a buffer system that is harsh and as collagen gel formation was compromised, this procedure was discontinued. However a decellularized ECM is only found in the solid form and easily purified therefore modification using SANH might be an advantage in surfaces that are currently insoluble.

### 3.3.6 Collagen adhesion utilizing the CAP

This employs a specific peptide shown to bind collagen derived from the collagenase digestive enzyme. This preparation requires centrifugation of the CaM-VEGF120 complex removing the supernatant and adding 10 X PBS to the CaM-VEGF120 pellet with addition of solubized collagen. Thus diluting the 10 X PBS to 1 X PBS gently mixing by pipetting up and down with placement onto the desired surface, with solidification at 37°C for one hour, thus suitable for cell culture experimentation.

**Table 3.1 - (FITC) CaM-VEGF120 concentrations for standard curve.** For use in figure 3.2a and 3.3b, fluorescent reading representative of molar amount.

µg/ml	µM
200.00	3.03
100.00	1.52
50.00	0.76
25.00	0.38
12.50	0.20
6.25	0.10
3.13	0.05
1.56	0.024
0.78	0.012
0.39	0.006

### **3.3.7 Isotherm construction, CaM-VEGF120 binding affinity and quantity per single CBP capped GNP**

#### **3.3.7.1 Standard curve construction to determine fluorescent values to established CaM-VEGF120 concentration**

Standard curve intended for 10 data points each at a twofold dilution was constructed for soluble (FITC) CaM-VEGF120 prepared in chapter II, with an initial concentration of 200  $\mu\text{g/ml}$ , displayed in table 3.1. The graph was plotted for fluorescence vs. known  $\mu\text{M}$  CaM-VEGF120, figure 3.2a and 3.3a. The required equipment to establish these measurements utilized the Nanodrop technology 3300 fluorospectrometer (serial no. 0860), once established construction of the actual isotherm can proceed.

#### **3.3.7.2 Isotherm plot construction**

The amount of adherence and binding of CaM-VEGF120 fusion construct in relation to the CBP capped GNPs was measured. Determination of the linear region of the curve is the first requirement as this implies a measured decrease in soluble CaM-VEGF120. The FITC labeled fusion construct prepared in chapter II having a known concentration and utilizing 10  $\mu\text{l}$  at 1  $\text{mg/ml}$  for 10 data points, a series of two fold dilutions was each added to a constant amount of CBP capped GNPs at  $2.24 \text{ E}+8$  GNPs, a total volume of 50  $\mu\text{l}$  per tube. This is with a twofold decreasing concentration of fluorescent construct as noted for the standard curve. Obtaining the region below saturation or better described as a rapid attenuation of fluorescent signal as the CBP capped GNPs absorb the soluble CaM-VEGF120 from solution. Establishing this linear portion of the curve, the actual isotherm can be constructed in the protocol just described (Jervis *et al.*, 2004; Doheny *et al.*, 1999).

To ten eppendorf tubes was added 40  $\mu$ ls of  $2.24 \times 10^8$  CBP capped GNPs in 1 X PBS, adding to the first tube was 10  $\mu$ l of 1 mg/ml of (FITC) CaM-VEGF120 providing a 200  $\mu$ g/ml starting concentration followed by 9 more samples at two fold dilution for the remaining tubes. This cocktail was incubated at room temperature for 4 hours with gentle rotation followed by centrifugation at 14,000 rpm with reading on the Nanodrop 3300 fluorospectrometer. The experiments were performed in triplicate. Following the plotting of the isotherm curve, isotherm analysis yielded the number of molecules absorbed per solid surface area and apparent dissociation constant.

## **3.4 Results**

### **3.4.1 In house production of the GNPs**

The protocol for the production of the GNPs is easily prepared in house, consistently producing a bright ruby red product, and is reproducible. Noting size determination as measured with visible spectroscopy the absorbance peak when maximum at 530 nm implies a 40  $\mu\text{m}$  GNP in diameter. Broad peaks in absorbance are indications of a wide size distribution. The protocol for the production of GNPs was simple and reproducible but difficulties were with capping efficiency, putative peptide capped GNPs frequently dissolved in PBS solution and therefore not efficient, especially if one wants to expand for tissue culture applications, thus commercially available GNPs were obtained.

### **3.4.2 Nanopartz GNP peptide capping**

Upon CBP capping one observed densely packed pellets as indicating of good stability in PBS. Stability and can only be the result of proper CBP cap formation, as mentioned GNPs uncapped are not stable in salt solutions. The problems of CBP binding to GNPs vanished with the purchase of GNPs obtained commercially from Nanopartz and proved to be extremely effective and reproducible following company's protocol. The Nanopartz GNPs permitted the production and analysis of quantifiable isotherm affinity. Final note, the amount of GNPs obtained during the reaction generally appeared constant as indicated by pellet size in PBS.

### **3.4.3 Characterization and properties of the CBP capped GNPs**

CBP capping protocols appeared successful as noted by stability in PBS. The percent of CBP capped GNPs cannot directly be determined, however considering the amount recovered after

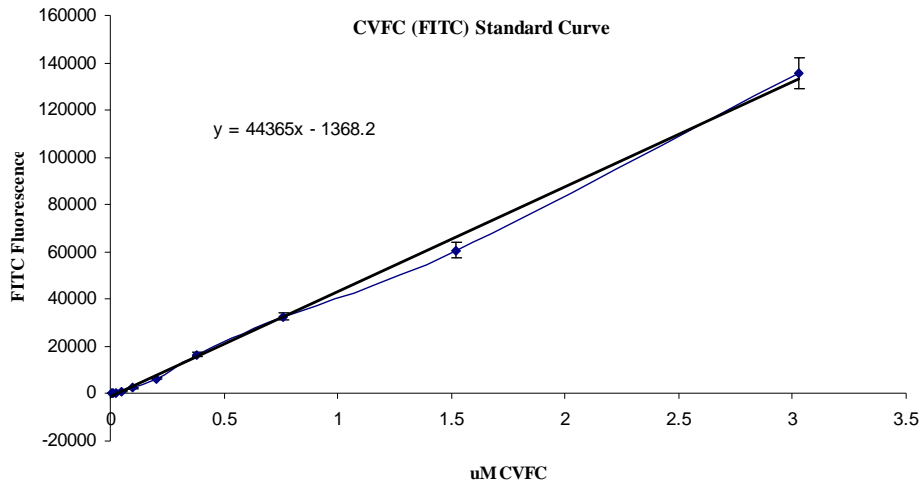
peptide capping, most of the reaction went to completion. Obtaining the OD at 534 nm comparing CBP capped in 1 X PBS to the CBP capped in ddH<sub>2</sub>O, an incomplete capping protocol should result in a drop in absorbance when comparing CBP capped GNPs suspended in PBS. This was not the case however, but if a complete reaction was required perhaps an increased reaction time or increased addition of CBP would be recommended. Noting any uncapped GNPs in a salt solution will dissolve therefore this is a measure of percent CBP capped GNPs. Other, more accurate techniques would require HPLC or TEM. As estimated from determining the spherical surface ( $4\pi r^2$ ) a maximum of  $4.0E+5$  CBPs can bind per GNP. Therefore, to ensure capped completion the capping protocol was adjusted so that double that amount was added per GNP, more than enough to be confident in going to completion; result was a product that is stable and reactive.

#### **3.4.4 Determination of CaM-VEGF120 per GNP**

Utilizing nanodrop technology is one means of data collection for the numerical determination obtaining a value for the number of (FITC) CaM-VEGF120 fusion constructs that covalently adhere to the saturated CBP gold surface. At saturation the CBP capped gold nanoparticles can bind  $2.8 E+4$  CAM-VEGF120 constructs derived from the isotherm analysis, noting the anti-parallel nature of the CaM-VEGF120 implies both ends consist of a CaM N-terminus, therefore one molecule should be able to bind two CBPs though not necessarily on the same particle. It is unclear at this point if steric hindrance is the limiting factor but is a reasonable assumption. Stability is reasonable as VEGF fusion construct adherence to the CBP capped GNPs remained intact even when exposed to many high stringency washes, very little

(FITC) CaM-VEGF120 fluorescent signal even after two days incubation at 37°C was detectable.

A



B

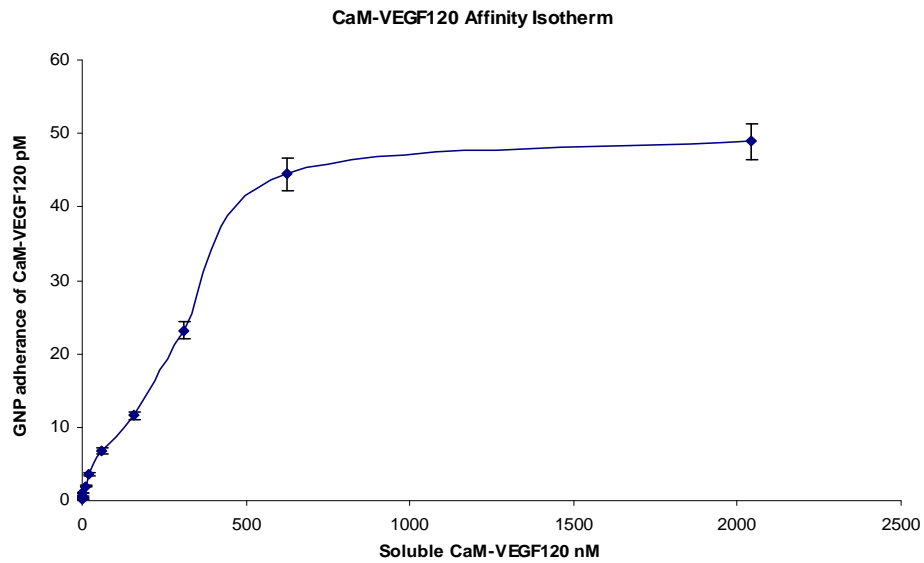


**Figure 3.2 - CaM-VEGF120 Isotherm and complementary standard curve.** A) A linear curve of known values of fluorescence vs. increasing amounts of FITC labeled CVFC as presented in table 3.1. B) CaM-VEGF120 binding to CBP capped GNPs, a measure of affinity and quantity per GNP, isotherm data derived from FITC labeled CaM-VEGF120.

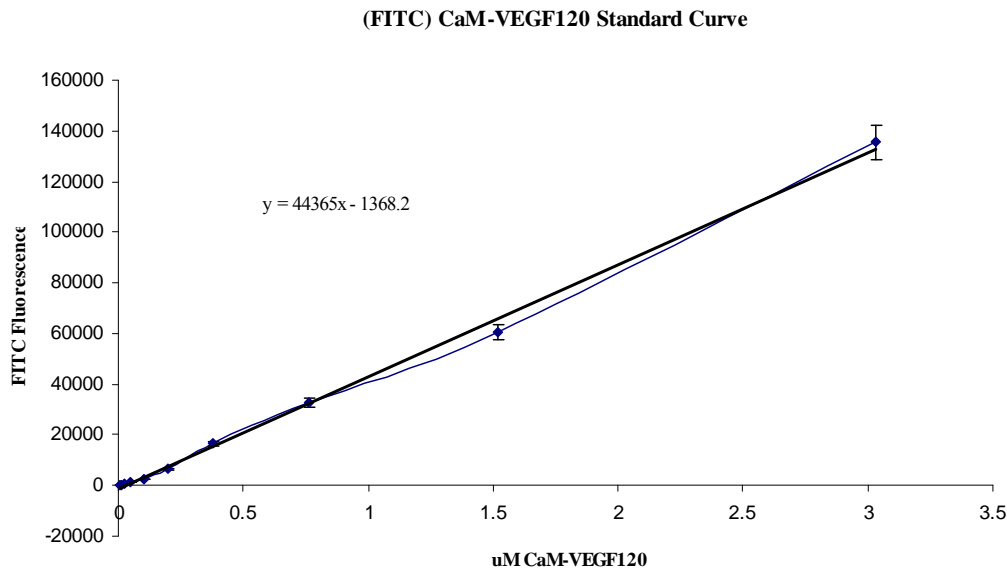
### 3.4.5 Isotherm

In isotherm plots the affinity is proportional to increasing slope and the plateau this includes the total amount of material that can bind. In the case of this project, the CaM-VEGF120 has a very high capacity for the CBP with a value of 28,000 CaM-VEGF120 molecules binding per GNP, however for experimental purposes 8,000 CaM-VEGF120 molecules were used per GNP.

To achieve this sensitivity CaM-VEGF120 required fluorescent labels. Another label with enhanced signal could be more suitable for these types of measurements. This implies a reduced amount of tags per molecule, noting from figure 3.3a the more tags per CaM-VEGF120 affinity is lost. Affinity from figure 3.2b is estimated at about 200 nM deduced from half way between the plateau and base of the curve on the y-axis and a value recovered from the x-axis, actual  $K_d$  for CaM CBP binding is between 1-10 nM.

With comparison to isotherm graphs increasing the number of FITC labels enhances the sensitivity of any labeled protein but in the case of the CaM-VEGF120 there appears to be a dramatic reduction in the affinity for binding of the fusion construct. Lysines are the target of FITC labeling reactions and as noted they occupy the active site required for CaM binding to the substrate region of the iNOS protein. Numerous FITC labels per CaM-VEGF120 may not interfere with total binding per capped GNP unless the FITC interferes in a steric fashion, that is binding may have compromised or a reduced adherence, some experiments to consider.

A



B

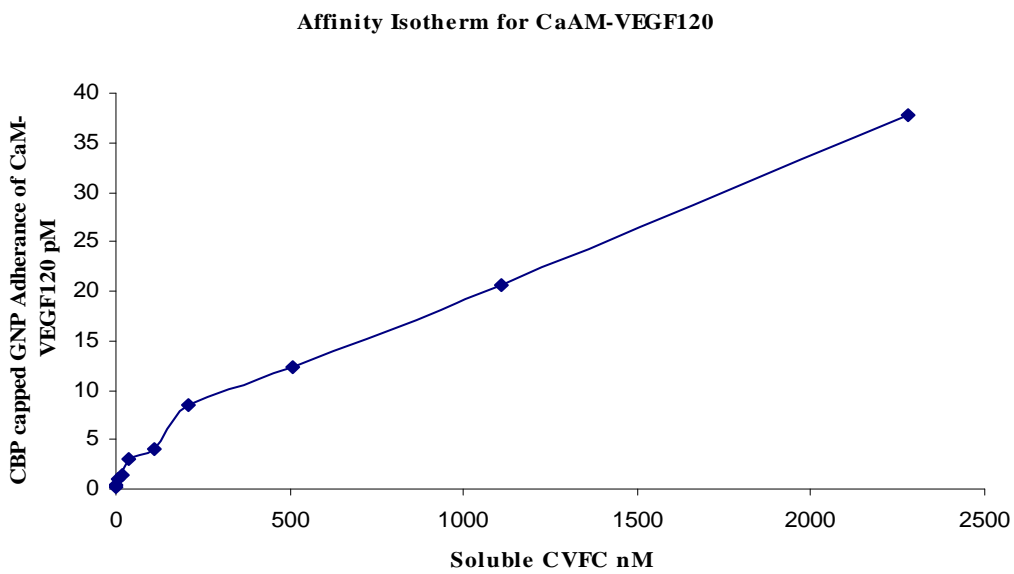


**Figure 3.3 - The original isotherm with 6 to 7 FITC labels per CaM-VEGF120. A)** Utilizing a 200  $\mu\text{g/ml}$  amount in a 2 fold series of dilutions demonstrates a robust standard curve. B) Isotherm results with enhanced FITC tagged CaM-VEGF120 noting the dramatic drop in affinity, a weak slope remaining in the linear phase.

## **3.5 Discussion**

### **3.5.1 In house GNP production and applicability**

The protocol and difficulties for the in house production of GNPs was very unpredictable, functionality was hard to reproduce to affectively bind sulfur moieties. For example as upon placement of the putative sample in PBS no pellet during the wash phase was recoverable. Briefly CBP capping experiments were problematic with very little product recovered, as they must have solubilized in the salt solution. In the literature it has been reported that the quality of the precursor gold ions are important as this will affect the quality of product. On average one in five batches of manually prepared GNPs was suitable.

### **3.5.2 CBP capped GNPs**

Successful peptide capping observed for the in house prepared GNPs collected following centrifugation had a characteristic pellet with expansion in size and a distinct pattern formation, notably more dense and concentrated when compared to the naked uncapped GNPs. Upon acquiring the GNPs from Nanopartz utilizing the same peptide capping protocol proved to be extremely effective and reproducible and was a huge advantage particularly for tissue culture experiments. Nanopartz GNPs permitted the production and charting of quantifiable isotherm affinity graphs. The commercially available GNPs are produced with a reducing agent that is proprietary but has the advantage of a much longer shelf life that readily exchanges with sulfur moieties, hence capping procedures were always successful as noted by the characteristic swelling of the pellet and binding of the CaM-VEGF120. Stability of the CaM-VEGF120 GNP complex was demonstrated by extensive wash protocols in PBS, consistently reproducible.

### **3.5.3 Potential properties enhancing the CBP capped GNPs**

Next it is logical to determine the percent of CBP capped GNPs, and from basic observation appeared to be complete. Given the current protocol mentioned in 3.5.3 generally ensures completion of capping of the GNPs producing a stable CBP capped GNP product, and if dried can be stable for an extended period of time. GNPs have the advantage acting as an intermediary for immobilization to scaffolding structures. Could the changes in types and lengths of peptide used to cap GNPs have alternative affects on the overall properties? Binding different substrate-types are flexible. This can include protease inhibitor like sequences intended to capture proteases within micro-environments. The design of peptides binding to the GNPs can have an intended affect on their cellular interactive properties, for example directed towards the prevention of cellular up-take as this can be an advantage when one is interested in receptor internalization studies. Alternatively the opposite can be employed if accelerated up-take is the intent, or they might be used as a sink to trap excess cytokines? Interestingly, they are very visible *in vivo* due to the characteristic plasmin resonance, therefore can be traced throughout a living system and do to the peptide cap are stable therefore secretion or trafficking can be studied.

### **3.5.4 Optimization of CaM-VEGF120 per GNP**

Achieving increased stability in relation to CaM-VEGF120 or CaM covalent absorbance to the CBP capped GNPs; a second sulfur group per capping peptide can be included, however this will reduce by half the number of CBPs per GNP. However if steric hindrance is playing a role the number of bound CaM-VEGF120 numbers would probably remain unchanged, but this has yet to be tested. To increase the binding capacity of the CaM portion perhaps this can be

accomplished by including a second CBP site within the target peptide, thus improving CaM access to the binding target sequence. If this proves to enhance stability with the inclusion of one or two extra cysteine caps perhaps much longer peptides can be considered with multiple CaM recognition sites, hence increased quantity of fusion construct binding offsetting any loss in total number of CBPs per gold nanoparticle. It should also be mentioned that gold can take on any shape, spherical tri-citrate GNPs are just one example, rod shapes are also available. At present there seems to be no limit to the possible combination of fusion constructs one wishes to obtain, maybe solubility issues can come into play utilizing bacterial preparations.

### **3.5.5 Isotherm constructs**

The quantification and affinity of molecules absorbed onto a surface, in this case the number of CaM-VEGF120s that can bind per GNP, or converting to a flat surface for example millimeter squared. CBP capped GNPs can bind a total of 28,000 CaM-VEGF120 molecules per 50 nm GNP as deduced by FITC tags, can FITC labels have a dampening affect on the numbers, seems to affect affinity as slope is much reduced, less tags demonstrate an augmented affinity as seen when comparing figures 3.2b and 3.3b. However it does work and can be used for other types of fusion constructs, nice system and with acquiring enhanced equipment a more refined value can be obtainable.

### **3.5.6 CaM-VEGF120 complex immobilization**

To briefly summarize, the CaM-VEGF120 fusion construct is optimal and able to bind irreversibly the CaM binding peptides, and through FITC labeling the numerical values for the CV fusion construct per gold particle has been established. A term best suitable to describe the

gold bound CaM-VEGF120 is the CaM-VEGF120 complex. The concepts this section is intended to address are one, how to immobilize the CaM-VEGF120 complex and the type of surface or material that can be considered as there are many suitable options. An obvious material type to consider seems to be type-I collagen as it can come in liquid form and when solidified is quite robust, and ideal concentrations of collagen are known for cell culture applications. This project has explored two means of CaM-VEGF120 complex immobilization, the SANH-SFB kit from SoluLink and a collagen binding peptide (Sistiabudi and Ivanisevic, 2008).

The first attempt was with the SANH-SFB kit that requires modification of the intended scaffold, as in the case of this project type-I rat tail collagen (BD Biosciences, Bedford MA). In theory a nice concept but is too harsh for solubilized collagen. The difficulties encountered after preparation of the modified collagen ranged in issues preventing solidification limiting suitability for tissue culture applications, noting cell culture surface adherence was compromised. Collagen gel solidification was only possible when blended with normal untreated collagen and always resulted in exaggerated gel concentrations, thus outside the limits for optimal cell culture interactions and discontinued, replaced with the CAP. Since type-1 collagen is suitable for tissue culture, and for practical purposes it must come in a soluble form, i.e. a low pH. Upon neutralizing the pH one can obtain solidification allowing variable shapes and concentrations, for example sandwich constructions or a standard slug trail.

CAP was discovered resulting from a literature search and noting the collagen adhesive properties, a 10 residue peptide, CAP; CQDSETRTFY. (Sistiabudi and Ivanisevic, 2008). This type of peptide construct can be expanded to include double or triple binding sequences with spacers. Other sequences that bind collagen can be considered or binding properties to other

materials, as fibronectin is another example, a very versatile and useful concept. CAP was chosen as it was readily available and is in possession of a cysteine cap, but quite short and probably compromised beneath all the CaM-VEGF120 molecules, however suitable for a first generation prototype. From what has been observed to this point is speed, a blend of 10:1 ratio of CBP to CAP prior to GNP capping seems to work. This probably will not affect numbers of fusion construct per GNP. The experimental numbers are not near saturation, noting 8000 CaM-VEGF120 per GNP are utilized in tissue culture. GNPs capped even with small percent of CAP have demonstrate increased adhesion to collagen coated surfaces, observed in collagen treated imaging chambers on a shaker, enhanced adhesion.

## Chapter IV

### CaM-VEGF120 bio-active response of VEGFR2 expressing cell lines

#### 4.1 Summary

Cell culture experiments to demonstrate CaM-VEGF120 bio-activity through the auto-phosphorylation of the VEGFR2; in particular the residue Tyr<sup>1175</sup> located within the tyrosine kinase domain. Tyr<sup>1175</sup> phosphorylation initiates several cellular activities such as migration and vasculogenesis. Other experiments to demonstrate bio-activity are included imaging of scratch assays which demonstrated a clear robust response to the sCaM-VEGF120. Cell free areas are quickly reclaimed by HUVECs or cBOECs exposed to sCaM-VEGF120 with notable cellular morphological differences compared to the controls.

When VEGFR2 expressing cell lines come into contact with the immobilized CaM-VEGF120 cellular differentiation is anticipated, and demonstrated when in contact with the CaM-VEGF complex (CaM-VEGF120 GNP bound) noting distinct pseudo-tube formation. Finally 3D collagen spot experiments demonstrate the effectiveness of the CAP important for the immobilization of the CaM-VEGF120 complex. The collagen blended CaM-VEGF120 complex lacking the CAP allows HUVECs to migrate towards the CaM-VEGF120 gradient whereas immobilized CaM-VEGF120 did not induce directed migration suggesting very low release of VEGF from the collagen matrix.

## **4.2 Introduction**

### **4.2.1 HUVEC properties**

HUVECs are one of the most important model systems of which endothelial *in vitro* research is based, as mature adult EC lines are not easily cultured (Labitzke and Friedl, 2001). HUVECs on the other hand are very abundant and inexpensive, however they cannot be assumed to represent all metabolic, physio-pathological and toxic response mechanisms when comparing to other ECs throughout the vascular network; therefore rigorous characterization would be helpful but appears to be lacking (Baudin *et al.*, 2007; Park *et al.*, 2006). HUVECs do have disadvantages, they display accelerated senescence and apoptosis with every passage and as a result attenuate the expression of proteins that define the endothelial phenotype, such as prostacyclin synthase, angiotensin I-converting enzyme, and includes the VEGFR2 (Baudin *et al.*, 2007; Mellberg *et al.*, 2009). HUVECs have served as effective model systems to demonstrate *in vitro* VEGF and bFGF angiogenesis including vascular sprouting and pathway signaling studies. Other authors have utilized HUVECs involving inhibition studies blocking receptor signaling, as an example the unique molecule EET and production noting VEGF-A angiogenic activity is blocked, but interestingly bFGF still works (Webler *et al.*, 2008). One final point are studies involving co-culture with Matrigel platforms, HUVECs can form pseudo-tube structures (Song *et al.*, 2009).

### **4.2.2 MSCs properties**

Briefly classified as a non-hematopoietic BM derived cell lines they are noted for their characteristic multipotent potential. Upon stimulation with G-CSF these cells can be mobilized from the BM. MSCs have the capacity to develop into a variety of lineages, includes SMCs, adipocytes, ligament cells and cardiomyocytes, and thus have therapeutic potential including the

enhancement of vasculogenesis and cardiac function (Jang *et al.*, 2011; Batten *et al.*, 2007). Attention is currently been given to MSCs as during transplantation they have been deemed safer than traditional embryonic stem cell therapies (Batten *et al.*, 2007). Recipient T-cell activity is not detected at the levels compared with traditional stem cell applications therefore inflammation is not as severe (Wang *et al.*, 2008). As an example, MSC pluripotency can be influenced by substrate stiffness, a physical stress, effecting cultured MSCs and predisposing these cell lines to differentiate into committed progenitors such as neuronal, muscular or osteo-related cells independent of growth factors (Jang *et al.*, 2011; Werbowetski-Ogilvie *et al.*, 2009).

#### **4.2.3 SMCs and pericytes**

The vascular wall is comprised of mature SMCs forming the muscular support as capillaries demonstrate very few or are completely free of all cell types except the lumen forming endothelial cells. When describing uncompromised vessels the SMCs are in the quiescent state, with minimal proliferative activity and are therefore resistant to vascular re-modeling (Hyedarkhan-Hagvall *et al.*, 2006).  $\alpha$ -Actin, caldesmon, and the ECM comprised of type-I collagen and elastin are some of the specific markers defining the vascular SMCs. These components coupled with the correct 3D placement of the vascular ECM are a product of SMC activity (Heydarkhan-Hagvall S *et al.*, 2006). Work of Sessa *et al.*, 2006 shows how vascular smooth muscle cells when not expressing inflammatory cytokines are not proliferative, as NO generated by the EC monolayer acts on SMCs enhancing the quiescent phenotype. Finally SMCs are responsible for the production of the Ang-1 cytokine a Tie-2 specific ligand inducing the quiescent vascular state.

## **4.2.4 Lineage committed stem cells**

### **4.2.4.1 EPC characterization**

The beginning of EPC characterization emerged with Asahara *et al.* (1997) and through enhanced neo-vascularization was shown to suppress symptoms of compromised regions such as myocardial ischaemia (Smadja *et al.*, 2008). In some instances Atherosclerotic lesions did experience reduced neointima formation including the suppression of SMC proliferation and accumulation (Zampetaki *et al.*, 2008).

Haemangioblasts can be committed to angioblast development of which EPCs derive or could be considered hematopoietic precursors, important to note no conclusive EPC phenotype has been agreed upon and is proving to be controversial. (Khoo *et al.*, 2008; Zampetaki *et al.*, 2008). EPCs are a population of mixed cells but remain the optimal cell for inducing vascular phenotypes. Why is EPC phenotypic characterization a challenge, one reason could be the multiple precursor cells, some being the non-haematopoietic MSCs. Currently the standard protocol selecting for the putative EPC population utilizes flow cytometry selecting for the markers CD34, CD133 and VEGFR2, however CD14 appears not to be a requirement at least for late out-growth EPCs. Smadja *et al.*, 2008 reports that VEGFR2 expression on peripheral blood cells defines a functionally competent cell population that has a demonstrated ability to contribute to re-endothelialization (Smadja *et al.*, 2007).

### **4.2.4.2 Early out-growth EPCs**

Early out-growth EPCs are initially noted for a spindle-like appearance following 4-7 days in culture, and are further characterized by a minimal level of proliferative activity that expire after 60 days even in the presence of high concentrations of growth factors (Smadja *et al.*, 2007;

Smadja *et al.*, 2008; Matsul H, 2007; Zampetaki *et al.*, 2008). Characteristically these cells actively express large amounts of angiogenic growth factors leading one to infer these cytokines act in a paracrine manner affecting neighboring tissues. Selecting for the CD14 marker lacking in the expression of VEGFR2 seems to be the criteria for the selection and isolation of this cell line (Mieno *et al.*, 2008). The current model suggests early out-growth EPCs seem to influence angiogenesis by means of integrating into sites of endothelial inflammation coupled with the production of large amounts of angiogenic growth factors, aiding anti-inflammatory properties and influencing development.

#### **4.2.4.3 Late out-growth EPCs**

Late out-growth EPCs are best characterized as endothelial lineage committed stem cells having the capacity to be expanded *ex vivo* (Smadja *et al.*, 2007; He *et al.*, 2004). Late out-growth EPCs lack the leukocyte markers CD14 and CD45 and are capable of expansion in culture for up to 12 weeks sustaining the EPC phenotype. The haematopoietic stem cell antigen CD133 is lost as EPCs are committed towards the late-EPC phenotype coupled with a reduced cytokine expression array in comparison to the early-outgrowth EPCs (Smadja *et al.*, 2007).

From experimental observations after 5 weeks in culture EPCs (BOECs) demonstrate an enhanced property for VEGF-A with induced angiogenesis (Smadja *et al.*, 2007). BOECs or late out-growth EPCs have shown excellent angiogenic potency *in vivo* when comparing to mature endothelial cells, but have a cobblestone pattern at confluency like mature ECs. They also have specialized features unique to BOECs such as urokinase activity and express a thrombin receptor that upon stimulation can induce pseudo-tube formation (Treichel *et al.*, 1998; Smadja *et al.*,

2009). These properties have been demonstrated *in vitro* and comparing to HUVECs stimulated responses are greatly enhanced (Smadja *et al.*, 2007; Serrati *et al.*, 2009).

#### **4.2.5 Objective**

This chapter will demonstrate bio-activity of HUVEC and cBOEC cell lines exposed to the putative CaM-VEGF120 in soluble and immobilized form. These experiments can be described as “scratch assays”, a means to demonstrate cellular migration and proliferation responding to bio-active cytokines to reclaim a cell free zone. However the more advanced experiments will consist of CaM-VEGF120 bound to GNPs capable of inducing pseudo-tube formation in comparison to control GNPs. Finally the most important of all the experiments is to demonstrate in 3D scaffold immobilization of the CaM-VEGF120. This project does touch on successful 3D collagen scaffolding models utilizing immobilized CaM-VEGF120 complex structures. Demonstrating the feasibility to create a platform where bio-active cytokines can be immobilized and accessible for a chosen cell type, a platform for future experimentation.

## **4.3 Methods**

### **4.3.1 Tissue culture**

Cell culture preparation, plastic surfaces require a form of insoluble protein coating including fibronectin (optimal), however alternatives can be used (Hughes *et al.*, 2010). Collagen coating in the form of gelatin, a .1% solution solubilized by autoclaving was used for routine culture growth and expansion. Type-I collagen favors differentiation intended for VEGF induced pseudo-tube formation as this has applications for imaging chambers when stimulated with bio-active cytokines. Initial seeding to obtain working cell numbers required 1-2 E+6 cells per T-75 flask, incubated o/n at 37°C with medium changed the following day to remove cryopreservation reagents. Upon progression towards confluence cells are passaged for expansion. Briefly, cells are washed once with 1 X PBS negative for Ca<sup>2+</sup> and Mg<sup>2+</sup> and inoculated with 1ml of trypsin per T-75 flask and left at room temperature for 1-5 minutes depending on cell type. The reaction is terminated with the addition of growth medium containing serum. Cells can continue to be passaged for experimental preparation and/or cryo-preservation.

### **4.3.2 Scratch assay preparation**

Scratch assays are measured by imaging of HUVECs or cBOECs when in contact with the sCaM-VEGF120 inducing migration into the cell free areas. 10 rectangular imaging chambers (3 X 1.5 cm) were treated with rat tail type-1 collagen prepared by over-night evaporation. Approximately 1.0 E+5 cells per chamber are seeded in rich medium and grown until confluent, as this is required for an optimal images. At confluency the rich medium is replaced by reduced medium containing 0.5% serum and further incubation for 12-24 hrs. A p200 pipette tip is “scratched” across the culture surface to clear a uniform path the length of the chamber. Cells

were then incubated with 100 ng/ml sCaM-VEGF120 or 50 ng/ml of the positive control VEGF165 (Invitrogen, Camarill CA). Images utilizing the Ziess Microscope Axiovert 200 (Model no. 37081, Göttingen Germany) were collected at 8 to 12 hour intervals for 30 to 48 hours.

#### **4.3.3 Random pseudo-tube formation**

The imaging chambers are set up in a similar fashion as the scratch assay with type-1 collagen as recommended by the manufacturer. The collagen treated chambers were seeded with  $1.0 \times 10^5$  cells per chamber in rich culture medium and allowed to reach 60-80% confluency, upon which reduced medium containing 0.1% serum was added with further incubation for 12-24 hrs before treatment. Control chambers were of two types; cells maintained in reduce medium only and the other included CBP capped GNPs. Experimental chambers for two types of conditions were evaluated; one with (FITC) sCaM-VEGF120 and the other set the (FITC) CaM-VEGF120 complex. Images were collected 12 hours upon addition of bio-active ingredients representative of time zero as this would continue for 1-2 weeks depending on cell quality, with collection of images every 8 to 12 hours and replacing the medium every 2 days.

#### **4.3.4 Advanced tissue culture**

Type-1 collagen coated imaging chambers were prepared as these experiments are set up intended to compare collagen gels blended with diffusible CaM-VEGF120 complex and its immobilized counter-part, however both are blended with type-1 collagen for the purposes of 3D suspension in collagen gel scaffolds.

Four imaging chamber preparations; control chamber having type-1 collagen coating only, second experimental control is included with 2  $\mu$ l collagen spots no additional ingredients. The experimental chambers consisted of 2  $\mu$ l collagen spots blended with diffusible CaM-VEGF120 complex and finally collagen spots blended with CaM-VEGF120 complex utilizing the CAP predisposing these GNPs or the CaM-VEGF120 complex structures to collagen immobilization.

Cell seeding was identical to the other chamber conditions however seeding with low serum conditions only to prevent collagen spot contamination, following 12 hrs for cell attachment, the initial medium was replaced with identical medium to remove unattached cells and imaging was started immediately, collecting images every 6 to 8 hrs for 8-10 days.

#### **4.3.5 IP and Western analysis of VEGFR2**

##### **4.3.5.1 Immunoprecipitation of the VEGFR2**

HUVECs cultured in 6-8 0.1% gelatin coated T-75 flasks grown to 90% confluency for enough cells to seed 6 large T-150 (0.1% gelatin) flasks to provide enough cells having low levels of the target antigen. Of the six T-150s flasks two T-150 flasks per treatment group were prepared. HUVECs were expanded to near confluency supplemented with rich medium, and media replaced with reduced medium (0.1% serum) with a further incubation for an additional 12-24 hrs. Preparation for five minute induction with growth factors utilizing standard concentrations (100 ng/ml sCaM-VEGF120). Following the 5 minute induction cells were placed on ice and washed twice with ice cold 1 X PBS supplemented with phosphatase inhibitors. Following with the addition of 1 ml lysis buffer (1 X PBS; 1% triton X-100, protease inhibitors (Roche Diagnostics, Indianapolis IL) and anti-phosphatase 1:100 (cocktail II, Sigma-Aldrich)) the cell layer was thinly coated while scrapping at 4°C, for 15 minutes per experimental group.

Cell lysate collected in eppendorf tubes followed by brief sonication of 10-15 second burst completed with gentle agitation for 20-30 minutes maximizing antigen solubility. The insoluble lysate was removed by centrifugation at high speed for 10 minutes and the supernatant recovered. Concentration measurement diluting the lysate to 100 mg/ml was precleared and doubled in volume averaging 600  $\mu$ l to which was added 0.5 to 1  $\mu$ g of capture antibody (poly clonal Goat anti-VEGFR2, Santa Cruz CA). Followed by o/n rotating incubation at 4°C followed by addition of protein G beads, 10  $\mu$ l per sample with further agitation utilizing the same conditions for 4 hours to o/n, washed 2 to 4 times in lysis buffer and resuspended in 40  $\mu$ l lysis buffer including 10  $\mu$ l sample buffer (-20°C storage possible if required). Prior to loading the running gel samples were heated at 95°C for five minutes, allowed with cooling to room temperature and centrifugation. Completed by loading 10-20  $\mu$ l of sample per well. A gradient running gel was run set at 100 volts for 4-6 hours followed by preparation for transfer to a nitrocellulose membrane.

#### **4.3.5.2 Western blotting**

Upon completion of the gel run, the gel was soaked for 20 minutes in ice cold transfer buffer (glycine 29 g, 121 MW tris 5.8 g, SDS 1 g and 20% methanol; 1 liter) and during this procedure and cutting the nitrocellulose membrane to size was briefly placed in transfer buffer, including two sheets of 3MM watman paper followed by construction of the transfer sandwich. The sandwich was placed into the apparatus maintained at 4°C for a 1 hr transfer at 100volts, followed by membrane removal, a brief wash in 1 X TBS, in preparation for antibody hybridization (Bhattacharya *et al.*, 2009). Pre-Hybridization, blocking Buffer (5% BSA, 0.1% tween 20 in 1 X TBS pH 7.4) utilizing 5 ml was added to the nitrocellulose membranes for agitated incubation at 4°C o/n followed by one wash (1XTBS, .05% tween 20).

Primary hybridization, minimal amounts of primary anti-bodies were required for this technique, 1  $\mu$ l per 4 ml of hybridization buffer (see blocking buffer) for both the rabbit polyclonal anti-VEGFR2 (Santa Cruz, CA) and the rabbit anti-VEGFR2 pTyr<sup>1175</sup> (Cell Signaling, Danvers MA) with rotational o/n 4°C incubation followed by 3 washes (1 X TBS, 0.05% tween 20) in preparation for the secondary hybridization.

Secondary hybridization, after three 10 minute washes (1 X TBS pH 7.4, 0.05% Tween 20) the blot is prepared for the secondary hybridization. The secondary antibody was a poly-HRP goat anti rabbit IgG (Thermo-Scientific, Rockford IL) used at 2 ng/ml in reduced hybridization buffer (4% BSA, 0.075% tween 20 in 1XTBS pH 7.4). A one hour agitated incubation at room temperature followed by 3 to 4 washes in wash buffer, with addition of Femto West chemiluminescent buffer (Thermo-Scientific, Rockford IL) for five extra minutes followed by removing the blot and excess liquid and placement into saran wrap in preparation for X-ray film exposure.

## **4.4 Results**

### **4.4.1 Scratch assay**

The scratch assay observes how a confluent lawn of endothelial cells or cBOECs proliferates or migrates onto a uniform path of cleared cells. A control chamber with serum reduced medium is compared to other chambers exposed to sCaM-VEGF120 at 100 ng/ml, as cell-free areas are reclaimed images are recorded as presented in figure 4.1 and 4.2. cBOECs do appear to be able to present an enhanced angiogenic sprouting profile, Figure 4.1f, as opposed to the HUVECs being predisposed to proliferation as expected, Figure 4.2f. Vasculogenic sprouting implies cBOECs are possibly expressing higher levels of VEGFR2 (Smadja *et al.*, 2008).

### **4.4.2 CaM-VEGF120 bio-active properties**

The first set of images demonstrate bio-activity of the CaM-VEGF120 complex compared to the control chambers, noting cell elongation and survivability as this pattern is apparent following figures 4.3 to 4.7. The more important images being the gold bound CaM-VEGF120 complex. The imaging chambers are coated with EtOH o/n dried type-I collagen ( $40 \mu\text{g}/\text{cm}^2$ ) providing the 2D surface allowing one to observe the CaM-VEGF120 complex cellular binding and up-take, aided by fluorescent imaging. These images demonstrate cell survivability in reduced medium (0.1% serum) imparted by the CaM-VEGF120 complex were the control samples in reduced medium display more cell debris and a thinning of the cell population. Interestingly from previous publications GNPs are anti-angiogenic, possibly by binding membrane proteins and perhaps interfering with the VEGFR2 directly (Kalishwaralal *et al.*, 2010).

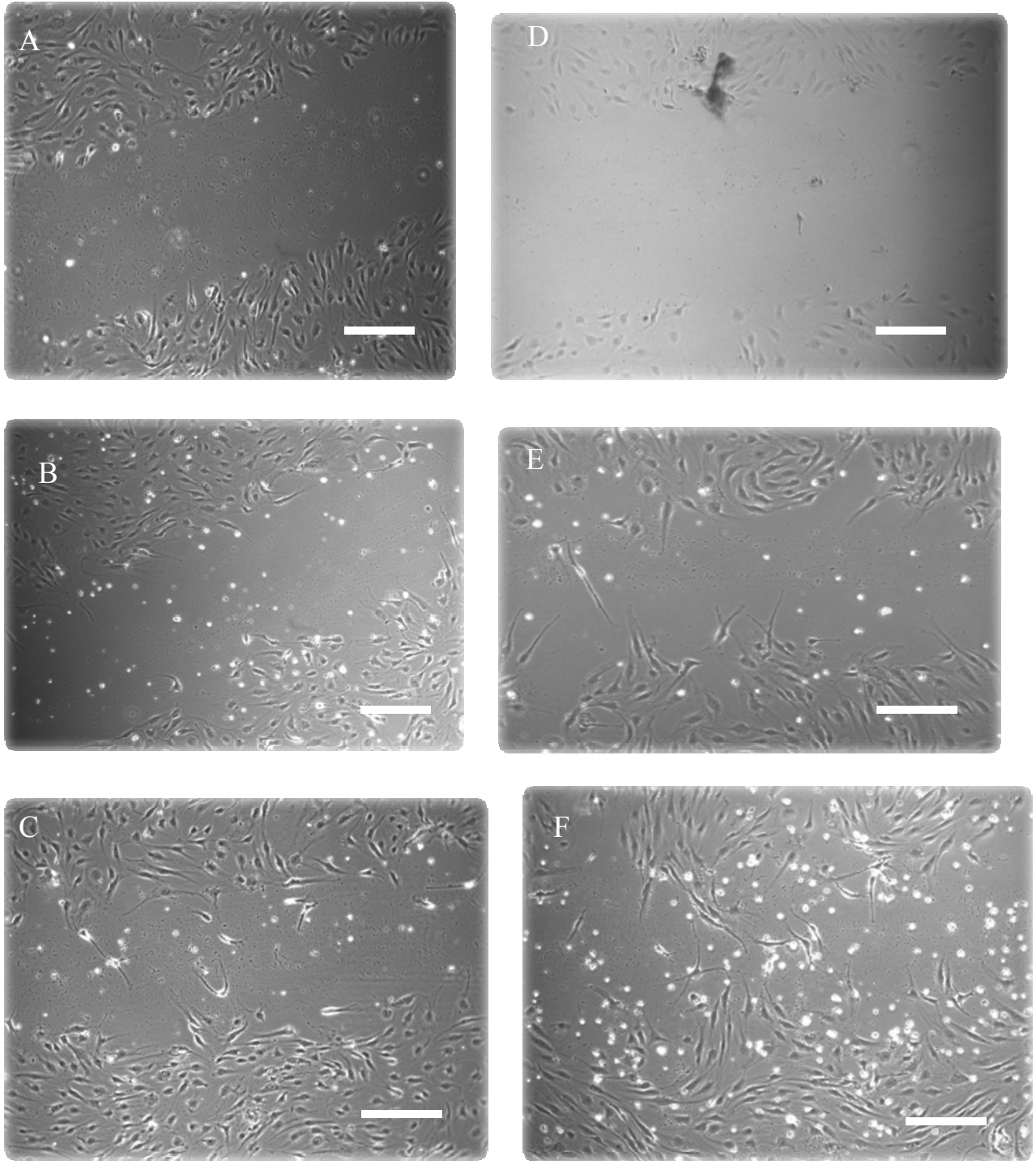


**Figure 4.1 - cBOEC scratch assay.** A-C are control chambers having no added growth factors. D to F are the experimental images exposed to 100 ng/ml sCaM-VEGF120. A and D are time zero, B and E 12 hours exposure as C and F represent 24 hours from the beginning of experiment the exposure to the sCaM-VEGF120, 10x objective imagery and 100 µm scale.

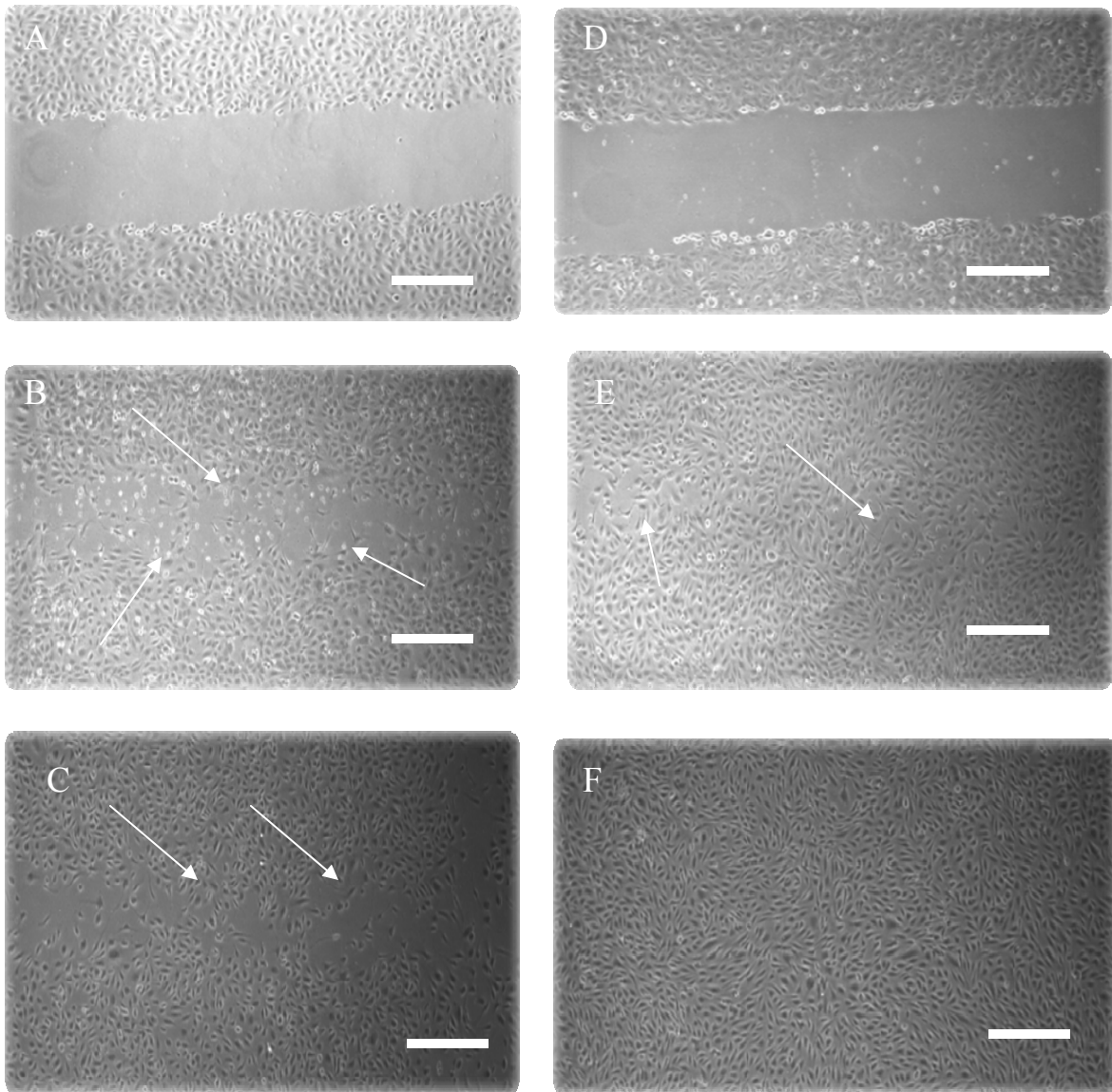


**Figure 4.2 - HUVEC scratch assay demonstrating sCaM-VEGF120 induced cell confluency.** A-C control images negative for bio-active cytokines, D-F experimental images with the addition of 100 ng/ml sCaM-VEGF120. A and D are time zero images, B and E images taken after 12 hours, noting in B indicated by arrows remaining cell free areas, much less in E. Finally C and F following the 24 hour induction as indicated by the arrows in C excess amounts of cell free areas remain, 5x objective imagery, 200  $\mu$ m scale.

The images presented in figures 4.3 to 4.7 one can observe that the CaM-VEGF120 complex is angiogenic, at least for the first 48hrs after induction. VEGF-A stimulation of the VEGFR2 augments its own regulation therefore cells expressing more of the VEGFR2 are expected to bind

more of the CaM-VEGF120 complex thus inducing enhanced survivability and augment tube forming structures noted in Figure 4.3 and 4.6c. It would then be assumed that the cells expected to scavenge the remaining CaM-VEGF120 complex are expressing the VEGFR2, cells not responding could be assumed to have little to no VEGFR2.

Comparing to the control images, HUVECs that do respond to the sCaM-VEGF120 or the CaM-VEGF120 complex present a definite elongated morphology up to 3 days, Figure 4.7e and f, and control HUVECs appear apoptotic and ultimately this must be what is happening. Another area to consider is protease production augmented by VEGFR2 activity and probably accelerates the reduction in the half-life of the CaM-VEGF120 complex, given the unprotected environment; this can be minimized through replacement of the culture medium or a flow chamber extending the life of the CaM-VEGF120 complex. This would favour conditions for physiological development. MMP activity such as MMP-2, 3, 7 and 9 can modify the surrounding ECM including the CaM-VEGF120 complex (Haas *et al.*, 1998).

#### **4.4.3 GNP internalization**

Examination of figure 4.3a, 4.4c and 4.5c representative of day one, robust angiogenic sprouting is evident, however it is random in nature as the gold particles have not been immobilized just permitted to settle onto cellular surfaces when added with the medium. At a later time point it becomes clear that the control samples are beginning to undergo apoptosis shown in Figure 4.6b and 4.7a and b, resulting from starvation conditions, as in the experimental groups this is not the case. Day two image Figure 4.6c comparing to time zero images in Figure 4.4a the sprouting is obvious noting Figure 4.6b is in the roughest shape, as staining for

apoptosis at this point would be advantageous to enhance the viable phenotype of these cells, but lacking in time and supplies.

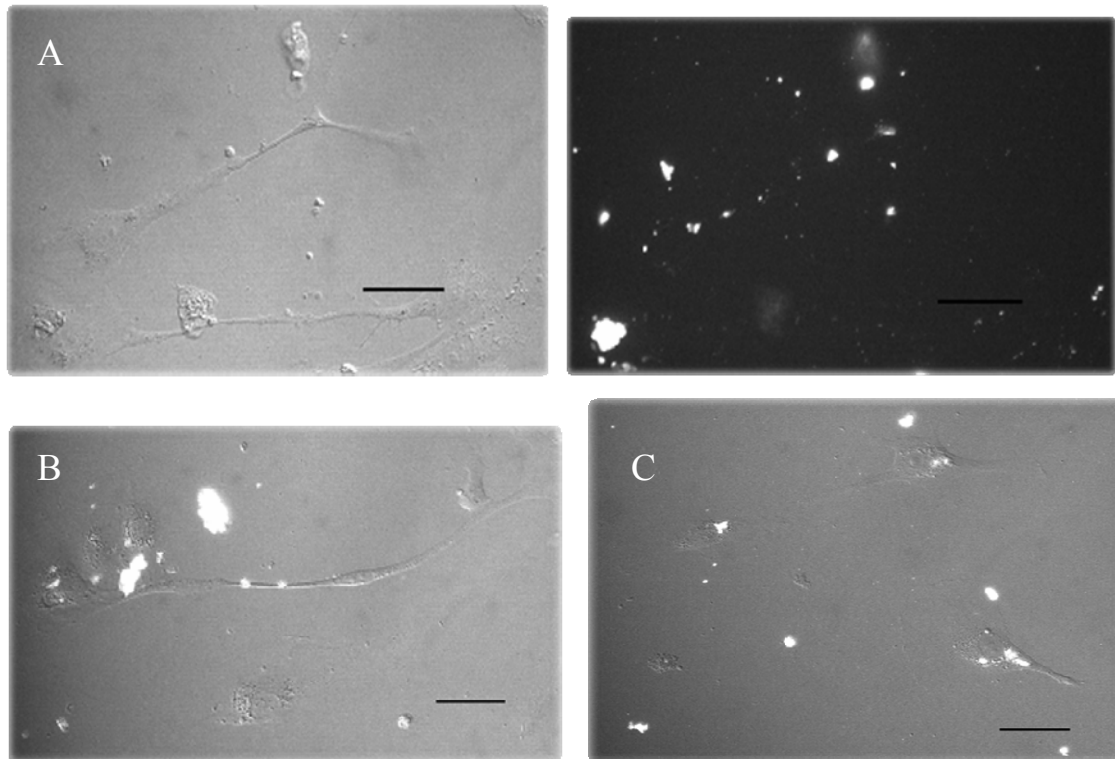


**Figure 4.3 – Day 1 to Day 4 HUVEC CaM-VEGF120 complex stimulation and response.** A) Day 1 comparing the phase contrast to the mirror fluorescent image on the right, representative of the interactive uptake and trafficking of the CaM-VEGF120 complex. B) Day 3 and C) Day 4 exposure times noting fluorescent signal visible in phase contrast, 40X objective imagery, scale 25µm.

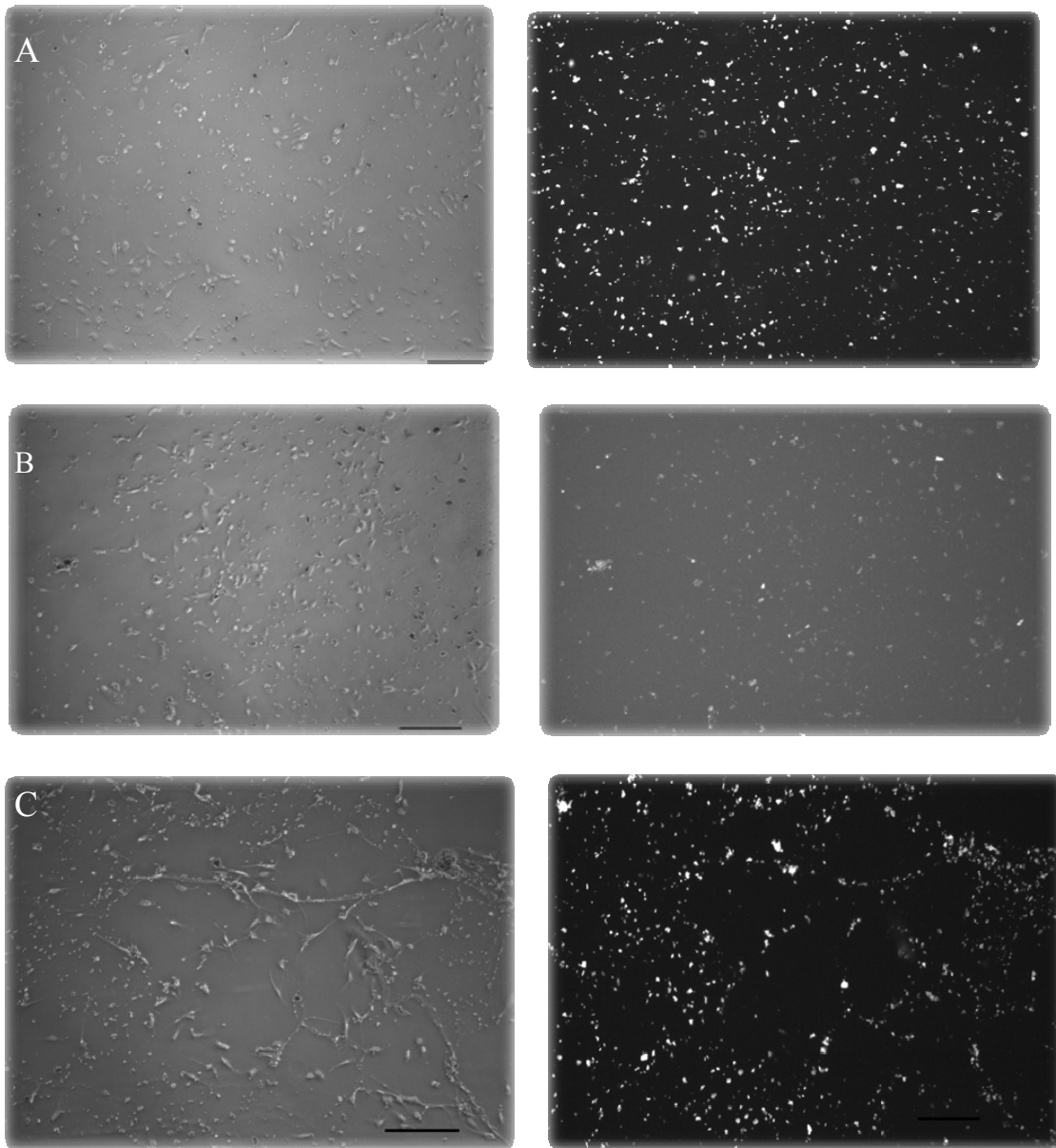


**Figure 4.4 – Image at time zero of HUVEC and CaM-VEGF120 stimulation and exposure.** A) CaM-VEGF120 complex, B) CBP capped GNPs ( $4.48 \text{ E}+8$  GNPs per chamber) for time zero. C) CaM-VEGF120 complex structures at 14 hours exposure or  $8,000$  CaM-VEGF120 per GNP, a total of  $4.48 \text{ E}+8$  GNPs per chamber. These images collected following 12hr reduced medium exposure and 12 hrs after addition of bio-active cytokines time zero, scale  $200\mu\text{m}$ , 5X imagery.

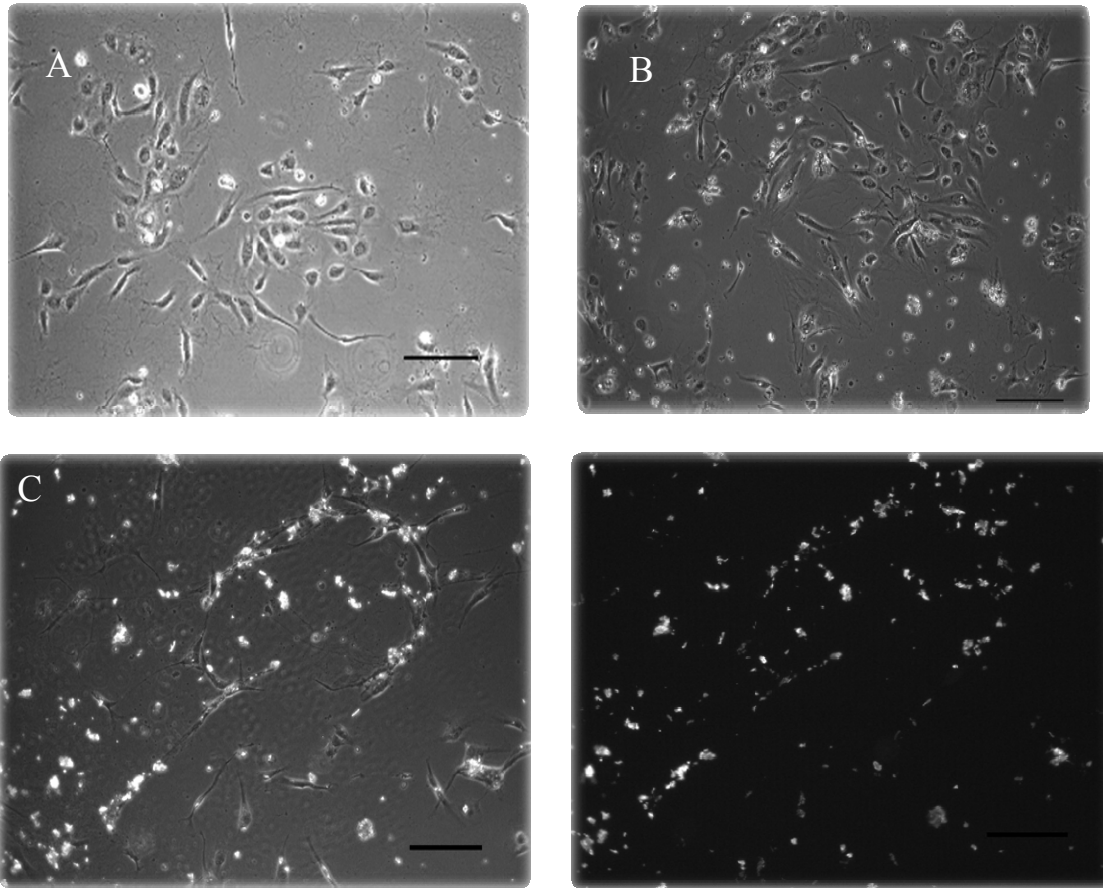


**Figure 4.5 - 14 hour HUVEC exposure to CaM-VEGF120 complex, with emphasis on tube formation.** A) Control no supplementation and B) CBP capped GNPs. C) CaM-VEGF120 complex with tube formation, noting column on the right is the fluorescent mirror image, scale 100um, 10x objective.

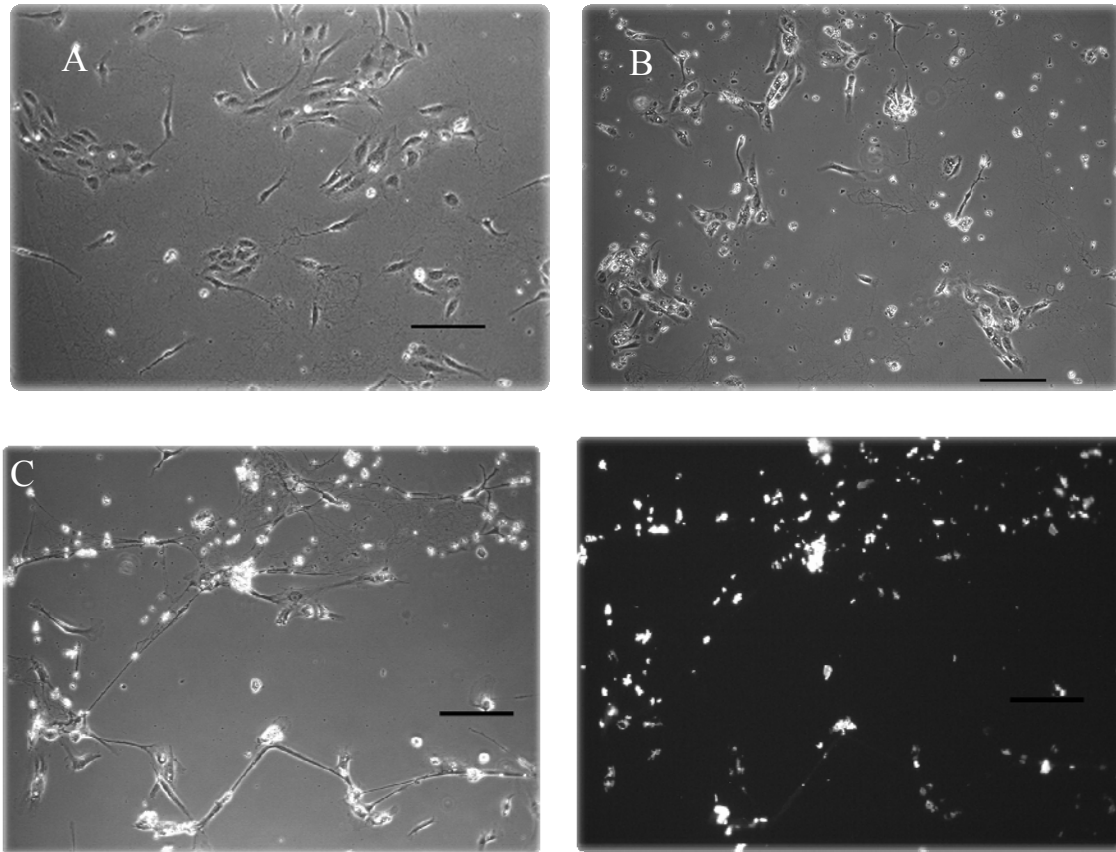


**Figure 4.6 - Day 2 imagery following CaM-VEGF120 complex exposure.** A) Control chamber no supplementation and B) CBP capped GNP noting lack of angiogenic sprouting and compromised survival. C) Extensive tube formation of HUVEC cells exposed to the CaM-VEGF120 complex and complimentary fluorescent image, 10x objective, scale 100um.

#### 4.4.4 3D Collagen gel structures

One of the last experiments for this project involving tissue culture was an *in vitro* demonstration of collagen gel spots blended with the CaM-VEGF120 complex with or without the collagen adhesion peptide. The procedure for immobilizing the GNPs to collagen required the binding or utilizing the CAP. Given the time frame collagen spots were possible consisting of 2  $\mu$ l spots at about 7-10 per imaging chamber. This produces sufficient evidence to demonstrate the bio-active capacity of the CaM-VEGF120 complex. Endothelial cells do not consider collagen suitable environments so are never seen migrating into this particular type of insoluble matrix unless a bio-active cytokine gradient is detected, optimally affective in reduced conditions

(Li and Claesson-Welsh, 2009; Serena *et al.*, 2008). To each imaging chamber was added 6-10 collagens spots consisting of 2  $\mu$ l each except for one control having no supplementation or collagen spots. Collagen spots were blended with either (FITC) CaM-VEGF120 complex or (FITC) CaM-VEGF120 adhesion complex noting the (FITC) CaM-VEGF120 complex is diffusible and should leach out of the collagen scaffold, and has demonstrated substantial cellular invasion. Collagen spots probably offer a form of protection and thus extending the shelf-life of the CaM-VEGF120 as compared to exposed 2D surfaces. Theses collagen spots were the first successful attempt at creating a suitable 3D scaffold with CAP immobilization. This is interesting as the collagen can solidify with any desired concentration but the concentration of collagen used here was optimal according to the manufacturer's protocol for cell culture. The same kind of experiment was performed earlier with SANH-SFB kit but the collagen spots were substantially denser as had to add normal collagen to the CaM-VEG120 adhesive collagen complex to obtain some form of gel formation. This did work but the collagen was overly concentrated and not optimal for cell culture and discontinued.

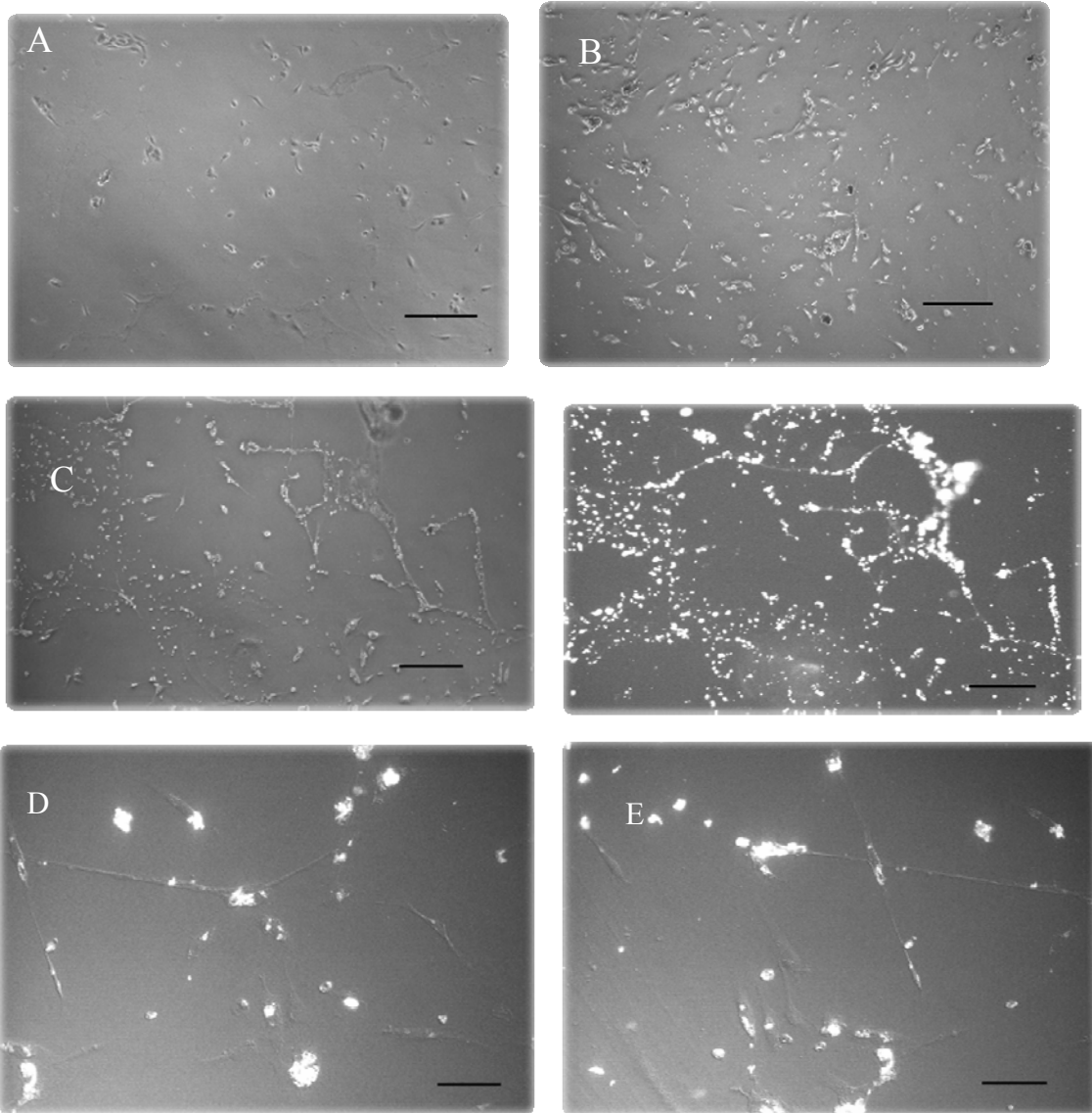


**Figure 4.7 – Final images at day three, emphasizing the robust pseudo-tube formation and fluorescent CaM-VEGF120.** A) Control comparing to B) CBP capped GNPs noting the probable apoptotic nature of the image and finally C), pseudo-tube formation is very robust when comparing to the controls but beginning to regress, 5X objective and scale 200  $\mu\text{m}$ . D and E) the complimentary image at 20x objective noting the fluorescent detail, scale 50 $\mu\text{m}$ .

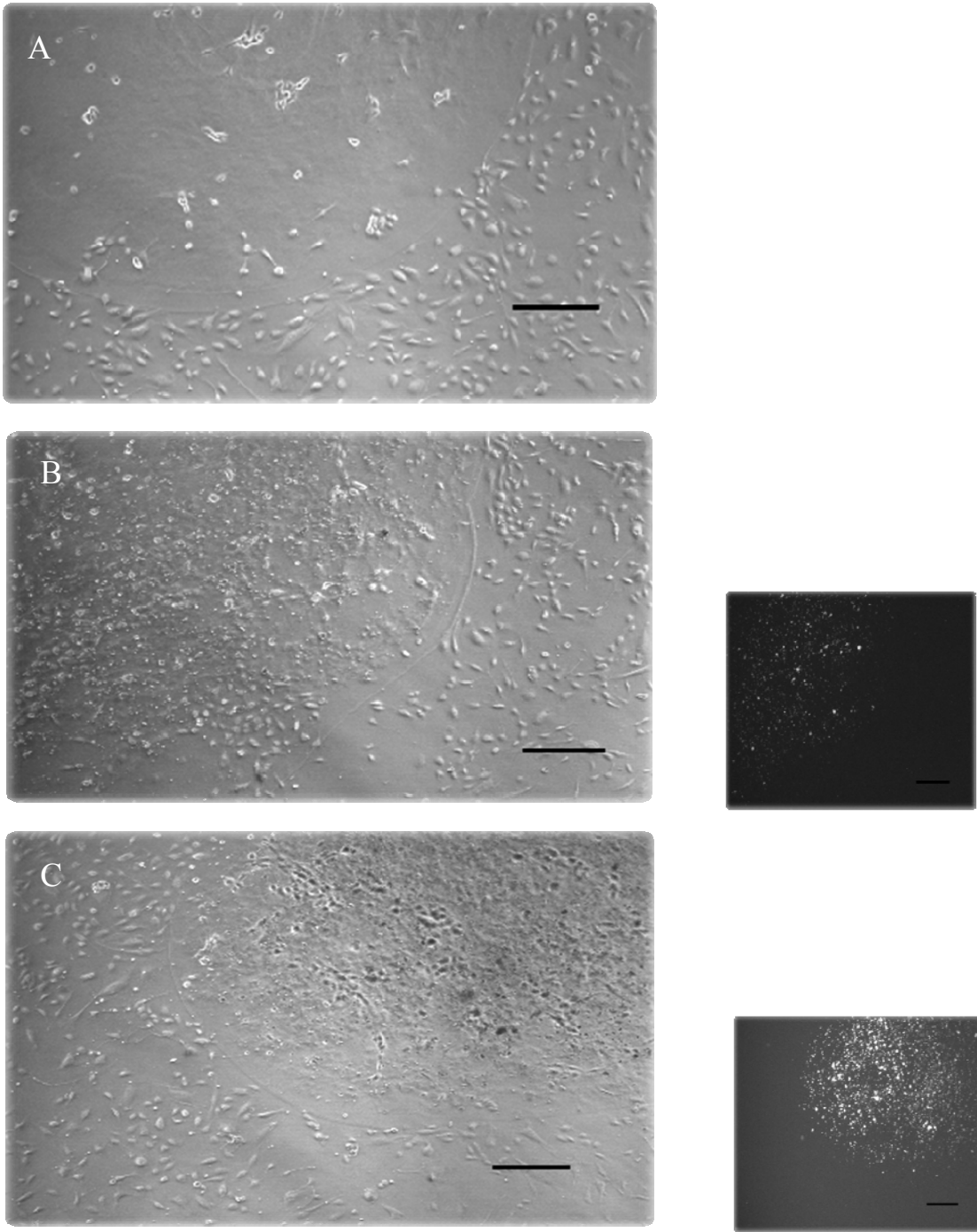


**Figure 4.8 - Collagen spot interaction with HUVECs, time zero.** A) A control collagen gel spot with no bio-active ingredients, B) collagen blended with (FITC) CaM-VEGF120 complex, and bottom C) are CaM-VEGF120 complexes with collagen adhesive properties, supplemented with a fluorescent images on the right, scale 200um, 5X objective.

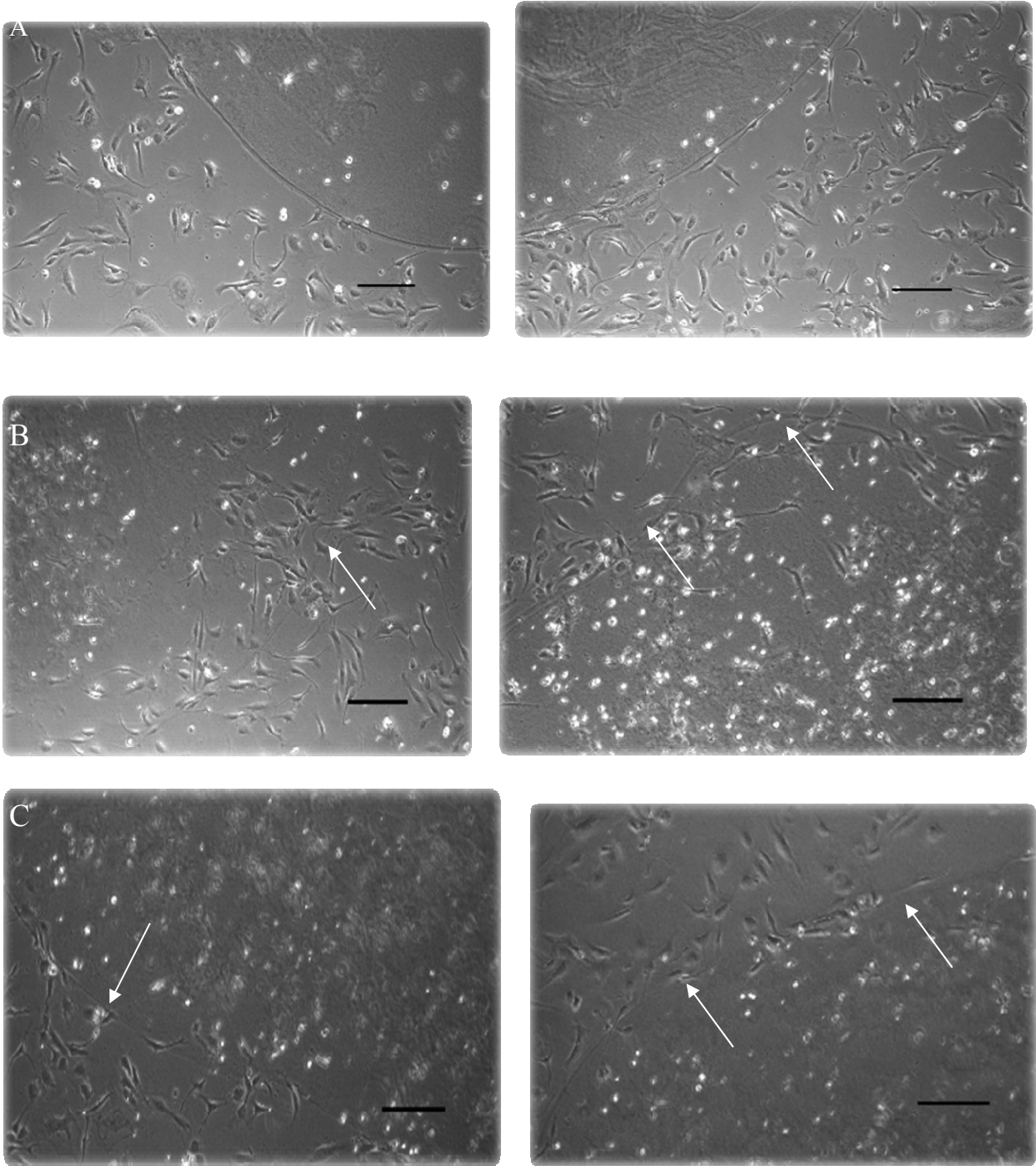
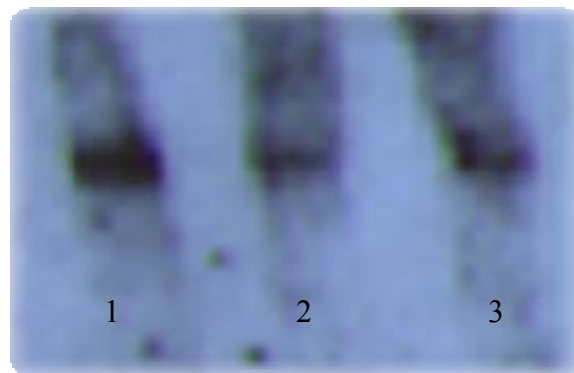


**Figure 4.9 - Day 3.5 cellular invasion into the collagen CaM-VEGF120 diffusible spot.** A) Control no cellular invasion but typically cells line the base of the collagen spot. B) Noting cellular invasion as the bio-active CaM-VEGF120 complex is not secure and arrow is pointing to the collagen edge. C) Bottom two images representative of the immobilized CaM-VEGF120 complex, cells cannot detect and the VEGF growth factor and therefore no or very little invasion detected, scale 100  $\mu\text{m}$ , 10X objective.

#### 4.4.5 VEGFR2 Tyrosine 1175 auto-phosphorylation

This part pertains to figure 4.11 demonstrating the phosphorylation of the Tyr<sup>1175</sup> do to sCaM-VEGF120 and VEGF165 VEGFR2 interaction. Clearly compared to the control lane 1 in Figure 4.10b there is no noticeable phosphorylation activity, cytokine exposure is five minutes and has been shown to be reproducible however it is evident that the level of VEGFR2 expression in this HUVEC cell line is rather weak hence the difficulty in obtaining a sizable signal.

A



B

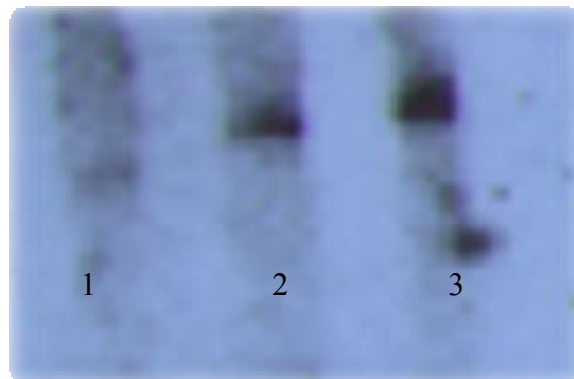


**Figure 4.10 - Western images of VEGFR2 IP demonstrating Tyr<sup>1175</sup> phosphorylation.** A) Representative image of total VEGFR2 signal, and B) were phosphorylation is detected in lane 2 CaM-VEGF120 100 ng/ml stimulation, lane 1 control no stimulation is rather weak in pTyr<sup>1175</sup> signaling. Lane 3 is VEGF165 stimulation at 50 ng/ml.

## **4.5 Discussion**

### **4.5.1 Cell culture, demonstration of CaM-VEGF120 bio-activity**

This chapter was concerned with the demonstration of CaM-VEGF120 bio-activity. The initial phases involved testing the first generation construct with tissue culture and possible applications for further follow-up experiments, a platform leading to animal model testing. Scratch assays confirmed the bio-activity of the CaM-VEGF120 fusion construct, as can be seen with HUVECs the cell free zone was completely re-claimed within 24 hours including angiogenic sprouting or elongation of the cellular phenotype. It has been reported that with increasing expression of the VEGFR2, cell VEGF-A stimulation attenuate in proliferative capacity but enhance pseudo-tube formation. This appears to be the case for the cBOECs as sprouting and migration are clearly evident in Figure 4.1. However the controls did not fare as well as is quite obvious. Finally these experiments probably can be improved with a reduction in serum from 0.5% to 0.1% as cellular proliferation especially with the HUVECs had a bit too much remaining momentum and the intent was to create a more dramatic contrast between the control and experimental groups.

### **4.5.2 CaM-VEGF120 Vasculogenesis**

Cells exposed to the CBP capped GNPs in reduced medium actually appear worse than unstimulated control chambers, however more work needs to be done to verify if the CBP capped GNPs are inducing any form of cell death programming. Restoring the chambers to rich medium might allow recovery of the stressed cells back to their original phenotype, but it would be interesting to include apoptotic analysis utilizing annexin V or Tunnel staining. However there may be no difference in the degree of programmed cell death comparing CBP capped GNP

cell exposure to the control preparation as GNPs are only anti-angiogenic, and non-toxic towards exposed cells (Kalishwaralal *et al.*, 2010). Finally the GNPs are CBP capped, cell apoptosis may be induced by removing the cellular CaM, and upon extracting these GNPs may prove to be CaM bound.

#### **4.5.3 CaM-VEGF120 complex interaction with putative VEGFR2**

Briefly it is interesting to speculate as to the stability of the (FITC) CaM-VEGF120 complex even during cellular internalization, perhaps the VEGFR2 receptor upon internalization was unable to quench the signaling cascade as the phosphorylated Tyrosine's might have more time to linger. The CaM-VEGF120 complexes appear to remain intact therefore what is the affect on the internalized receptor. Presented in figures 4.3 To 4.7 the CaM-VEGF120 complex molecules were left in the aggregated state perhaps slowing internalization, this must have an effect on the signaling cascade generated by the VEGFR2.

After one day the (FITC) CaM-VEGF120 complex structures were visible in the cell from internalization, noting this spans the length of the pseudo-tube during formation evident in figure 4.3. An alternative perspective can be provided using an FITC labeled construct not recognized by the cell or blocking the VEGFR family of receptors to determine if internalization is prevented, however time constraints meant it is beyond the boundaries of this project. As gold particles have been reported to be taken up by cells as found in literature, and noted for the CBP capped GNPs in this chapter, but appears to lack a defined pattern. This leads one to speculate as to the different types of peptides or proteins that can be bound to these gold particles. Describing CBP capped GNPs they are not associated with tube formation therefore one cannot see or detect CPB capped GNPs along the length of vasculogenic sprout, and only appear in the cytoplasm

around the nucleus, hence no evidence for intercellular trafficking. The most prudent experiment to perform would be the use of the FITC labeled CaM preparations and perform similar experiments and record the process of cellular uptake and compare to the CaM-VEGF120 complex.

#### **4.5.4 Enhancing GNP immobilization to survive rigorous conditions**

Animal models are where this project would come to life, as inoculation would be the next logical step. Were vasculogenic development *in vitro* becomes a means for inducing angiogenesis, connecting to the host vascular network. Given the plasmon resonance of gold, *in vivo* tracking and therefore a detectable difference between the immobilized GNPs to diffusible GNPs would make for an interesting comparison.

Adhesion enhancement if required as the strength of CAP binding and has yet to be tested. So how do we know for sure this peptide is providing collagen adhesive properties? From what has been mentioned and presented the system is proving successful. Without changing the peptide perhaps a collagen gel can be constructed and subject to an electric current comparing the CBP capped GNPs to the CAP peptide capped GNP noting differences in migration rates. However an interesting experiment would be cellular uptake, immobilized CaM-VEGF120 complexes attached to a collagen surface, how this compares to the diffusible CaM-VEGF120 complex with regards to uptake and trafficking. As mentioned in chapter III ECM adhesive peptides can be extended in length with repeats or a blend of different adhesive properties to enhance binding to choice of scaffold so lots of room for improvement.

Finally from figure 4.9b the HUVECs are abundant under the collagen gel spots probably due to detecting the diffusible CaM-VEGF120 complex, as it is speculated a gradient pattern has

developed. The IP analyzed by western blot with regards to the phosphorylation of the Tyr<sup>1175</sup> is in fact induced by the CaM-VEGF120. However if time was permitting a robust VEGFR2 expressing cell line would enhance this protocol substantially, thus permitting quantitative experimental analysis of immobilized CaM-VEGF120. This implies a possible sustained phosphorylated state as mentioned the cells may not easily internalize the CaM-VEGF120 complex bound to the scaffolding material, possibly interfering with phosphatase activity.

## Chapter V

### Conclusion

#### 5.1 Alternatives to the CaM-VEGF120

As we have seen CaM can be the foundation for construct considerations, but if attempting to replace the VEGF120 with other potential protein molecules what are some of the potential difficulties or advantages? The difficulties that might be encountered is the isolation from a bacterial source. The CaM-VEGF120 was possible as this construct is fairly acidic and very soluble. What about something like the bFGF cytokine, much less soluble thus might present some challenges. As far as angiogenesis is concerned VEGF-A splice variants like the VEGF165 would probably generate an enhanced angiogenic response at least when compared to the soluble VEGF120. Making clones at the DNA level should not be a problem, but with the protocol utilized in chapter II, the isolation of intact bio-active proteins solubility issues can affect the final outcome, but has yet to be attempted.

Constructing a myriad of potential fusion constructs, a functional library can be considered and modeled were these constructs could be available depending on the possible demands. One could consider the replacement of CaM, but it is a very versatile molecule. A fusion construct could be made with collagen binding peptides incorporated. However the GNPs have the advantage of *in vivo* tracking, and are measurable in terms of the isotherm constructs pertaining to the number of molecules binding per GNP, outlined in chapter III. Noting GNPs can come in many shapes and can be packed with constructs of varying types. Other fusion constructs considered relative to vasculogenesis would be the VEGF188 and Ang-1. If successful all three VEGF-A isoforms can be blended or perhaps creative patterns can be considered, thus observe

and compare *in vitro* angiogenesis for morphological differences. This could prove very interesting; however this would imply a much enhanced experimental platform. Final note, is the immobilized VEGF120 similar to the VEGF165 in regards to the induction of the VEGFR2?

## **5.2 Modifications to tissue culture**

We have seen the possibilities of different cytokines, how about tissue culture. If time was permitting it would be prudent to get data from a co-culture system. The initial cell choice for a co-culture system logically would be MSCs or pericytes to be included when the primary cell line expressing the VEGFR2 receptor is phosphorylated. If development is following a physiologically induced migratory path pericyte activity will be measurable. This would be especially true compared to the control CBP capped GNP, a very important comparison. However to date enhanced stability results from the addition of SMC/pericyte, and is required for any developing vasculature or at least provides an extended period of stability to the *in vitro* vasculature. HUVECs provide a good model system for this study however mixing pericyte and HUVEC cell lines prior to seeding has shown to have no effect, therefore timing appears to be important when blending the different cell types.

Since time has been a factor the experiments have to come to a conclusion, but these 3D collagen gel structures can be placed in many shapes including the collagen sandwich model. A collagen-fibronectin blend has been recommended, at the very least it would be interesting to compare to the scaffolds constructed of pure type-1 collagen.

Therefore to bring this project to fruition it would be ideal to have a blend of immobilized cytokines and co-culture cell types, but this is when it begins to get complex. The ensuing events

however can be monitored by cellular responses comparing gene expression to endogenous systems, comparing to ideal model organ transplant recipients. It would be interesting to see if functional lumens do form from these 3D structures allowing flow through. A form of laminar flow is essential for enhancing the physiological phenotype. For example capillary dispensed tube trails blended with cells or direct seeding onto the micro-slug trails to observe a vasculogenic sprouting pattern and properties with applications of laminar flow, a platform for physiological vascular development.

## References

- Ali N, Yoshizumi M, Fujita Y, Izawa Y, Kanematsu Y, Ishizawa K, Tsuchiya K, Yano S, Sone S and Tamaki T (2005). A novel Src kinase inhibitor, M475271, inhibits VEGF-induced human umbilical vein endothelial cell proliferation and migration. *J Pharmacol* 98 130-141.
- Andruss BF, Bolduc C and Beckingham K (2004). Movement of calmodulin between cells in the ovary and embryo of *Drosophila*. *Genesis* 38, 93-103.
- Asahara T, Murohara T, Sullivan A, Silver M, van der Zee R, Li T, Witzenbichler B, Schatteman G and Isner JM (1997). Isolation of putative progenitor endothelial cells for angiogenesis. *Science* 275, 964-967.
- Bahram F and Claesson-Welsh L (2010). VEGF-mediated signal transduction in lymphatic endothelial cells. *Pathophysiology* 17, 253-261.
- Batten P, Rosenthal NA and Yacoub MH (2007). Immune response to stem cells and strategies to induce tolerance. *Phil Trans R Soc B* 362, 1343-1356.
- Baudin B, Bruneel A, Bosselut N and Vaubourdolle M (2007). A protocol for isolation and culture of human umbilical vein endothelial cells. *Nat Protoc* 2, 481-485.
- Benest AV and Augustin HG (2009). Blood vessels kept quiet. *Nature* 458, 41-42.
- Bhattacharya R, Junhye K, Xiujuan L, Wang E, Patra S, Bida JP, Bajzer Z, Claesson-Welsh L and Mukhopadhyay D (2009). Distinct role of PLC $\beta$ 3 in VEGF-mediated directional migration and vascular sprouting. *Journal of Cell Science* 122, 1025-1034.
- Bodin A, Ahrenstedt L, Fink H, Brumer H, Risberg B and Gatenholm (2007). Modification of nanocellulose with a xyloglucan-RGD conjugate enhances adhesion and proliferation of endothelial cells: implications for tissue engineering. *Biomacromolecules* 8, 3697-9704.
- Burchfield JS and Dimmeler S (2008). Role of paracrine factors in stem and progenitor cell mediated cardiac repair and tissue fibrosis. *Fibrogenesis & Tissue Repair* 1, 1-11
- Carmona G, Chavakis E, Koehl U, Zeiher AM and Dimmeler S (2008). Activation of Epcac stimulates integrin-dependent homing of progenitor cells. *Blood* 111, 2640-2647.
- Chachques JC, Trainini JC, Lago N, Cortes-Morichetti M, Schussler O and Carpentier A (2008). Myocardial assistance by grafting a new bioartificial upgraded myocardium (MAGNUM Trial): clinical feasibility study. *Ann Thorac Surg* 85, 901-908.
- Claesson-Welsh L (2008). VEGF-B taken to our hearts; specific effect of VEGF-B in myocardial ischemia. *Arteriosclerosis, Thrombosis, and Vascular Biology* 28, 1575-1579.
- Doheny JG, Jervis EJ, Guarna MM, Humphries RK, Warren RAJ and Kilburn DG (1999). Cellulose as an inert matrix for presenting cytokines to target cells: production and properties of a stem cell factor-cellulose-binding domain fusion protein. *Biochem J* 339, 429-434.
- Fernandes H, Dechering K, van Someren E, Steeghs I, Apotheker M, Leusink A, Bank R, Karolina Janeczek K, van Blitterswijk C, and de Boer J (2009). The role of collagen crosslinking in differentiation of human mesenchymal stem cells and MC3T3-E1 cells. *Tissue Engineering* 15, 3857-3867.
- Fleury ME, Boardman KC and Swartz MA (2006). Autologous morphogen gradients by subtle interstitial flow and matrix interactins. *Biohys J* 91, 113-121.

- Francis ME, Uriel S and Brey EM (2008). Endothelial cell-matrix interactions in neovascularization. *Tissue Engineering* 14, 19-33.
- Gabhann FM and Popel AS (2008). Systems biology of vascular endothelial growth factors. *Microcirculation* 15, 715-738.
- Gao F, Vasquez SX, Su F, Roberts S, Shah N, Grijalva V, Imaizumi S, Chattopadhyay A, Ganapathy E, Meriwether D, Johnston B, Anantharamaiah GM, Navab M, Fogelman AM, Reddy ST and Farias-Eisner R (2011). L-5F, an apolipoprotein A-1 mimetic, inhibits tumor angiogenesis by suppressing VEGF/basic FGF signaling pathways. *Integr Biol* 3, 479-489.
- Gifford JL, Walsh MP and Vogel HJ (2007). Structures and metal-ion-binding properties of the Ca<sup>2+</sup>-binding helix-loop-helix EF-hand motifs. *Biochem J* 405, 199-221.
- Gill SC and von Hippel PH (1989). Calculation of protein extinction coefficients from amino acid sequence data. *Analytical Biochemistry* 182, 319-326.
- Gong J and Ito Y (2008). Peptide immobilized on gold particles enhances cell growth. *Cytotechnology* 58, 141-144.
- Haas TL, Davis SJ and Madri JA (1998). Three-dimensional type-I collagen lattices induce coordinate expression of matrix metalloproteinases MT1-MMP and MMP-2 in microvascular endothelial cells. *JBC* 273, 3604-3610.
- Haiss W, Thanh NT, Aveyard J and Fernig DG (2007). Determination of size and concentration of gold nanoparticles from UV-vis spectra. *Anal Chem* 79, 4215-4221.
- He T, Peterson TE, Holmuhamedov EL, Terzic A, Caplice NM, Oberley LW and Datusic ZS (2004). Human endothelial progenitor cells tolerate oxidative stress due to intrinsically high expression of manganese superoxide dismutase. *Arterioscler Thromb Vasc Biol* 24, 2021-2027.
- Helm CL, Fleury ME, Zisch AH, Boschetti F and Swartz MA (2005). Synergy between interstitial flow and VEGF directs capillary morphogenesis in vitro through a gradient amplification mechanism. *Natl Acad Sci UAS* 102, 15779-15784.
- Henriksen NA, Yadete DH, Sorensen LT, Ågren MS and Jorgensen LN (2011). Connective tissue alteration in abdominal wall hernia. *British Journal of Surgery* 98, 210-219.
- Heydarkhan-Hagvall S, Esguerra M, Helenius G, Söderberg R, Hohansson BR and Risberg B (2006). Production of extracellular matrix components in tissue-engineered blood vessels. *Tissue Engineering* 12, 831-842.
- Hoeben A, Landuyt B, Highly MS, Wildiers H, van Oosterom AT, de Bruijn EA (2004). Vascular Endothelial Growth Factor and Angiogenesis. *Pharmacol Rev* 56 549-580.
- Holderfield MT and Hughes CCW (2008). Crosstalk between Vascular endothelial growth factor, notch, and transforming growth factor- $\beta$  in vascular morphogenesis. *Circ Res* 102, 637-652.
- Houck KA, Leung DW, Rowland AM, Winer J and Ferrara N (1992). Dual regulation of vascular endothelial growth factor bioavailability by genetic and proteolytic mechanisms. *JBC* 267, 26031-26038.
- Hu W, Criswell MH, Fong SL, Temm CJ, Rajashekhar G, Cornell TL and Clauss MA (2009). Differences in the temporal expression of regulatory growth factors during choroidal neovascular development. *Experimental Eye Research* 88, 79-91.
- Hughes CS, Lynne M, Postovit LM and Lajoie GA (2010). Matrigel: A complex protein mixture required for optimal growth of cell culture. *Proteomics* 10, 1886-1890.

- Jakobsson L and Claesson-Welsh L (2008). Vascular basement membrane components in angiogenesis-an act of balance. *The Scientific World Journal* 8, 1246-1255.
- Jakobsson L, Kreuger J, Holmborn K, Lundlin L, Eriksson I, Kjellen L and Claesson-Welsh L (2006). Heparan sulfate in trans potentiates VEGFR-mediated angiogenesis. *Developmental Cell* 10, 625-634.
- Jang JY, Lee SW, Park SH, Shin JW, Mun C, Kim SH, Kim DH, Shin JW (2011). Combined effects of surface morphology and mechanical straining magnitudes on the differentiation of mesenchymal stem cells without using biochemical reagents. *J Biomed Biotechnol* 2011, Article ID 860652.
- Jervis EJ, Guarna MM, Doheny JG, Haynes CA and Kilburn DG (2005). Dynamic localization and persistent stimulation of factor-dependent cells by a stem cell factor/cellulose binding domain fusion protein. *Biotechnol Bioeng* 91, 314-324.
- Kalishwaralal K, Sheikpranbabu S, BarathManiKanth S, Haribalaganesh R, RamkumarPandian S and Gurunathan S (2011). Gold nanoparticles inhibit vascular endothelial growth factor-induced angiogenesis and vascular permeability via Src dependent pathway in retinal endothelial cells. *Angiogenesis* 14, 29-45.
- Keck RG, Berleau L, Harris R and Keyt BA (1997). Disulfide structure of the heparin binding domain in vascular endothelial growth factor: characterization of posttranslational modifications in VEGF. *Arch Biochem Biophys* 344, 103-113.
- Khoo CP, Pozzilli P and Alison MR (2008). Endothelial progenitor cells and their potential therapeutic applications. *Regen Med* 3, 863-876.
- Kim BS, Chen J, Weinstein T, Noiri E and Goligaorsky MS (2002). VEGF expression in hypoxia and hyperglycemia: reciprocal effect on branching angiogenesis in epithelial-endothelial co-cultures. *J Am Soc Nephrol* 13, 2027-2036.
- Kim S, Mohamedali KA, Cheung LH and Rosenblum MG (2007). Overexpression of biologically active VEGF121 fusion proteins in *Escherichia coli*. *Journal of Biotechnology* 128, 638-647.
- Koch S, Tugues S, Li X, Gualandi L and Claesson-Welsh L (2011). Signal transduction by vascular endothelial growth factor receptors. *Biochem J* 437, 116-183.
- Krpetić Ž, Nativo P, Porta F and Brust M (2009). A multidentate peptide for stabilization and facile bioconjugation of gold nanoparticles. *Bioconjugate Chem* 20, 619-624.
- Labitzke R and Friedl P (2001). A serum-free medium formulation supporting growth of human umbilical cord vein endothelial cells in long-term cultivation. *Cytotechnology* 35, 87-92.
- Lee SLC, Rouhi P, Jensen LD, Zhang D, Ji H, Hauptmann G, Ingham P and Cao Y (2009). Hypoxia-induced pathological angiogenesis mediates tumor cell dissemination, invasion, and metastasis in zebrafish tumor model. *PNAS* 106, 19485-19490.
- Levy R (2006). Peptide-capped gold nanoparticles: towards artificial proteins. *ChemBioChem* 7, 1141-1146.
- Li X and Claesson-Welsh L (2009). Embryonic stem cell models in vascular biology. *Journal of Thrombosis and Haemostasis* 7, 53-56.
- Linares PM and Gisbert JP (2011). Role of growth factors in the development of lymphangiogenesis driven by inflammatory bowel disease: a review. *Infamm bowel Dis* 17, 1814-1821.
- Loffredo F and Richard TL (2008). Therapeutic Vasculogenesis : It Takes Two. *Circ Res* 103, 128-130.
- Lokmic Z and Mitchell GM (2008). Engineering the microcirculation. *Tissue Engineering* 14, 87-103.

- Majzik A, Patakfalvi R, Hornok V and Dékány I (2009). Growing and stability of gold nanoparticles and their fictionalization by cysteine. *Gold Bulletin* 42, 113-123.
- Matsul H, Shibata M, Brown B, Labelle A, Hegadorn C, Andrews C, Hebbel RP, Galipeau J, Hough C and Lillicrap D (2007). Ex vivo gene therapy for haemophilia A that enhances safe delivery and sustained in vivo factor VIII expression from lentivirally engineered endothelial progenitors. *Stem Cells* 25, 2660-2669.
- Mellberg S, Diberg A, Bahram F, Hayashi M, Rennel E, Ameer A, Orzechowski Westholm J, Larsson E, Lindahl P, Cross MJ and Claesson-Welsh L (2009). Transcriptional profiling reveals a critical role for tyrosine phosphatase VE-PTP in regulation of VEGFR2 activity and endothelial cell morphogenesis. *The FASEB Journal* 23, 1490-1502.
- Mertsching H, Schanz J, Steger V, Schandar M, Schenk M, Hansmann J, Dally I, Friedel G and Walles T (2009). Generation and transplantation of an autologous vascularized bioartificial human tissue. *Transplantation* 88, 203-210.
- Mieno S, Clements RT, Boodhwani M, Sodha NR, Ramlawi B, Bianchi C and Sellke FW (2011). Characteristics and function of cryopreserved bone marrow-derived endothelial progenitor cells. *Ann Thorac Surg* 85, 1361-1366.
- Mihardja SS, Gao D, Sievers RE, Fang Q, Feng J, Wang J, Vanbrocklin HF, Larrick JW, Huang M, Dae M and Lee RJ (2010). Targeted in vivo extracellular matrix formation promotes neovascularization in a rodent model of myocardial infarction. *PLoS ONE* 5, e10384.
- Mohan MJ, Seaton T, Mitchell J, Howe A, Blackburn K, Burkhart W, Moyer M, Patel I, Waitt GM, Becherer JD, Moss ML and Milla ME (2002). The tumor necrosis factor- $\alpha$  converting enzyme (TACE): a unique metalloproteinase with highly defined substrate selectivity. *Biochemistry* 41, 9462-9471.
- Moss AJ, Sharma S and Brindle NPJ (2009). Rational design and protein engineering of growth factors for regenerative medicine and tissue engineering. *Biochem Soc Trans* 37, 717-721.
- Muller YA, Li B, Christinger HW, Wells JA, Cunningham BC and De Vos AM (1997). Vascular endothelial growth factor: crystal structure and functional mapping of the kinase domain receptor binding site. *PNAS* 94, 7192-7197.
- Nacak TG, Alajati A, Leptien K, Fulda C, Weber W, Miki T, Czepluch FS, Waltenberger J, Wieland T, Augustin HG and Kroll J (2007). The BTB-kelch protein KLEIP controls endothelial migration and sprouting angiogenesis. *Circ Res* 100, 1155-1163.
- Nerem RM (2006). Tissue engineering: the hope, the hype, and the future. *Tissue Engineering* 12, 1143-1150.
- Nillesen STN, Geutjes PJ, Wismans R, Schalkwijk J, Daamen WF and van Kuppevelt TH (2007). Increased angiogenesis and blood vessel maturation in acellular collagen-heparin scaffolds containing both FGF2 and VEGF. *Biomaterials* 28, 1123-1131.
- O'Neil KT and DeGrado WF (1990). How calmodulin binds its targets: sequence independent recognition of amphiphilic  $\alpha$ -helices. *Trends Biochem Sci* 15, 59-64.
- Ott HC, Matthiesen TS, Goh SK, Black LD, Kren SM, Netoff TI and Taylor DA (2008). Perfusion-decellularized matrix: using nature's platform to engineer a bioartificial heart. *Nature Medicine* 14, 213-221.
- Park HJ, Zhang Y, Georgescu SP, Johnson KL, Kong D and Galper JB (2007). Human umbilical vein endothelial cells and human dermal microvascular endothelial cells offer new insights into the relationship between lipid metabolism and angiogenesis. *Stem Cell Rev* 2, 93-102.
- Petersen W, Pufe T, Unterhauser F, Zantop T, Mentlein R and Weiler A (2003). The splice variants 120 and 164 of the angiogenic peptide vascular endothelial cell growth factor (VEGF) and expressed during achilles tendon healing. *Arch Orthop Trauma Surg* 123, 475-480.

- Prahs C, Héroult M, Lanahan AA, Uziel N, Kessler O, Shraga-Heled N, Simons M, Neufeld G and Augustin HG (2008). Neuropilin-1-VEGFR2 complexing requires the PDZ-binding domain of neuropilin-1. *JBC* 283, 25110-25114.
- Robinson CJ and Stringer SE (2001). The splice variants of vascular endothelial growth factor (VEGF) and their receptors. *J Cell Sci* 114, 853-865.
- Rophael JA, Craft RO, Palmer JA, Hussey AJ, Thomas GP, Morrison WA, Penington AJ and Mitchell GM (2007). Angiogenic growth factor synergism in a murine tissue engineering model of angiogenesis and adipogenesis. *Am J Pathol* 171 2048-2057.
- Roy H, Bhardwaj S and Yia-Herttuala S (2006). Biology of vascular endothelial growth factors. *FEBS letters* 580, 2879-2887.
- Rusnati M and Presta M (2006). Extracellular angiogenic growth factor interactions: an angiogenesis interactome survey. *Endothelium* 13, 93-111.
- Serena E, Flaibani M, Carnio S, Boldrin L, Vitiello L, de Coppi P and Elvassore N (2008). Electrophysiologic stimulation improves myogenic potential of muscle precursor cells grown in a 3D collagen scaffold. *Neurological Research* 30 207-214.
- Serrati S, Margheri F, Pucci M, Cantelmo AR, Cammarota R, Dotor J, Borràs-Cuesta F, Fibbi G, Albini A and del Rosso M (2009). TGF $\beta$ 1 antagonistic peptides inhibit TGF $\beta$ 1-dependent angiogenesis. *Biochem Pharmacol* 77 813-825.
- Shibuya M (2006). Differential roles of vascular endothelial growth factor receptor-1 and receptor-2 in angiogenesis. *Journal of Biochemistry* 39, 469-478.
- Sistiabudi R and Ivanisevic A (2008). Collagen-binding peptide interaction with retinal tissue surfaces. *Langmuir* 24, 1591-1594.
- Smadja DM, Basire A, Amelot A, Conte A, Bièche I, Le Bonniec BF, Aiach M and Gaussem P (2008). Thrombin bound to a fibrin clot confers angiogenic and haemostatic properties on endothelial progenitor cells. *J Cell Mol Med* 12, 975-986.
- Smadja DM, Bièche I, Helley D, Laurendeau I, Simonin G, Muller L, Aiach M and Gaussem P (2007). Increased VEGFR2 expression during human late endothelial progenitor cells expansion enhances in vitro angiogenesis with up-regulation of integrin  $\alpha_6$ . *J Cell Mol Med* 11, 1149-1161.
- Smadja DM, Bièche I, Susen S, Mauge L, Laurendeau I, d'Auquier C, Grelac F, Emmerich J, Aiach M and Gaussem P (2008). Interleukin 8 is differently expressed and modulated by PAR-1 activation in early and late endothelial progenitor cells. *J Cell Mol Med* 12, 2534-2546.
- Smadja DM, Cornet A, Emmerich J, Aiach M and Gaussem P (2007). Endothelial progenitor cells: characterization, in vitro expansion, and prospects for autologous therapy. *Cell Biol Toxicol* 23, 223-239.
- Smadja DM, Gaussem P, Mauge L, Israël-Biet D, Dignat-George F, Peyrard S, Agnoletti G, Vouhé PR Bonnet D and Lévy M (2009). Circulating endothelial cells a new candidate biomarker of irreversible pulmonary hypertension secondary to congenital heart disease. *Circulation* 119, 374-381.
- Smadja DM, Mauge L, Susen S, Bieche I and Gaussem P (2009). Blood outgrowth endothelial cells from cord blood and peripheral blood: angiogenesis-related characteristics in vitro “a rebuttal”. *Journal of Thrombosis and Haemostasis* 7, 506-508.

Song H, Suehiro JI, Kanki Y, Kawai Y, Inoue K, Daida H, Yano K, Ohhashi T, Oettgen P, Aird WC, Kodama T and Minami T (2009). Critical role for GATA3 in mediating Tie2 expression and function in large vessel endothelial cells. *JBC* 284, 29109-29124.

Sugihara T, Wadhwa R, Kaul SC and Mitsui Y (1998). A novel alternatively spliced form of murine vascular endothelial growth factor, VEGF 115. *JBC* 273, 3033-3041.

Tam J, Duda DG, Perentes JY, Quadri RS, Fukumura D and Jain RK (2009). Blockade of VEGFR2 and not VEGFR1 can limit diet-induced fat tissue expansion: role of local versus bone marrow-derived endothelial cells. *PLoS ONE* 4, e4974.

Terpos E, Anargyrou K, Katodritou E, Kastiris E, Papatheodorou A, Christoulas D, Pouli A, Michalis E, Delimpasi S, Gkotsamanidou M, Nikitas N, Koumoustiotis V, Margaritis D, Tsionos K, Stefanoudaki E, Meletis J, Zervas K and Dimopoulos MA (2012). Circulating angiopoietin-1 to angiopoietin-2 ratio is an independent prognostic factor for survival in newly diagnosed patients with multiple myeloma who received therapy with novel antimyeloma agents. *Int. J. Cancer* 130, 735-742.

Thomas M and Augustin HG (2009). The role of the angiopoietins in vascular morphogenesis. *Angiogenesis* 12, 125-137.

Tozer GM, Akerman S, Cross NA, Barber PR, Björndahl MA, Greco O, Harris S, Hill SA, Honess DJ, Ireson CR, Pettyjohn KL, Prise VE, Reyes-Aldasoro CC, Ruhrberg C, Shima DT and Kanthou C (2008). Blood vessel maturation and response to vascular-disrupting therapy in single vascular endothelial growth factor- $\alpha$  isoform-producing tumors. *Cancer Res* 68, 2301-2311.

Tran PK, Agardh HE, Tran-Lundmark K, Ekstrand J, Roy J, Henderson B, Gabrielsen A, Hansson GK, Swedenborg J, Paulsson-Berne G and Hedin U (2007). Reduced perlecan expression and accumulation in human carotid atherosclerotic lesions. *Atherosclerosis* 190, 264-270.

Treichel JA, Reddington M and Kreutzberg GW (1998). Regulation of plasminogen activator inhibitor-1 mRNA accumulation by basic fibroblast growth factor and transforming growth factor- $\beta$ 1 in cultured rat astrocytes. *J Neurochem* 71, 1944-1952.

Turkevich J (1985). Colloidal Gold. Part II, Colour, coagulation, adhesion, alloying and catalytic properties. *Gold Bull* 18, 125-131.

Wang CH, Cherng WJ and Verma S (2008). Drawbacks to stem cell therapy in cardiovascular diseases. *Future Cardiol* 4, 399-408.

Webler AC, Michaelis UR, Popp R, Barbosa-Sicard E, Murugan A, Falck JR, Fisslthaler B and Fleming I (2008). Epoxyeicosatrienoic acids are part of the VEGF-activated signaling cascade leading to angiogenesis. *Am J Physiol Cell Physiol* 295, 1292-1301.

Werbowski-Ogilvie TE, Bossé M, Stewart M, Schnerch A, Ramos-Mejia V, Rouleau A, Wynder T, Smith MJ, Dingwall S, Carter T, Williams C, Harris C, Dolling J, Wynder C, Boreham D and Bhatia M (2009). Characterization of human embryonic stem cells with features of neoplastic progression. *Nature Biotechnology* 27, 91-97.

Wiesmann C, Fuh G, Christinger HW, Eigenbrot C, Wells JA and de Vos AM (1997). Crystal structure at 1.7Å resolution of VEGF in complex with domain 2 of the Flt-1 receptor. *Cell* 91, 695-704.

Yaun A, Lin CY and Chang C (2011). Functional and structural characteristics of tumor angiogenesis in lung cancers overexpressing different VEGF isoforms assessed by DCE- and SSCE-MRI. *PLoS One* 6, e16062.

Zachary I and Glick G (2001). Signaling transduction mechanisms mediating biological actions of the vascular endothelial growth factor family. *Cardiovascular Research* 49, 568-581.

Zahlten J, Steinicke R, Opitz B, Eitel J, N'guessan PD, Vinzing M, Witzernath M, Schmeck B, Hammerschmidt S, Suttrop N and Hippenstiel S (2010). TLR2 and nucleotide-binding oligomerization domain 2-dependent krüppel-like factor 2 expression down regulates NF- $\kappa$ B-related gene expression. *J Immunol* 185, 597-604.

Zampetaki A, Kirton JP and Xu Q (2008). Vascular repair by endothelial progenitor cells. *Cardiovascular Research* 78, 413-421.

Zelzer E, McLean W, and Olsen BR (2002). Skeletal defects in VEGF(120/120) mice reveal multiple roles for VEGF in skeletogenesis. *Development* 129, 1893-1904.

Zhou HS, Honma I and Komiyama H (1994). Controlled synthesis and quantum-size effect in gold-coated nanoparticles. *Physical Review* 50, 12052-12056.

Zygalaki E, Kaklamanis L, Nikolaou NI, Kyzopoulos S, Hourri M, Kyriakides Z, Lianidou ES and Kremastinos DT (2008). Expression profile of total VEGF, VEGF splice variants and VEGF receptors in the myocardium and arterial vasculature of diabetic and non-diabetic patients with coronary artery disease. *Clinical Biochemistry* 41, 82-87.